NASA CR-72563
FHR 3612-1

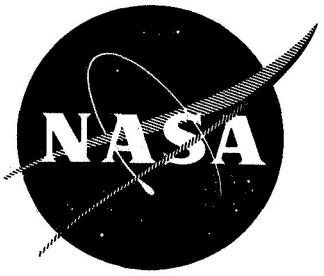

DEVELOPMENT OF HIGH TEMPERATURE POLYIMIDE ROD SEALS

by

J. Lee

FAIRCHILD HILLER
REPUBLIC AVIATION DIVISION

prepared for

NATIONAL AERONAUTICS AND SPACE ADMINISTRATION

NASA Lewis Research Center
Contract NAS 3-11170
D.P. Townsend, Project Manager
W.R. Loomis, Research Advisor

NOTICE

This report was prepared as an account of Government-sponsored work. Neither the United States, nor the National Aeronautics and Space Administration (NASA), nor any person acting on behalf of NASA:

A.) Makes any warranty or representation, expressed or implied, with respect to the accuracy, completeness, or usefulness of the information contained in this report, or that the use of any information, apparatus, method, or process disclosed in this report may not infringe privately-owned rights; or

B.) Assumes any liabilities with respect to the use of, or for damages resulting from the use of, any information, apparatus, method or process disclosed in this report.

As used above, "person acting on behalf of NASA" includes any employee or contractor of NASA, or employee of such contractor, to the extent that such employee or contractor of NASA or employee of such contractor prepares, disseminates, or provides access to any information pursuant to his employment or contract with NASA, or his employment with such contractor.

Requests for copies of this report should be referred to

National Aeronautics and Space Administration
Scientific and Technical Information Facility
P.O. Box 33
College Park, Md. 20740

NASA CR-72563
FHR 3612-1

FINAL REPORT

DEVELOPMENT OF HIGH TEMPERATURE POLYIMIDE ROD SEALS

by

J. Lee

FAIRCHILD HILLER
REPUBLIC AVIATION DIVISION
Farmingdale, Long Island, New York 11735

prepared for

NATIONAL AERONAUTICS AND SPACE ADMINISTRATION

21 August 1969

CONTRACT NAS 3-11170

NASA Lewis Research Center
Contract NAS 3-11170
D.P. Townsend, Project Manager
W.R. Loomis, Research Advisor

FOREWORD

The work described herein was conducted by Republic Aviation Division of Fairchild Hiller under NASA Contract NAS 3-11170. The program was initiated by the Fluid Systems Components Division of NASA Lewis Research Center, under the direction of Mr. R. L. Johnson, with Mr. D. P. Townsend acting as NASA Project Manager, and Mr. W. R. Loomis, Research Advisor.

Work on this program at Republic Aviation Division was under the direction of Mr. J. Lee, Project Manager - Fluid Systems Laboratory, with Mr. J. J. Brown, Chief - Hydromechanical Department, providing overall program supervision.

TABLE OF CONTENTS

TABLE OF CONTENTS (Cont'd)

LIST OF ILLUSTRATIONS

LIST OF ILLUSTRATIONS (Cont'd)

LIST OF TABLES

Development of High-Temperature Polyimide Rod Seals

by J. Lee

Fairchild Hiller Corporation
Republic Aviation Division

ABSTRACT

A polyimide V-seal evolved and tested with considerable success in a previous program under NASA Contract NAS 3-7264 was redesigned to improve the seal's fatigue life and to provide a more efficient and controllable loading of the seal. Two redesigned versions of the original seal were tested in conjunction with a spring-loaded lip seal using the original V-seal as the control specimen. Both of the improved V-seal configurations demonstrated exceptionally good sealing performance in meeting the program objective of 20 million short-stroke cycles of operation at 500°F (260°C). The original V-seal design failed after approximately 11 million cycles, which was approximately the operating life obtained in previous testing. The spring-loaded lip seal developed excessive leakage after 3.3 million cycles due to shrinkage of the polyimide material. Results obtained on the modified V-seals demonstrated the validity of the techniques used to improve the performance of the seals.

SUMMARY

The objective of this program, conducted under NASA contract NAS 3-11170, was to develop high performance polyimide rod seals for use with hydraulic fluids in advanced aircraft. The developed seals were intended for use as the low pressure, zero leakage, sealing element in a two-stage seal arrangement. In pursuing this objective, investigations were conducted to 1) further develop the polyimide V-seal evolved under a previous NASA contract (NAS 3-7264), 2) develop other seal designs, and 3) conduct long-term short-stroke cycling tests in chlorinated phenyl methyl silicone fluid at 500°F (260°C) on the most promising seal configurations to verify their sealing capability.

The V-seal evaluated in Contract NAS 3-7264 was redesigned based on thorough analyses of its configuration, the physical properties of the material, and known failure modes. Two improved versions of the original V-seal design were evolved and were designated as Design B-1 and Design HB-1. Unique features of these seals are their geometry and method of loading. Design B-1 incorporates longer seal legs than those used in the original design and utilizes a dual load path loading device which permits independent and controllable loading to the inner and outer surfaces of the seal. To minimize the notch sensitivity effects of the material, Design HB-1 incorporates linearly tapered legs to decrease the bending stresses at the transition area of the seal. The dual loading device is also used in this design. Both configurations met the 20 million cycle goal of the program without failure. Total fluid leakage accumulated during 1172 hours of operation was 27.5 cc for Design B-1 and 25,5 cc for Design HB-1, which was well within the specified leakage of 3 cc per hour. The performance of these two configurations represents a substantial improvement over that of the original V-seal configuration, which failed after approximately 11 million cycles during the same test. Fatigue failure of the material, experienced in previous testing, was essentially eliminated in the redesigned seals.

In addition to Designs B-1 and HB-1, a spring-loaded lip seal was also developed and tested. However, failure of this seal due to excessive leakage

occurred after 3.3 million cycles. Although the lip seal offers simplicity in design and low operating friction, further development work is required to refine the design.

Based on the results of this research effort, substantial progress has been made toward developing workable rod seal configurations for high temperature hydraulic applications. The polyimide seals designed and evaluated during the course of this work have shown greatly improved performance over the polyimide V-seal designs of the earlier program.

INTRODUCTION

The continuing need for increased reliability and efficiency of fluid power systems for advanced aircraft has spurred development in the area of new and improved sealing devices. One approach to meeting the rigorous operating environment anticipated for future aircraft is the use of two-stage seals for fluid containment in hydraulic actuators. This report summarizes the results of a program to develop high temperature resistant rod seals for use as zero leakage second-stage seals for such multiple seal arrangements. This effort was directed specifically towards the use of a polyimide plastic as the material of construction for the developed seals. The polyimides, which are organic condensation polymers derived from the reaction between pyrometallic dianhydrides and aromatic diamines, have undergone considerable investigation in earlier work conducted under NASA Contract NAS 3-7264. In this early effort, polyimide seals were evolved which exhibited an operational life of 1300 hours at fluid temperature up to 500°F (260°C).

In the program reported herein, a concerted effort was made to improve upon the earlier seal designs, develop other designs which most effectively use the mechanical properties of the polyimide, and conduct long-term cycling tests at 500°F (260°C) on the most promising seal configurations to evaluate design improvements.

This report presents the results and conclusions of this research undertaking. Descriptions of test equipment and test procedures are also included.

SECTION I
SEAL DESIGN AND DEVELOPMENT

A. GENERAL

The 45° V-seal developed and tested under Contract NAS 3-7264 (ref. 1) was used as the basis for the design and development effort. The primary objective of this task was to extend the operating life of the V-seal configuration through design improvements based on a thorough analysis of its configuration, failure modes, and physical behavior of the polyimide material. Additional seal designs were evolved based on the foregoing analyses. Seven basic seal concepts were developed and subjected to bench testing to verify the designs. Of these seals, three candidates were selected for testing along with the original V-seal design.

B. ANALYSIS

Based on previous test results obtained on the one-inch diameter (2.54 cm) polyimide V-seals (ref. 1), failure of the seal after 1300 hours of operation was believed to have been caused primarily by fatigue as a consequence of the seal's shape and loading condition. A time-dependent factor may have also been significant: namely, that slow relaxation of the material at temperature caused changes in geometry and loading conditions that were of sufficient magnitude eventually to cause failure.

Seal failure (Figures 1, 2, and 3) usually occurred at the inboard element, with progressively less damage to the middle and outboard elements. The inboard element received the full effects of fluid pressure, distributing some of the load to the cavity walls and the balance to the other two elements. These factors point again to geometry and loading as the determinants of failure, since the most heavily loaded member consistently sustained the worst damage. The seals usually failed cleanly around a well-defined circumference or on a radius. The circumferential failures were close to the point of support by the inboard load ring, indicating either a point of inflection in bending or a shear plane.

Figure 1. 45° V-Seal, 1300 Hours of Operation (No. 1 Seal - Inboard)

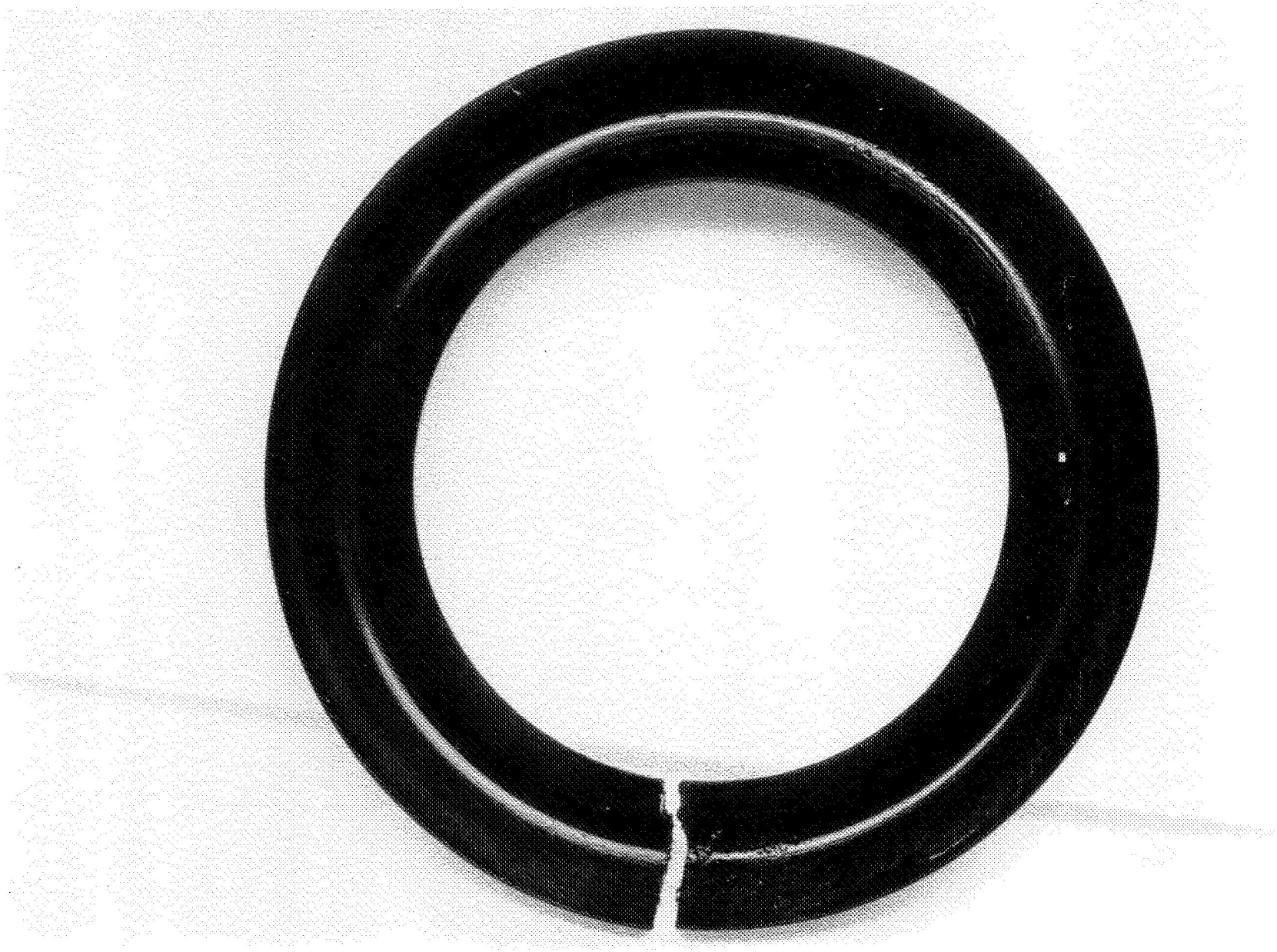

Figure 2. 45° V-Seal, 1300 Hours of Testing (No. 2 Seal)

Figure 3. 45° V-Seal, 1300 Hours of Testing (No. 3 Seal - Outboard)

The radial cracks may have been tensile failures due to shrinkage resulting from thermal cycling. The polyimide material is known to be quite notch sensitive, and an imperfection may have caused some of these failures. In either case, loading and geometry were considered to be the fundamental causes of failure.

1. Dimensional Study of 45° V-Seal

Results of the dimensional analysis of the 45° V-seal used in the endurance test conducted in reference 1 substantiate most of the early findings relating to its failure. Dimensional changes and changes in the basic geometry of the seal due to plastic deformation are evidenced in Figures 4, 5, and 6. Figures 4 and 5 show the detailed dimensions obtained from a cross-sectional sample of the tested and untested seals, respectively. Relative changes in the basic geometry of the tested seal is shown in the composite views depicted in Figure 6. Dimensions of the cross-sectional seal samples were obtained on an optical comparator at a 20 times enlargement. The shapes of the seals were traced from the comparator at the same magnification.

Of particular interest are the findings obtained in the study of the seal as installed in the gland. Figure 7 shows the V-seal laid out in the assembled condition in the gland cavity. This layout was obtained by projecting a section of the seal on an optical comparator; a tracing was then made of the seal's shape. To accomplish this, the seal was confined in a slotted plate (Figure 8), which simulated the gland cavity.

As shown in Figure 7, the clearance between the inner seal leg and backup ring is insufficient to permit adequate seal deflection. A mismatch between the center line of the seal and the center line of the backup ring and load ring also exists. The amount of offset between the center lines is approximately 0.005 - 0.006 inch (0.127 - 0.152 mm) radially. Under these conditions, the load ring makes its initial contact with the outer leg of the seal, while a clearance of approximately 0.007 inch (0.178 mm) exists between the inner leg of the seal and the load ring. With this condition, initial loading occurs on the outer leg; contact of the load ring is made on the inner leg only after the outer leg has deflected against the gland. However, as this latter condition is reached,

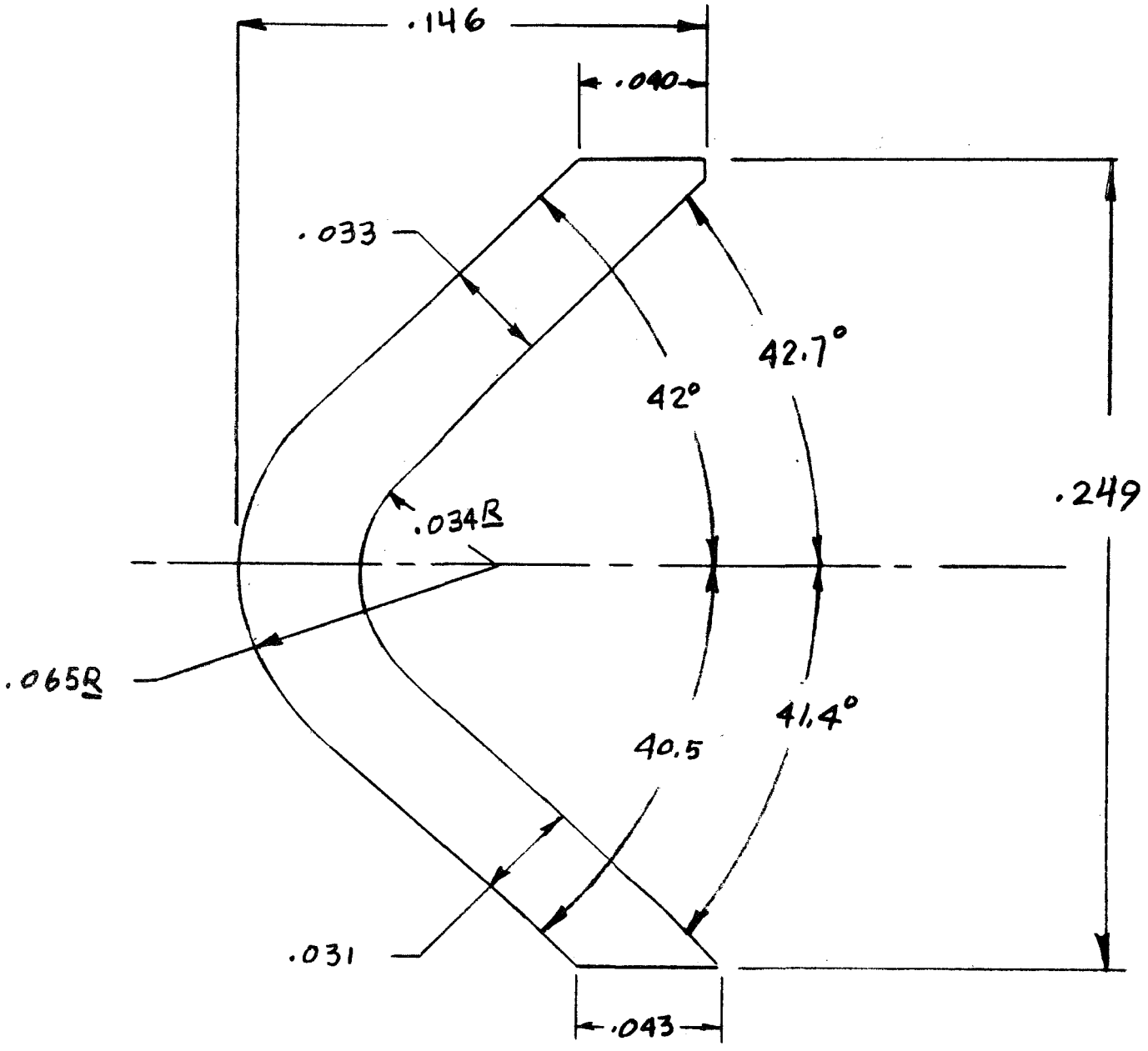

Figure 4. 45° V-Seal - Dimensions After 1300-Hour Endurance Test

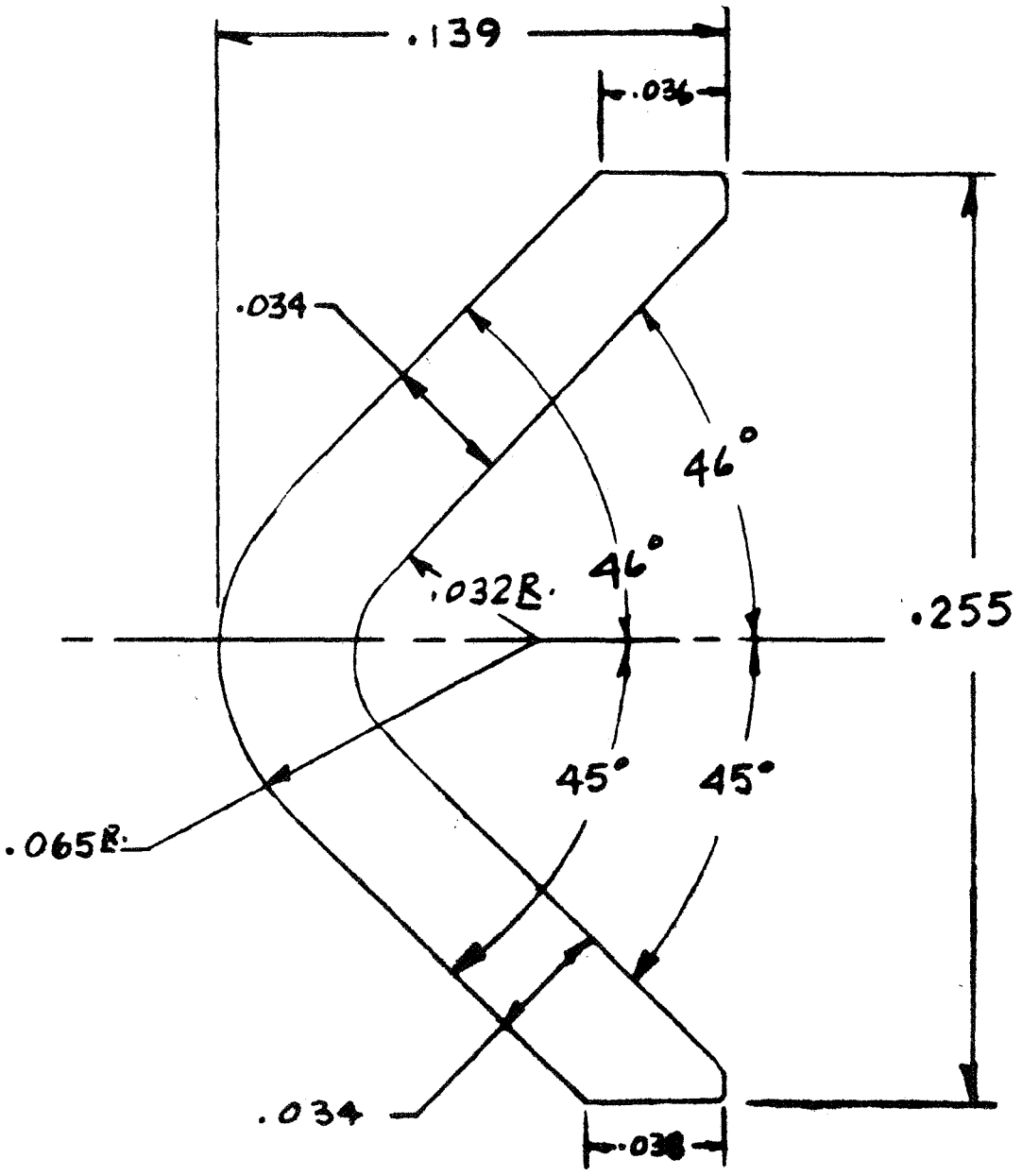

Figure 5. New 45° V-Seal

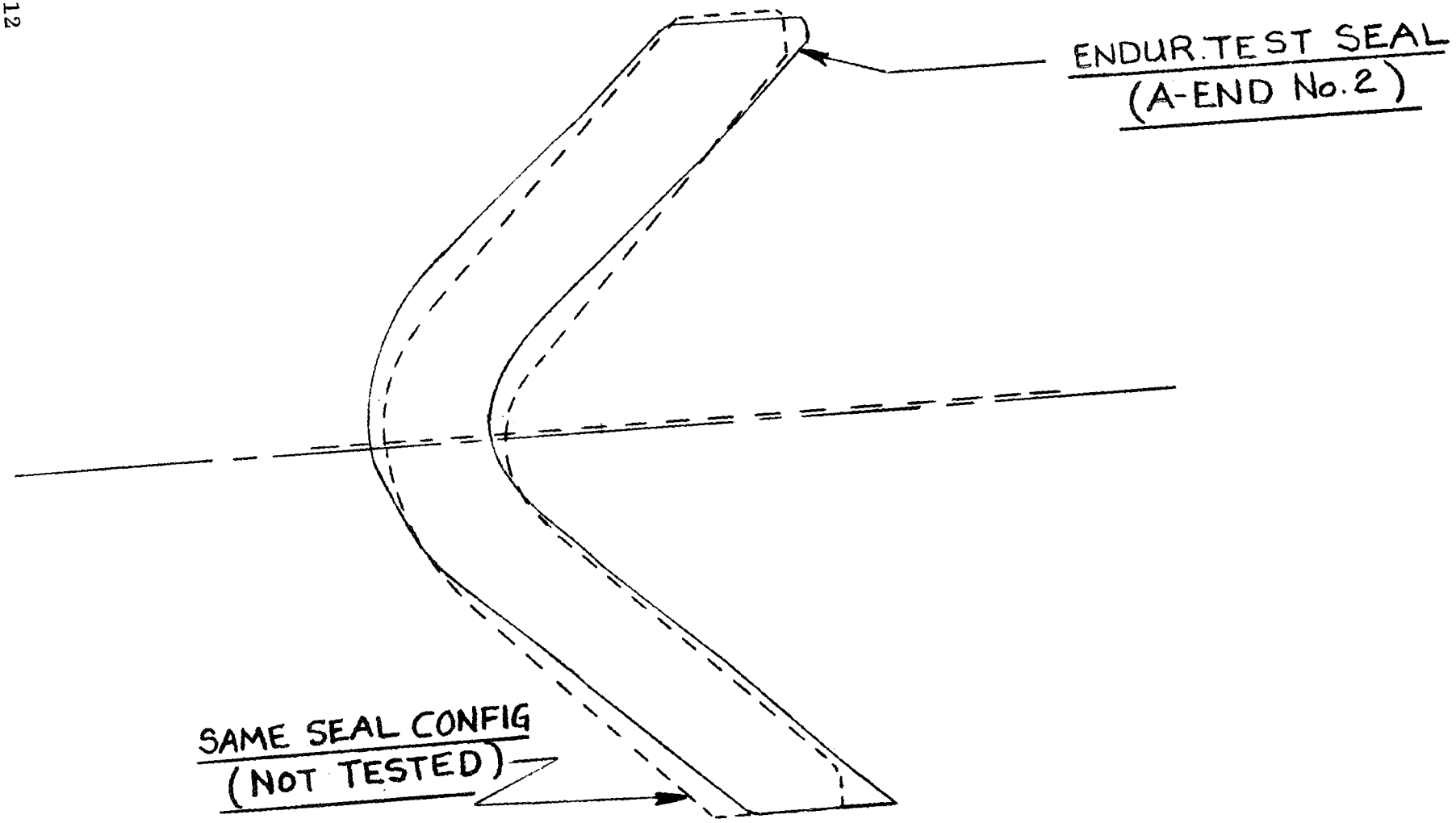

Figure 6. Comparison of Endurance Test Seal and Untested Seal

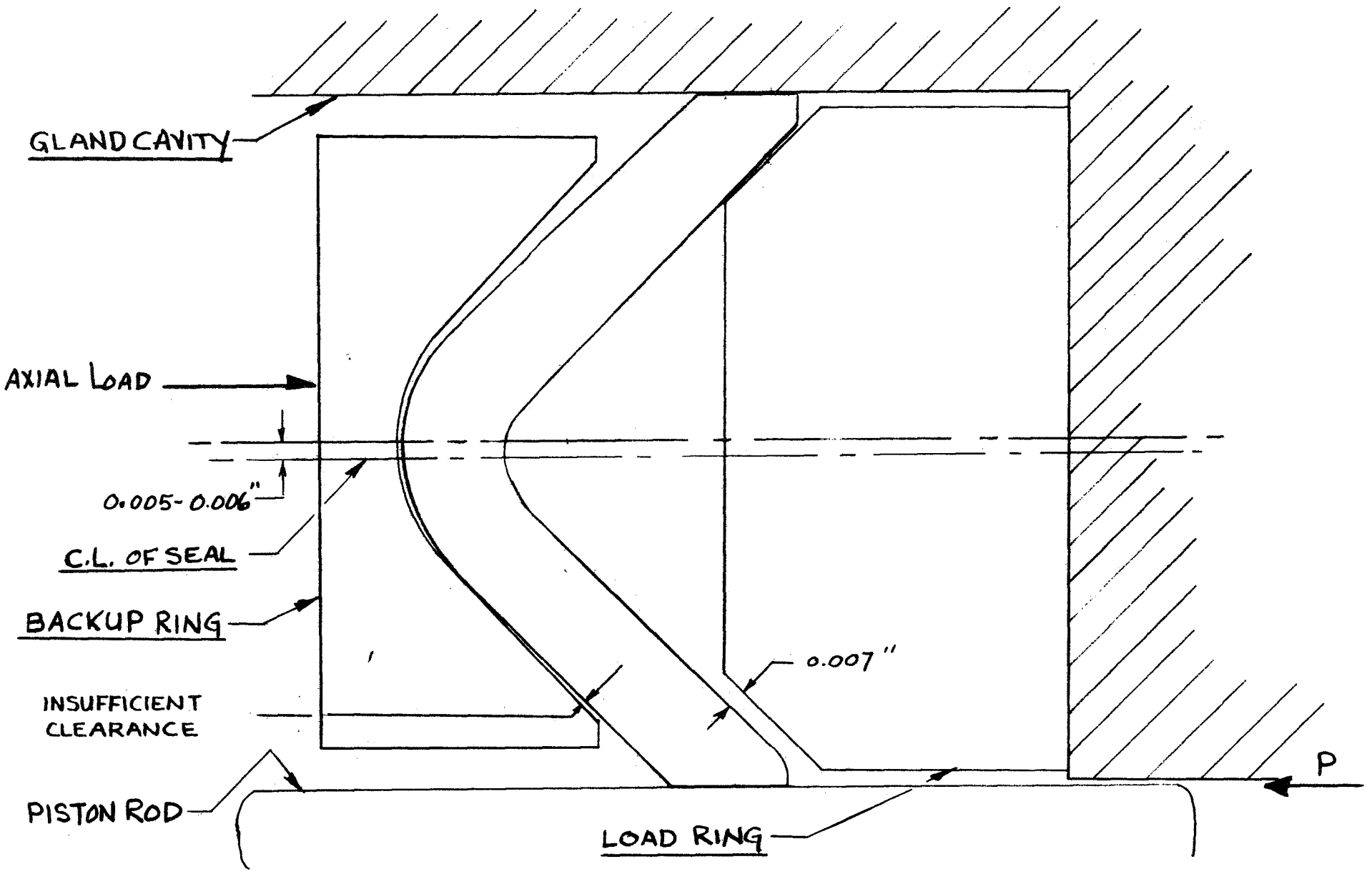

Figure 7. V-Seal Endurance Test Configuration

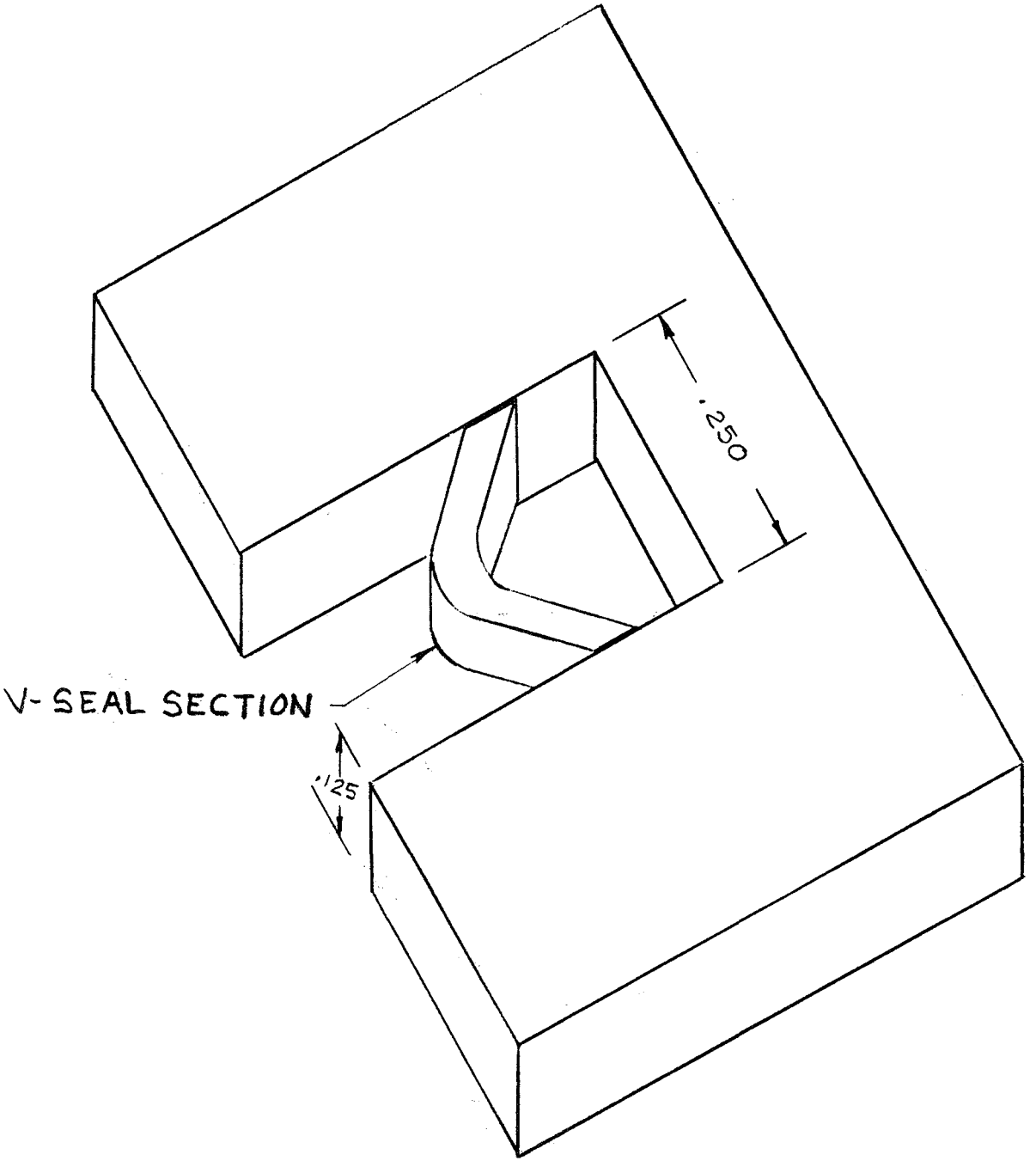

Figure 8. Simulated Gland Cavity

deflection of the inner leg would be limited because of the symmetrical design of the load ring. Consequently, in order to obtain further deflection of the inner leg, the axial load must be increased substantially, which results in over-stressing the outer leg. This latter condition was believed to be one of the causes of seal breakage experienced in the endurance test conducted in reference 1. Figure 9 shows that even under the best assembly conditions where perfect alignment of the seal components is achieved, deflection of the seal legs are limited due to insufficient clearance between the seal and backup ring.

2. Analysis of Operating Stresses of 45° V-Seal

Analysis of the V-seal was made to determine the operating stresses experienced by the seal during the endurance testing reported in reference 1. The primary stress producing conditions were the mechanical seal load, which was approximately 200 pounds (889.6 N); operating temperature of 500°F (260°C); and 100 psi (6.9×10^5 N/m^2) fluid pressure.

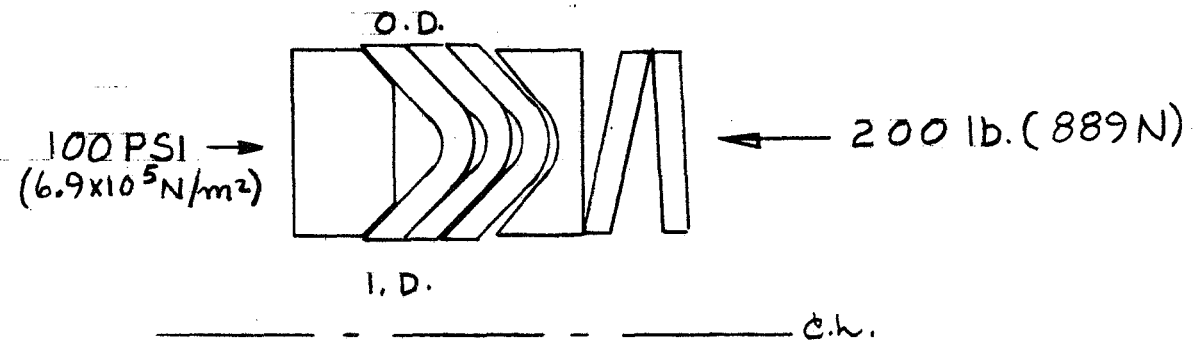

As shown by the installed configuration, the axial seal load of 200 pounds generated by the spring washers is split between the outer and inner legs of the "V". This load produces a radial seal force (P_R) on the inner and outer legs of the "V" which is assumed to be evenly distributed over the three seals. Therefore: for the inner leg, the radial load (P_R) is:

$$P_R = \frac{P}{2\pi r \times 3} = \frac{100}{2\pi \times 0.521 \times 3} = 10.6 \text{ pounds/inch of circumference } (1.86 \times 10^3 \text{ N/m of circumference})$$

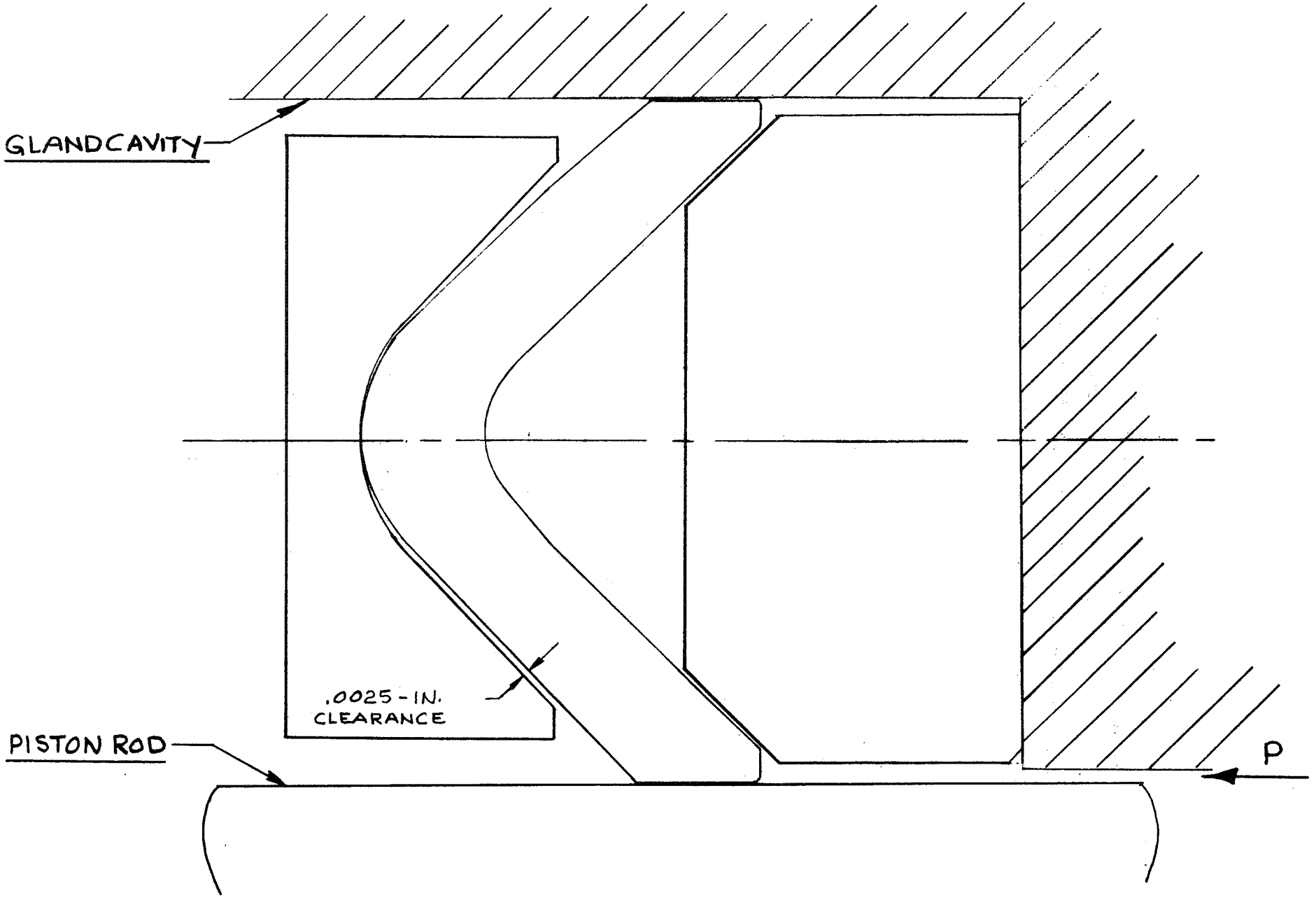

Figure 9. V-Seal Assembly - Matched Center Lines

The radial load on the outer leg is:

$$P_R = \frac{100}{2\pi \times 0.75 \times 3} = 7.1 \text{ pounds/inch of circumference}$$
(1243 N/m of circumference)

For purpose of this study, the V-seal was treated as a conical shell having the following characteristics:

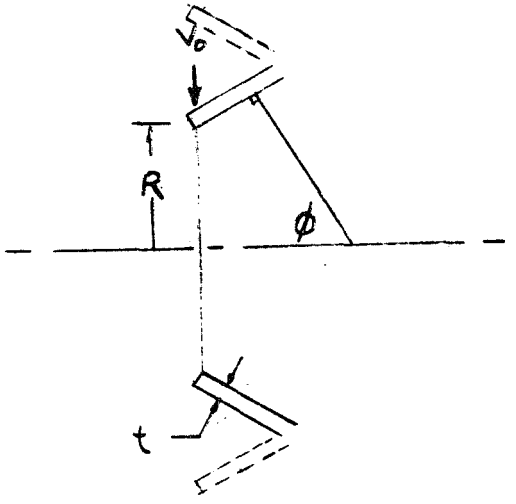

t	= 0.032 in. (0.082 cm)
R	= 0.521 in. (1.32 cm)
$V_o = P_R$	= 10.6 lb/in. - inner leg (1856 N/M)
$V_o = P_R$	= 7.1 lb/in. - outer leg (1243 N/m)
ϕ	= 45°
v	= 0.45 (Poisson's ratio)
E	= 450,000 psi @ R. T. (3.1×10^9 N/m^2)
E	= 250,000 psi @ 500° F (1.725×10^9 N/m^2)
S_{ty}	= 6,000 psi @ 500° F (4.136×10^7 N/m^2 @ 260° C)
S_{cy}	= approx 12,000 psi @ 500° F (8.264×10^7 N/m^2 @ 260° C)

Based on the geometry of the seal, the principal stresses consist primarily of hoop stresses. These are determined by the basic equation (ref. 2).

$$S_2 = \frac{-2\,V_o}{t} \lambda\, R \sqrt{\sin \phi} \quad \text{(at end)} \qquad (1)$$

where:

S_2 = Hoop membrane stress psi (N/m^2)

V_o = Radial load on seal (lb/in. (N/m) circumference)

t = Thickness of leg - in. (m)

$$\lambda = \sqrt[4]{\frac{3(1-v^2)}{R_2^{\,2}\, t^2}}$$

R = Mean radius - in. (m)

Rearranging terms, Equation (1) becomes

$$S_2 = \frac{-2\,V_o \sqrt[4]{3(1-\nu^2)} \times \sqrt{R} \times \sqrt{\sin\phi}}{t^{3/2}} \qquad (2)$$

Substituting the boundary conditions of the seal in Equation (2) the hoop membrane stress (S_2) on the inner leg is:

$$S_2 = \frac{-2(10.6) \sqrt[4]{3(1-(0.45)^2} \times \sqrt{0.521} \times \sqrt{0.707}}{(0.032)^{3/2}}$$

$$S_2 = \frac{-21.2 \times 1.242 \times 0.723 \times 0.842}{0.00573}$$

$$S_2 = -2790 \text{ psi (inner leg) } (-1.925 \times 10^7 \text{ N/m}^2)$$

The hoop membrane stress on the outer leg is:

$$S_2 = \frac{-2(7.1) \times 1.242 \times 0.867 \times 0.842}{0.00573}$$

$$S_2 = -2245 \text{ psi (outer leg) } (-1.55 \times 10^7 \text{ N/m}^2)$$

Radial deflection (R.D.) of the inner and outer legs of the "V" under the above conditions was determined by Equation (3).

$$\text{R.D.} = \frac{V_o}{2D\lambda^3} \times \sqrt{\sin\phi} \qquad (3)$$

where:

$$D = \frac{Et^3}{12(1-\nu^2)}; \quad \lambda = \sqrt[4]{\frac{3(1-\nu^2)}{R^2 t^2}}$$

Solving for D and λ and substituting in Equation (3), radial deflections are 0.0036-in. (0.0000914 m) and 0.0041-in. (0.000104 m) for the inner and outer legs, respectively, at room temperature. At the 500°F condition, the deflections are approximately 1.8 times greater because of the lower modulus of elasticity of the polyimide.

Superimposed on the hoop stresses are the stresses generated due to thermal expansion. These stresses were determined by assuming no external constraints on the seal legs. Thus, the dimensions the seal would assume under thermal expansion can be calculated. The thermal stresses are then determined by calculating the stresses required to force the seal legs back to their original dimensions.

Using a coefficient of thermal expansion of 27.5×10^{-6} in./in./°F (ref. 3) for the polyimide material, expansion of the inner diameter of the seal at 500°F (260°C) is:

$$27.5 \times 10^{-6} \times \Delta T \times L = 27.5 \times 10^{-6} \times 423 \times 1 = 0.0117 \text{ in. } (0.000297 \text{ m})$$

Expansion on the outer diameter is:

$$27.5 \times 10^{-6} \times 423 \times 1.5 = 0.017 \text{ in. } (0.000432 \text{ m})$$

Equivalent radial loads (V_o) induced by the thermal expansion can be determined by substituting the above values in Equation (3) and solving for V_o. Thus, the equivalent radial load (V_o) for the inner leg is:

$$V_o = \frac{2 \times (0.76)\,(9.65)^3 \times 0.0058}{0.842} = 9.4 \text{ pounds/inch } (1646 \text{ N/m})$$

For the outer leg:

$$V_o = \frac{2 \times (0.76) \times (8.1)^3 \times 0.0085}{0.842} = 8.15 \text{ pounds/inch } (1427 \text{ N/m})$$

Substituting the above values in Equation (1), the additional stresses (S_2') generated are:

$S_2' = 2480$ psi (1.710×10^7 N/m^2) on the inner leg and

$S_2' = 2575$ psi (1.775×10^7 N/m^2) for the outer leg

In addition to these stresses, a stress generated by the 100 psi (6.9×10^5 N/m^2) fluid pressure is also present. Equivalent hoop stresses generated by the 100 psi (6.895×10^5 N/m^2) pressure are determined as follows:

$$S_2'' = \frac{PR}{t} \times \cos \phi$$

$$S_2'' = \frac{100 \times 0.526 \times 0.866}{0.032} \qquad (4)$$

$$S_2'' = 1420 \text{ psi } (9.76 \times 10^6 \text{ N/m}^2) \text{ for the inner leg,}$$

and

$$S_2' = 2030 \text{ psi } (1.4 \times 10^7 \text{ N/m}^2) \text{ for the outer leg.}$$

Based on the foregoing analysis, the combined operating stresses

for the inner leg $= S_2 + S_2' + S_2''$

$= 2790 + 2480 + 1420 = 6690$ psi $(4.62 \times 10^7$ N/m$^2)$

and for the outer leg $= 2245 + 2575 + 2030 = 6850$ psi $(4.72 \times 10^7$ N/m$^2)$

Although the above stresses are primarily in compression, they are considered quite high as compared to an ultimate compressive stress of approximately 12,000 psi (8.264×10^7 N/m^2) at 500° F (260° C) for the polyimide material. Ultimate tensile strength of the polyimide is approximately 6000 psi (4.132×10^7 N/m^2) at 500° F (260° C). From this analysis it is believed that the main cause of seal failure in the endurance test conducted under Contract NAS3-7264 was due to the seals being overstressed. The analysis also shows that thermal stresses represent approximately 30% of the total stress. Because of the inherent characteristic of the material, reduction of the thermal stresses is difficult. The stress resulting from the working pressure is also a fixed parameter. However, it is believed that stresses induced by mechanical loading can be minimized through design.

The foregoing analysis is rather conservative as it assumes that the seal load exerted by the load ring is applied equally to the I. D. and O. D. surfaces of the seals and that the load is evenly distributed over the three sealing elements.

However, the analysis does illustrate the consequences of unequal loading, which is a more realistic condition as revealed by the geometry study. It should also be pointed out that the method of analysis was based on equations derived from classical formulas used in the stress analysis of materials whose behavior more closely follows Hooke's Law of stress-strain relationships. Consequently, the results obtained are considered approximations of actual conditions.

3. Thermal Effects on Polyimide

The dimensional stability and physical behavior of the polyimide at elevated temperatures were evaluated by subjecting the material to thermal cycling and high-temperature aging under confined and unconfined conditions. Accordingly, V-seals were fabricated and tested under the following conditions:

a. Confined in gland, spring loaded, and pressurized with silicone fluid.
b. Confined in gland, spring loaded, and in contact with air.
c. Unconfined, in contact with silicone fluid.
d. Unconfined, in contact with air.

As shown in Figure 10, the test assembly for the confined aging test consists of three V-seals, which were loaded with an approximately 200 pound (889 N) spring washer. This configuration, which is representative of the actual seal installation, enables the seals to be subjected to mechanical and thermal stresses. The test assembly for the unconfined aging test is shown in Figure 11. The seals in this configuration were permitted to expand and contract without restraints on their geometric shape.

The aging tests were run concurrently at 500° F (260° C) fluid/air temperature for 160 hours continuously, and the specimens were then allowed to cool to room temperature for inspection. This procedure was repeated until failure of the seals occurred or until completion of 1000 cumulative hours of soaking.

The initial test (Run No. 1) was terminated after 500 hours due to a malfunction in the oven heat controller, which caused the oven to overheat,

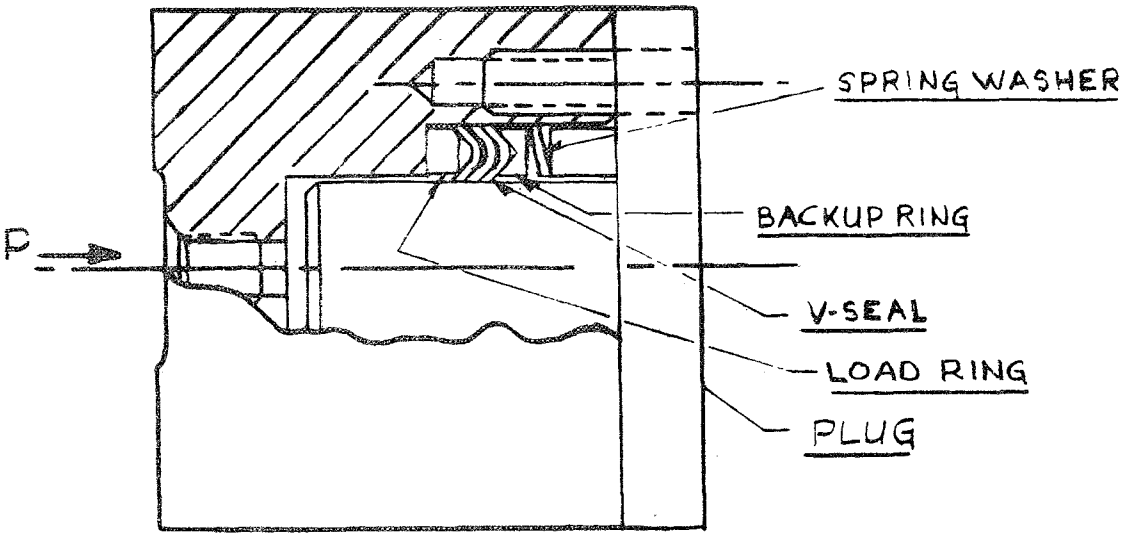

Figure 10. Confined Aging Assembly

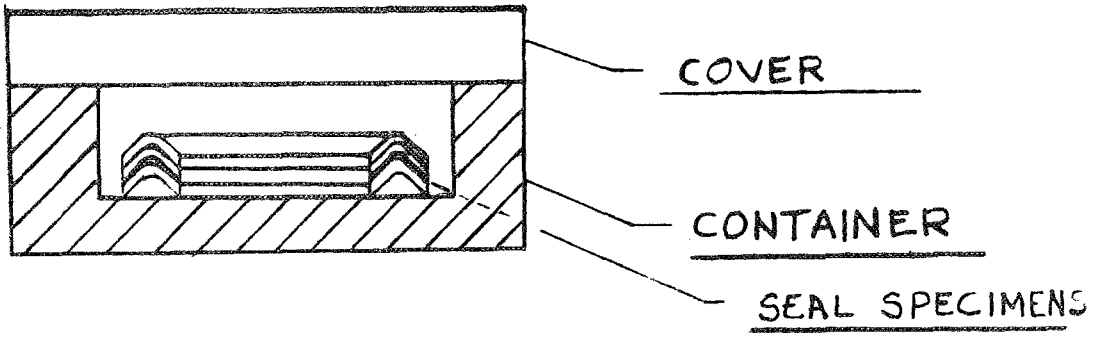

Figure 11. Unconfined Aging Assembly

resulting in the disintegration of the test specimens. At the time of shut-down, the temperature in the oven had risen from 500° F (normal operating) to 1300° F (705° C).

Although the specimens were destroyed in the test, significant data were obtained, which covered 416 hours of aging at 500° F (260° C). Table 1 shows the dimensional changes that occurred on the seal specimens during this period of aging. Figure 12 shows the dimensional changes on the inner and outer diameters of typical specimens for each test condition. These results show that the specimens experienced their greatest shrinkage after the first thermal cycle. Shrinkage was gradual after subsequent thermal cycling. As the polyimide material was annealed for two hours at 525° F, to relieve molding stresses prior to machining, the amount of shrinkage was greater than anticipated.

As shown in Figure 12, the confined and unconfined specimens which were in contact with F-50 fluid showed less decrease in their respective I. D. and O. D. dimensions as compared to those specimens in contact with air.

Due to the premature termination of the test, a rerun of the test was made. The oven equipment was repaired and a backup heat regulator installed in the temperature control circuit to provide fail-safe operation. This run successfully completed the 1000-hour test.

Based on visual inspection, the seals all appeared to be in good condition and showed no evidence of degradation. Loss of weight was experienced by the specimens during the aging. The greatest weight loss (Table 2) was experienced by those specimens exposed to an air atmosphere. These specimens showed weight loss of 0. 86-0. 96% and 1. 04-1. 17% for the unconfined and confined conditions, respectively. Weight losses exhibited by the specimens in contact with oil were 0. 65-0. 76% and 0. 63-0. 68%, for the unconfined and confined specimens.

TABLE 1. HIGH TEMPERATURE AGING TEST - RUN NO. 1

416 HOURS AT 500°F (260°C)

Seal No.	Test Condition	O.D. Dimensions					I.D. Dimensions				
		Orig.		Final			Orig.		Final		
		(in.)	(cm)	(in.)	(cm)	% Chge	(in.)	(cm)	(in.)	(cm)	% Chge
4	Unconfined, F-50 silicone fluid	1.504	3.820	1.5015	3.814	0.167	0.996	2.530	0.995	2.527	0.1
11		1.504	3.820	1.5015	3.814	0.167	0.9955	2.528	0.993	2.524	0.25
2	Unconfined, air atmosphere	1.504	3.82	1.499	3.807	0.33	0.998	2.534	0.995	2.527	0.3
9		1.5045	3.821	1.4995	3.808	0.33	0.998	2.534	0.993	2.522	0.5
3	Confined in gland, F-50 silicone fluid	1.505	3.822	1.493	3.792	0.8	0.995	2.527	0.991	2.517	0.4
6		1.505	3.822	1.491	3.787	0.93	0.995	2.527	0.991	2.517	0.4
7		1.504	3.82	1.492	3.789	0.8	0.995	2.527	0.991	2.517	0.4
1	Confined in gland, air atmosphere	1.5045	3.821	1.489	3.782	1.03	0.997	2.532	0.990	2.514	0.7
5		1.504	3.82	1.489	3.782	1.03	0.994	2.524	0.990	2.514	0.4
10		1.504	3.82	1.491	3.789	0.865	0.994	2.524	0.989	2.512	0.5

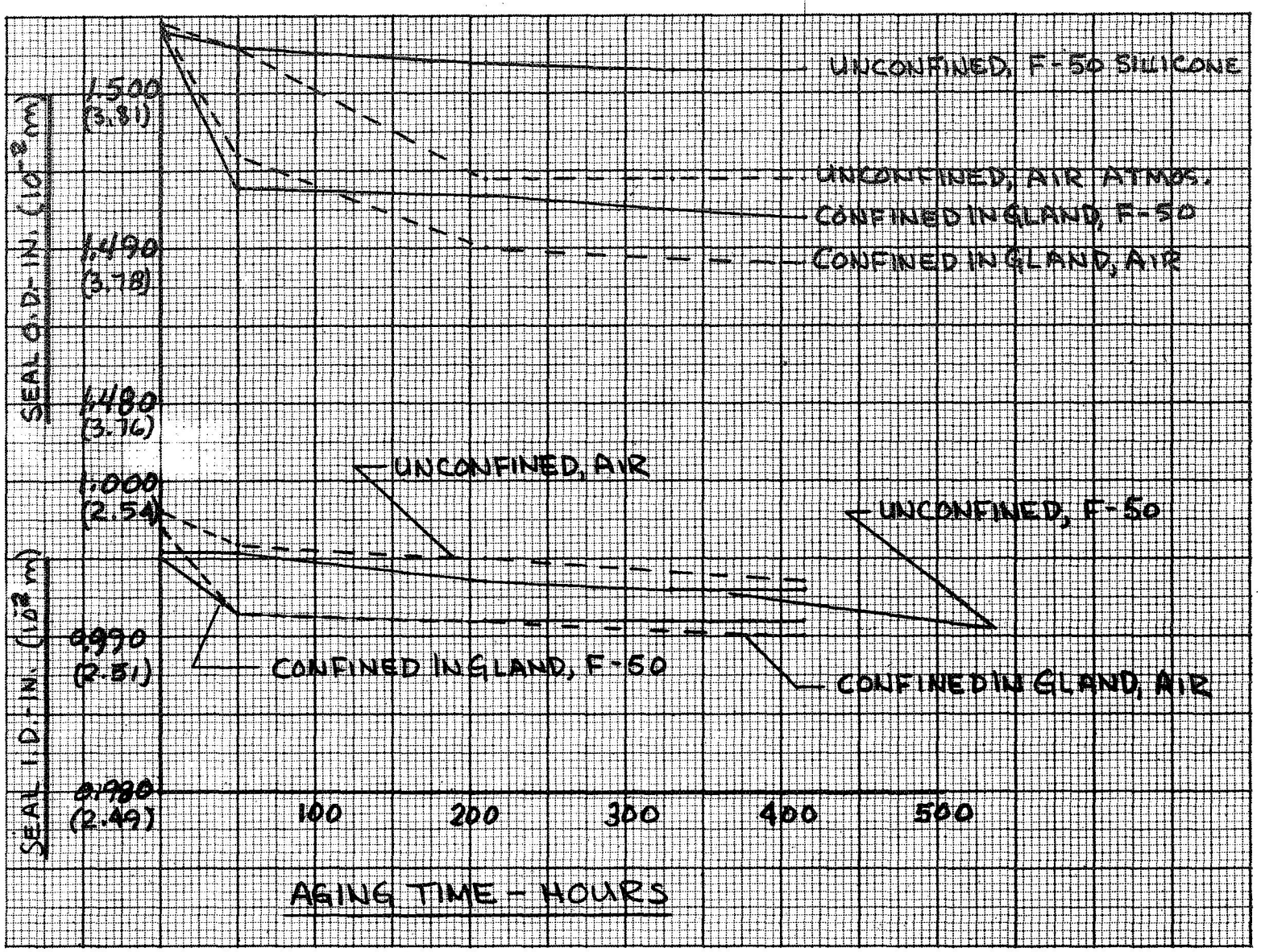

Figure 12. Seal Shrinkage vs Aging Time - Run No. 1, 416 Hours at 500°F (260°C)

TABLE 2. HIGH TEMPERATURE AGING TEST - RUN NO. 2, 1000 HOURS AT 500°F (260°C)

Seal No.	Test Condition	O.D. Dimensions					I.D. Dimensions					Wt Loss %
		Orig.		Final		% Chge	Orig.		Final		% Chge	
		(in.)	(cm)	(in.)	(cm)		(in.)	(cm)	(in.)	(cm)		
4	Unconfined, F-50 silicone fluid	1.504	3.820	1.5015	3.814	0.167	0.995	2.527	0.944	2.524	0.1	0.65
8		1.503	3.817	1.5005	3.811	0.23	0.995	2.527	0.944	2.524	0.1	0.76
2	Unconfined, air atmosphere	1.504	3.820	1.503	3.817	0.067	0.995	2.527	0.993	2.522	0.2	0.86
9		1.504	3.820	1.5015	3.814	0.167	0.995	2.527	0.994	2.524	0.1	0.96
3	Confined in gland, F-50 silicone fluid	1.504	3.820	1.491	3.789	0.86	0.995	2.527	0.9905	2.515	0.45	0.68
6		1.504	3.820	1.490	3.786	0.93	0.995	2.527	0.991	2.517	0.4	0.63
7		1.504	3.820	1.491	3.789	0.86	0.994	2.524	0.991	2.517	0.32	0.65
1	Confined in gland, air atmosphere	1.5035	3.818	1.4915	3.790	0.8	0.995	2.527	0.990	2.514	0.5	1.17
5		1.504	3.820	1.4925	3.793	0.76	0.995	2.527	0.9915	2.518	0.35	1.1
10		1.504	3.820	1.494	3.796	0.67	0.995	2.527	0.992	2.520	0.3	1.04

Seal measurements taken during inspection (Figure 13) show that dimensional shrinkage of the seals seems to follow the trend noted in the first run. The greatest amount of shrinkage occurred after the first thermal cycle and appears to be independent of time, as it was found that shrinkage for an initial heating period of 4 hours was approximately the same as that obtained for an initial heating period lasting 48 hours. As experienced in the first run, shrinkage after subsequent thermal cycling was gradual.

Variations in the inner and outer diameters of the seals (Table 2) after testing indicate that the unconfined specimens showed the least shrinkage. In the confined test condition, the specimens in contact with oil exhibited slightly greater shrinkage than those exposed to air. A possible explanation for the greater shrinkage is that these specimens were subjected to an additional unit load due to the pressure (100 psi) of the fluid in the test unit.

The greater dimensional shrinkage experienced by the confined specimens is believed to be due to plastic deformation of the material caused by thermal stresses and stresses resulting from the springload on the seal. As shown below, differential expansion between the seal and gland housing causes a substantial compressive stress on the seal resulting in permanent deformation of the seal.

Stresses developed on the O.D. of the seal due to the differential thermal expansion at 500°F (260°C) are as follows:

$$\Delta L \text{ (polyimide)} = 27.5 \times 10^{-6} \times 427 \times 1.504 = 0.0176 \text{ in. } (0.0447 \text{ cm})$$

$$\Delta L \text{ (gland)} = 7 \times 10^{-6} \times 427 \times 1.500 = 0.0045 \text{ in. } (0.0114 \text{ cm})$$

Therefore: seal O.D. at 500°F becomes 1.504 + 0.0176 = 1.5216 in. (3.865 cm) and gland I.D. at 500°F becomes 1.500 + 0.0045 = 1.5045 in. (3.820 cm). The seal-to-gland interference is: 1.5216 - 1.5045 = 0.0171 in. (0.0434 cm), therefore:

$$\text{Strain} = \frac{\Delta L}{L} = \frac{0.017}{1.522} = 0.0112 \text{ or } 1.1\%$$

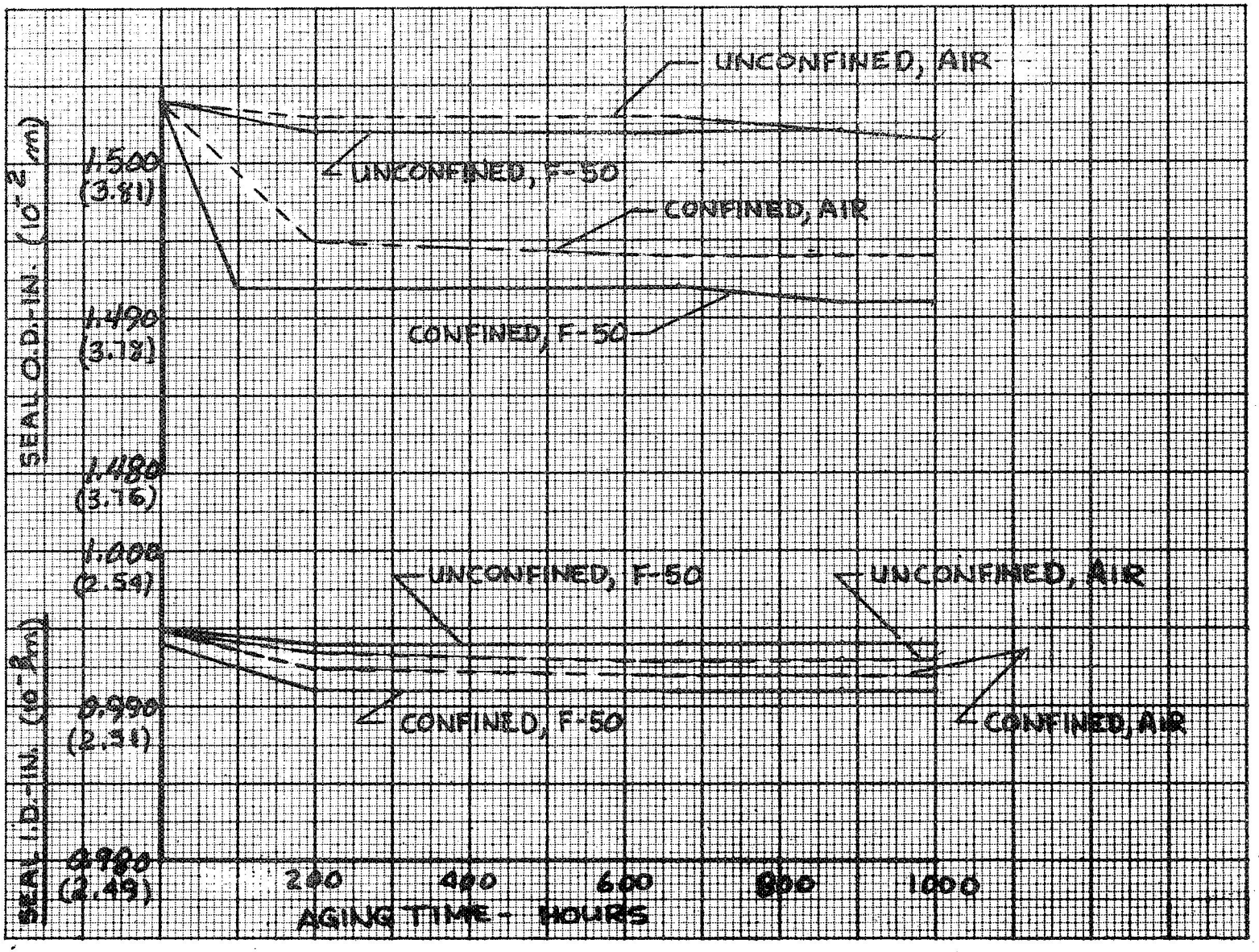

Figure 13. Seal Shrinkage vs Aging Time - Run No. 2, 1000 Hours at 500°F (260°C)

The 1.1% strain represents a stress level of approximately 3000 psi (2.068×10^7 N/m^2) (Reference 3) at 500°F (260°C), which could be high enough to induce permanent deformation of the material. Based on this analysis, a similar condition exists on the I.D. of the seal.

The foregoing results indicate that the polyimide material is capable of withstanding at least 1000 hours at 500°F (260°C). Although dimensional shrinkage due to plastic flow appears to be an inherent characteristic of the material, it is believed that the shrinkage can be minimized to some extent by decreasing the seal load. The weight loss exhibited by the specimens was negligible and could be attributable to the evaporation of the moisture content of the material.

4. Fabrication Methods

The selection of fabrication techniques is based on the geometry of the part and the need for maximum utilization of the material's properties. Three possible methods of fabricating polyimide seals are 1) stamping from rolled sheets, 2) machining from billets, and 3) direct forming (molding). There are, however, certain limitations to each of these basic techniques.

For example, the rolled sheets exhibit higher tensile and elongation properties (Table 3) but the sheets are limited in thickness to approximately 0.070 inch (0.15 cm), which restricts their application to a limited number of seal shapes.

TABLE 3. ROOM TEMPERATURE PROPERTIES OF POLYIMIDE

Type	Tensile Strength	Elongation (Percent)	Specific Gravity (gm/cc)
Rolled Sheet	17,000 psi (11.7×10^7 N/m^2)	12	1.43
Machined Parts (Billets)	12,000 psi (8.27×10^7 N/m^2)	8	1.43
Direct-Formed Parts	10,000 psi (7.24×10^7 N/m^2)	6.5	1.43

The direct formed (molded) parts have a lower specific gravity and accompanying lower strength and elongation (Table 3). For complex shapes, such as the V-seal, densities lower than those shown in Table 3 could result, particularly at the transition section of the "V". Because of the close tolerances usually required for seals, final machining of the formed part would be necessary. In general, direct forming probably provides the most efficient use of the polyimide material and for large quantities, direct forming of parts could result in the lowest cost. However, it is felt that at the present time, the techniques for the direct forming of parts such as the V-seal would require further development.

Machining of seals from molded polyimide billets appears to be the most attractive method at the present time. To obtain the best balance of properties, the part to be machined should be oriented so that the higher tensile properties of the polyimide (perpendicular to the direction of molding) are utilized. In machining, a good surface finish on the part is essential to minimizing stress concentrations, as the polyimide is quite notch sensitive.

As part of the study on fabrication methods for polyimide seals, a modified annealing process was investigated. This method consists of initially machining a piece of polyimide material into a hollow cylindrical shape, 2 inches long by 1.6 inches O.D. by 0.95 inch I.D. (5.08 cm x 4.06 cm x 2.41 cm), and annealing it for two hours at 600°F (316°C). Following this annealing period, "V" shaped specimens were rough machined from the material and annealed for an additional hour at 600°F (316°C), prior to final machining.

A short-term aging test at 500°F (260°C), was conducted with the finished specimens to determine if the double annealing cycle produced any improvements in dimensional stability. A dimensional check of the seals after 200 hours of aging showed a considerable reduction in shrinkage on the seal O.D. These results (Table 4) are compared with those obtained on seals aged for the same length of time during Run No. 2. Although the data were obtained over a short aging period, it is believed that the double annealing cycle could improve the dimensional stability of the polyimide seals. As indicated in previous aging tests, the bulk of the shrinkage usually occurs during the first few hours at

temperature. Therefore, it is believed that the shrinkage exhibited by the double annealed specimens after 200 hours of aging represents the bulk of the change.

TABLE 4. V-SEAL AGING TEST - 200 HOURS AT 500° F (260° C)

Seal No.	Test Condition	O. D. Change - %		I. D. Change - %	
		Run No. 2	Run No. 3	Run No. 2	Run No. 3
3	Confined in gland;	0.8	0.27	0.5	0.3
6	200 lb spring load,	0.83	0.47	0.5	0.5
7	F-50 silicone fluid	0.8	0.47	0.3	0.4

Note:

Run No. 2 - Material annealed 2 hours at 600° F (316° C) prior to machining

Run No. 3 - Material annealed 2 hours at 600° F (316° C), rough machined, and annealed 1 hour at 600° F (316° C) before final machining

C. DESIGN STUDY

The foregoing analyses and investigations indicate that the following modifications to the original V-seal were required:

- Redesign the seal to operate at a lower stress level
- Redesign the loading device to permit asymmetrical loading of the seal
- Redesign the backup ring to ensure adequate clearance between it and the seal
- More accurate machining of the seal to ensure dimensional compatibility with its mating members
- Revise annealing schedule to improve dimensional stability of the polyimide.

1. Redesign of Original V-Seal

From a stress standpoint, redesign of the 45° V-seal was based on the following critical conditions which the seal undergoes in its operating environment.

a) The O. D. surface of the seal (Figure 14) expands and contracts at a greater rate than the gland housing during heating and cooling. High thermal stresses induced during expansion cause plastic deformation of the material resulting in shrinkage of the O. D. surface. During cooling, the O. D. surface of the seal tends to contract away from the gland, resulting in loss of seal contact. This condition becomes progressively worse during the life of the seal because of shrinkage.

b) The same differential expansion and contraction is experienced on the I. D. surface of the seal but with opposite effects. On heating (see Figure 15), the I. D. surface tends to expand away from the piston rod, resulting in loss of sealing contact between the two surfaces. During cooling, the I. D. surface tends to contract against the piston rod. This condition induces high thermal stresses in the material causing plastic deformation, which results in a reduction of the inner diameter.

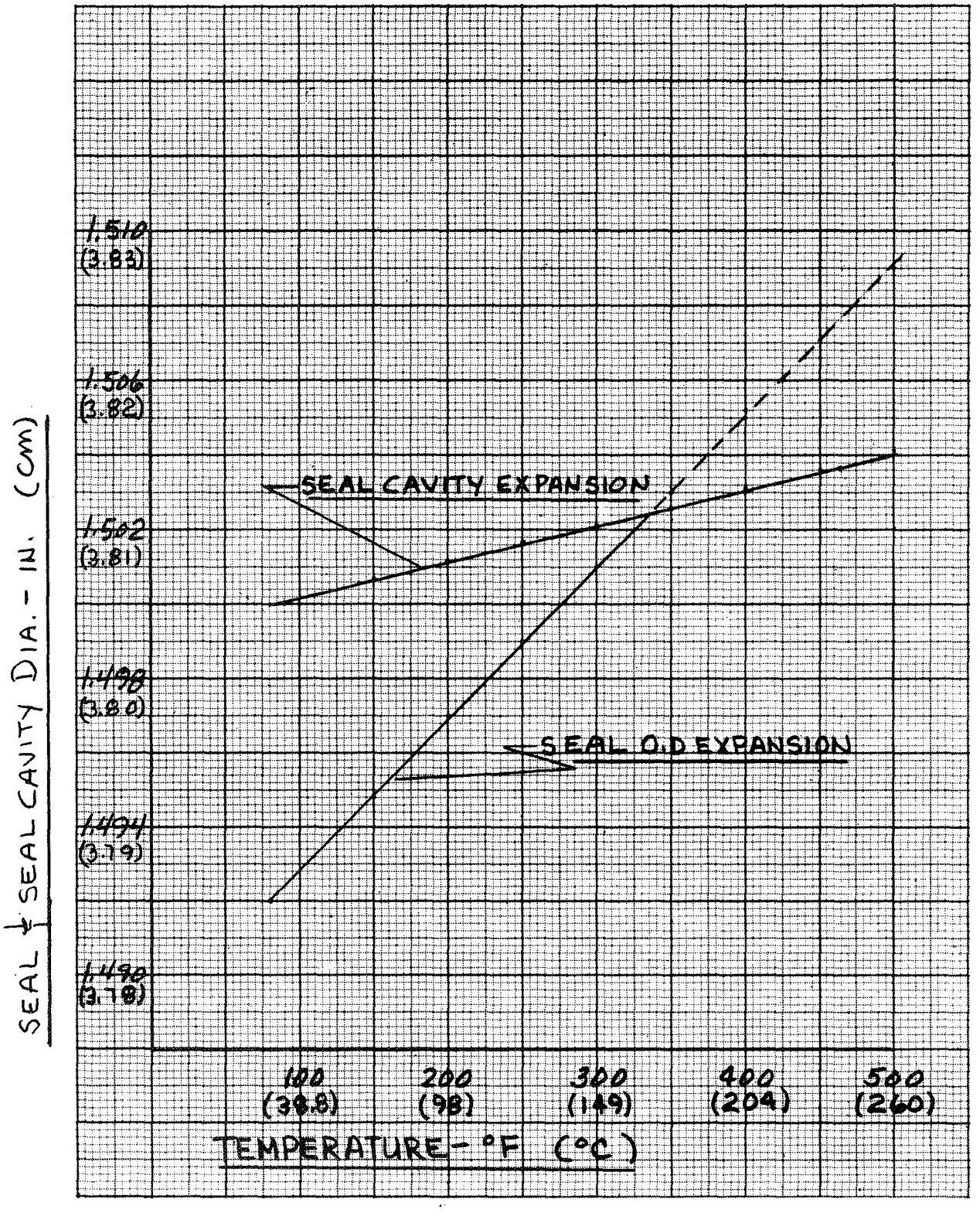

Figure 14. Differential Expansion between V-Seal O. D. and Seal Cavity

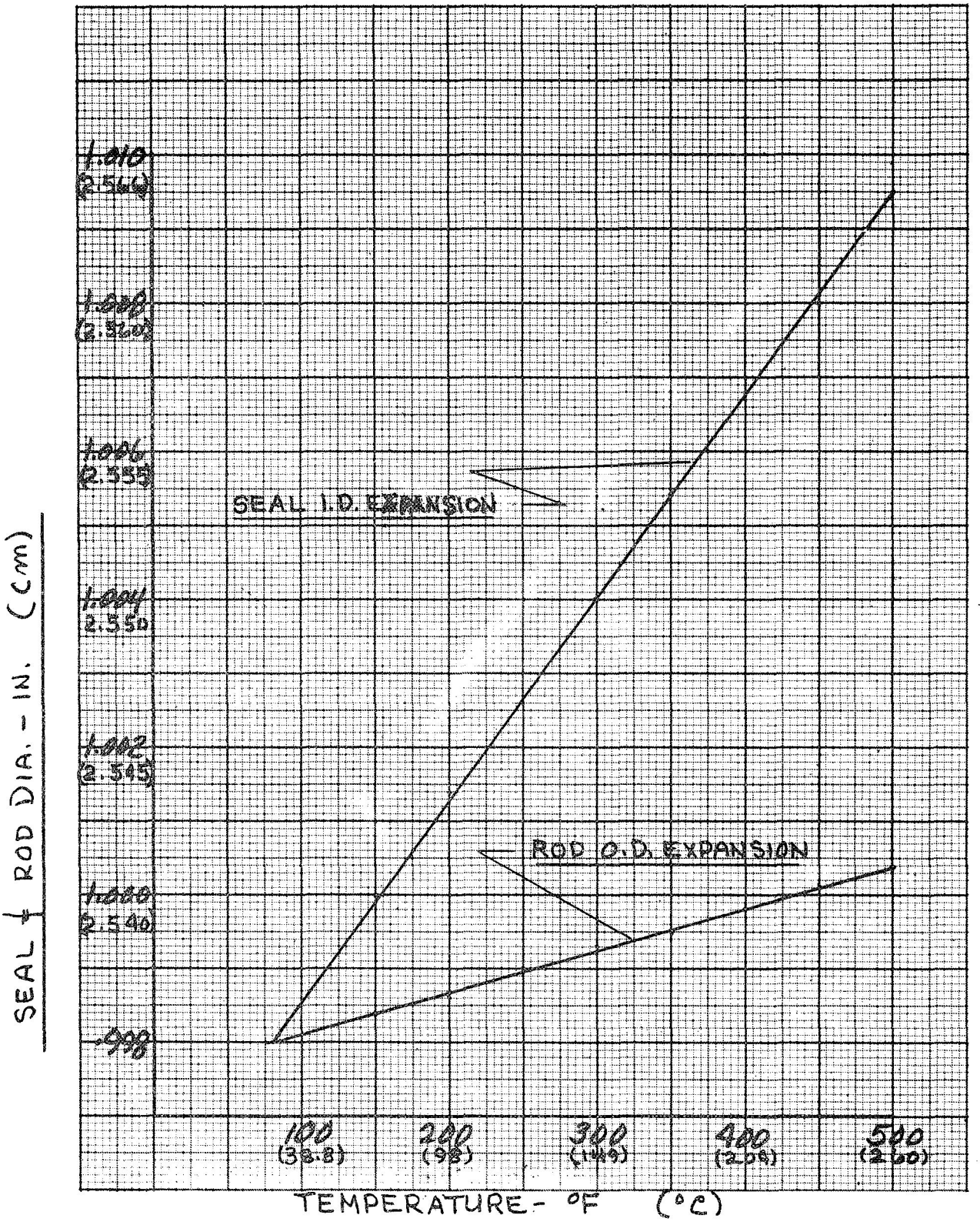

Figure 15. Differential Expansion between V-Seal and Piston Rod

From the above, it is evident that for condition a), a seal load of sufficient magnitude is required to prevent the O. D. surface of the seal from losing contact with the gland bore during cooling. For condition b), a seal load is required to restrain the seal from expanding away from the piston rod in order to maintain an effective seal at this interface. Based on the thermal aging test (Table 2), a seal O. D. deflection of approximately 0. 010 inch (0. 0254 cm) is necessary to compensate for shrinkage. A deflection of approximately 0. 009 inch (0. 0228 cm) of the seal I. D. is required to offset the differential expansion between the seal and piston rod at 500°F (260°C).

The seal loads required to meet the foregoing conditions represent the principal stresses imposed on the seal.

A model of the V-seal is depicted below; a seal leg angle of 30° was selected, as this provides longer legs for greater flexibility. Data relevant to the design of the seal are listed below:

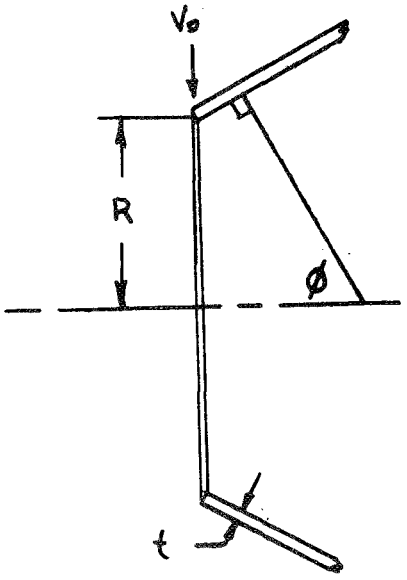

Seal material - polyimide

Tensile yield strength at 600°F - 6000 psi

Modulus of elasticity at 500°F - 250,000 psi

Modulus of elasticity at room temperature - 450,000 psi

Seal leg angle - 30°

Required seal O. D. deflection - 0.010-in.

Required seal I. D. deflection - 0.009-in.

Allowable hoop stress - 2000 psi

Poisson's ratio (ν) - 0.45

Coefficient of thermal expansion (α) - 27.5×10^{-6} in./in./°F

As a first step in redesigning the V-seal to meet the above requirement, the cross-sectional dimension of the seal was determined. Rearranging eq. (2) and substituting appropriate values for each term, the cross-sectional thickness of the seal was obtained in terms of seal load (V_o).

For the I. D. :

$$t = \left(\frac{-2V_o \sqrt[4]{3(1-\nu^2)} \times \sqrt{R} \times \sqrt{\sin\phi}}{S_2} \right)^{2/3}$$

$$t = \left(\frac{-2V_o \times 1.242 \times 0.72 \times 0.932}{2000} \right)^{2/3}$$

$$t = (0.000834\ V_o)^{2/3}$$

and, for the O. D. :

$$t = \left(\frac{-2V_o \times 1.242 \times 0.86 \times 0.932}{2000} \right)^{2/3}$$

$$t = (0.000995\ V_o)^{2/3}$$

Figure 16 depicts seal cross-sectional thickness as a function of seal load (V_o) at a stress level of 2000 psi (1.38×10^7 N/m^2). From this plot,

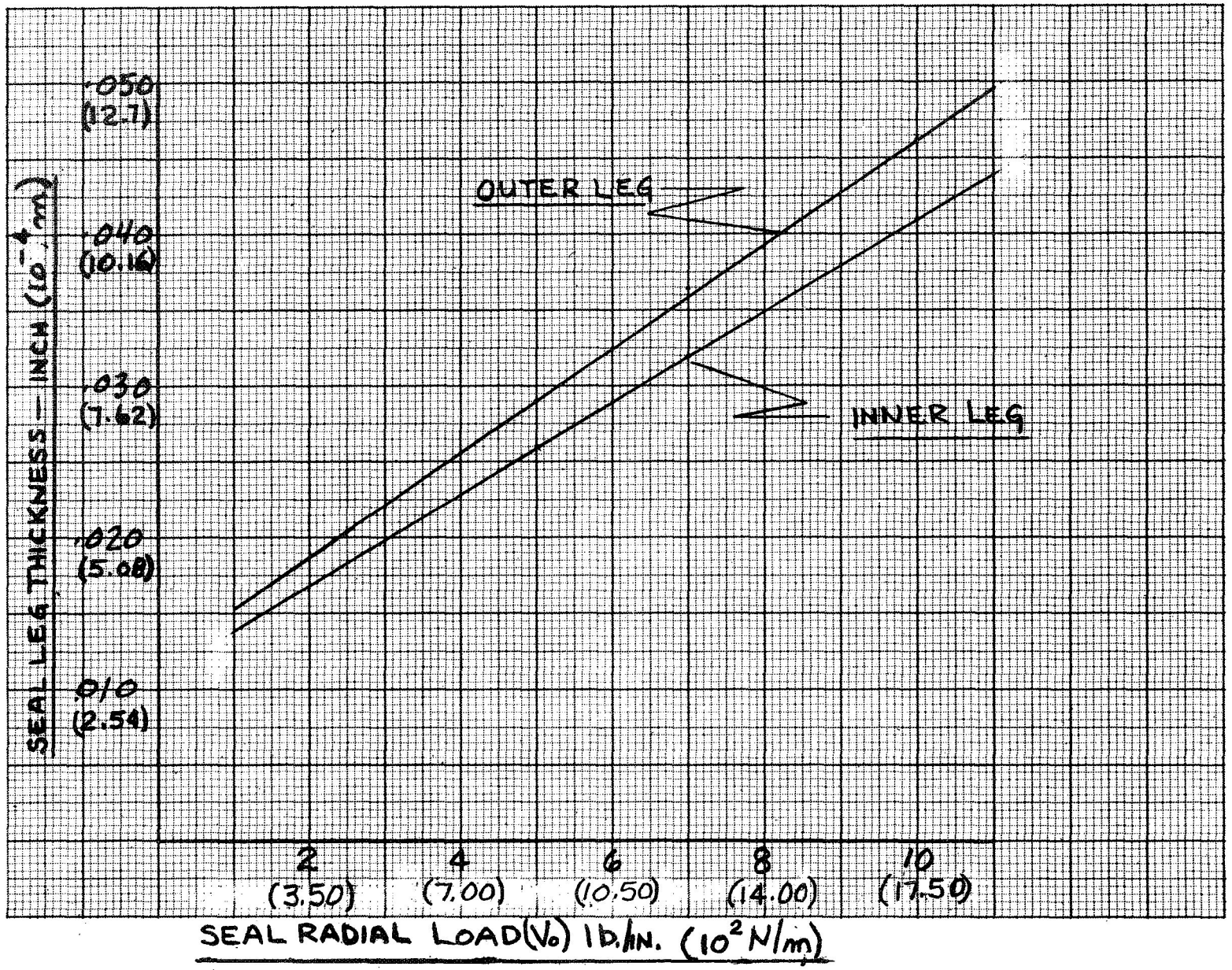

Figure 16. Seal Leg Thickness vs Seal Radial Load (Hoop Stress 2000 psi)

a nominal seal thickness of 0.032 inch (0.0812 cm) was selected, as this would facilitate manufacturing. Corresponding to this thickness, the seal load (V_o) is 7 and 6 pounds per inch (1226 and 1051 N/m) of circumference for the inner and outer legs, respectively. Substituting these values in eq. (3) yields the following deflections required for the I. D. and O. D. of the seal at the critical conditions previously stated.

Therefore, the radial deflection (R. D.) of seal I. D. at 500°F (260°C) becomes:

$$\text{R. D.} = \frac{-V_o}{2D\lambda^3} \times \sqrt{\sin\phi} \qquad (3)$$

R. D. = - 0.0048 inch (0.0122 cm)

and the radial deflection of seal O. D. at room temperature becomes:

$$\text{R. D.} = \frac{-6}{2.72 \times 414} \times 0.932$$

R. D. = - 0.005 inch (0.0127 cm)

These values satisfy the required deflection characteristics of the seal at both temperature extremes within the allowable working stress of the polyimide. The axial spring load required to produce the necessary circumferential seal load to provide the required deflections at the I. D. and O. D. of the seal was determined as follows:

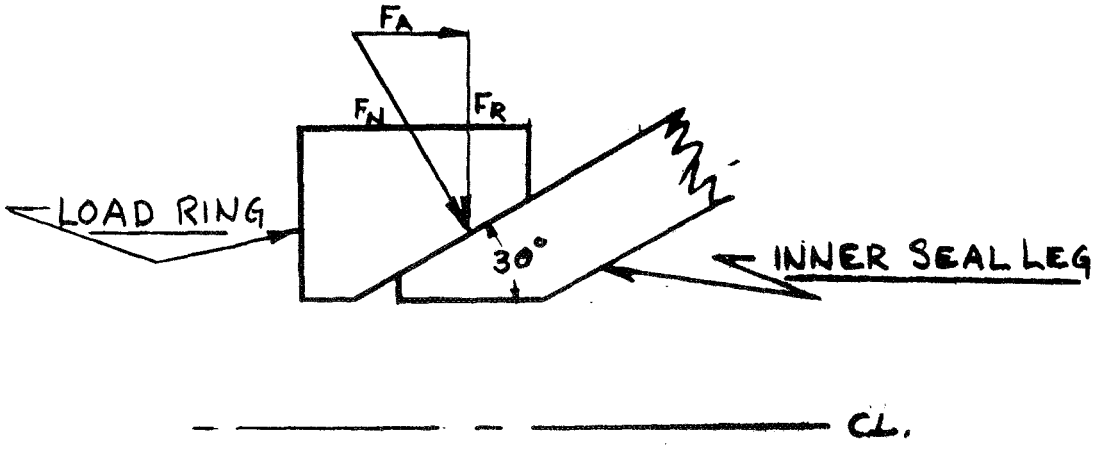

The axial load is found by

$$F_A = F_N (\sin\alpha + \mu \cos\alpha) \tag{5}$$

where:

$$F_N = \frac{P}{(\cos\alpha - \mu \sin\alpha)} \tag{6}$$

The circumferential load (P) is found by:

$$P = F_R \times 2\pi r \tag{7}$$

The circumferential load (P) for the I. D. surface of the seal is:

$$P = 7 \times 2 \times \pi \times 0.516 = 22.6 \text{ pounds (101N) per seal}$$

For the O. D. surface of the seal:

$$P = 6 \times 2\pi \times 0.734 = 27.6 \text{ pounds (123N) per seal}$$

Substituting these values for (P) in eq. (6) yields:

$$F_N = \frac{22.6}{(0.866 - (0.15 \times 0.500))}$$

F_N = 28.6 pounds (127N) for I. D. surface

F_N = 35 pounds (156N) for O. D. surface

Thus, from eq. (5) the axial load is:

$$F_A = 28.6\ (0.500 + (0.15 \times 0.866))$$

F_A = 18 pounds (80.1N) for I. D. surface

F_A = 22 pounds (97.9N) for O. D. surface

Since there are three seals per assembly, the axial load is multiplied by three and becomes 54 pounds (240N) and 66 pounds (294N) for the I. D. and O. D. surfaces, respectively.

Based on the foregoing analysis, it can be seen that the loads required to deflect the I. D. and O. D. of the seal vary considerably.

Consequently, the one-piece load ring used in the 45° V-seal configuration was redesigned to provide a dual load path so that independent loading of the sealing surfaces can be achieved. The backup ring was also redesigned to provide sufficient clearance between it and the seal to ensure full deflection of the seal. Figure 17 depicts the complete seal assembly, which was designated Design B-1. As shown in the assembly, the modified load ring permits asymmetrical loading of the seal. Upon initial application of the axial load, the inner load ring makes contact with the inner seal leg; as the inner load ring is spring-loaded, it moves inward while maintaining a predetermined load on the seal, thus permitting the outer loading surface to make contact with the outer seal leg.

An alternate seal design, identified as Design HB-1, was developed which also offers improvements over the original 45° V-seal design. As shown in Figure 18, the seal is configured with linearly tapered legs, which minimize the bending stresses at the transition area of the leg. Because of the reduced thickness at the sealing portion of the leg, a leg deflection (radially) of 0.0025 inch (0.00635 cm) at a seal load of 4.5 pounds per inch (788 N/m) of seal circumference was obtained. At these conditions, a maximum bending stress (at maximum seal deflection) of approximately 1500 psi (1.034×10^7 N/m^2) is generated, which occurs between the fixed end and the sealing end of the leg. This stress level is well within the strength limits of the polyimide material. The lower seal loading also reduces the contact stresses and sliding friction at the seal interface.

Analysis of this seal configuration was based on the same method used in analyzing the 30° V-seal, except that values for "t" (cross-sectional thickness) were based on the average thickness of the seal leg.

2. Additional Seal Designs

Five additional seal designs were evolved that offered potential improvements over the original 45° V-seal. In these designs, attempts were made to establish a good balance in operating stresses, wear compensation, and friction.

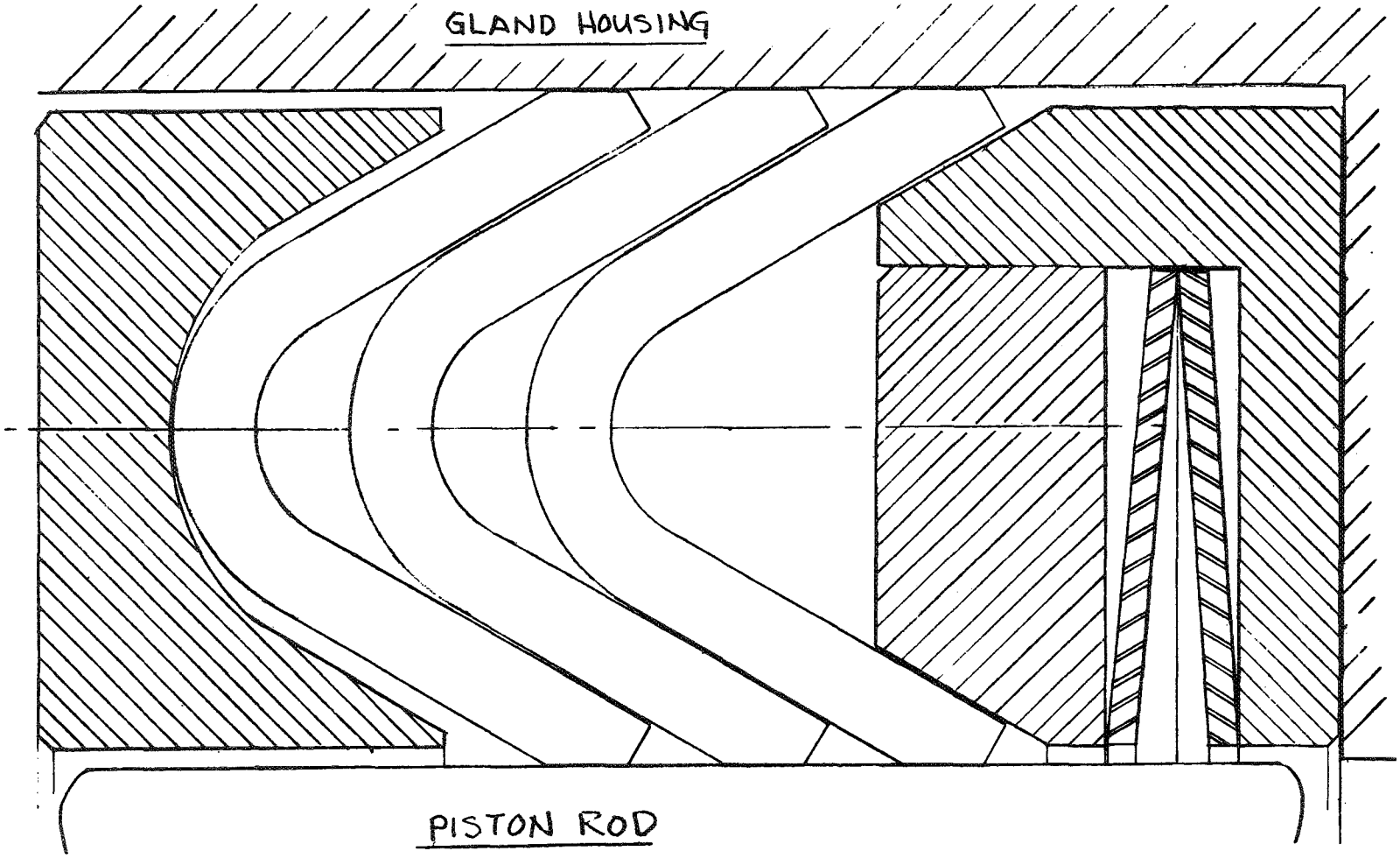

Figure 17. Modified V-Seal Assembly - 30° Leg Angle (Design B-1)

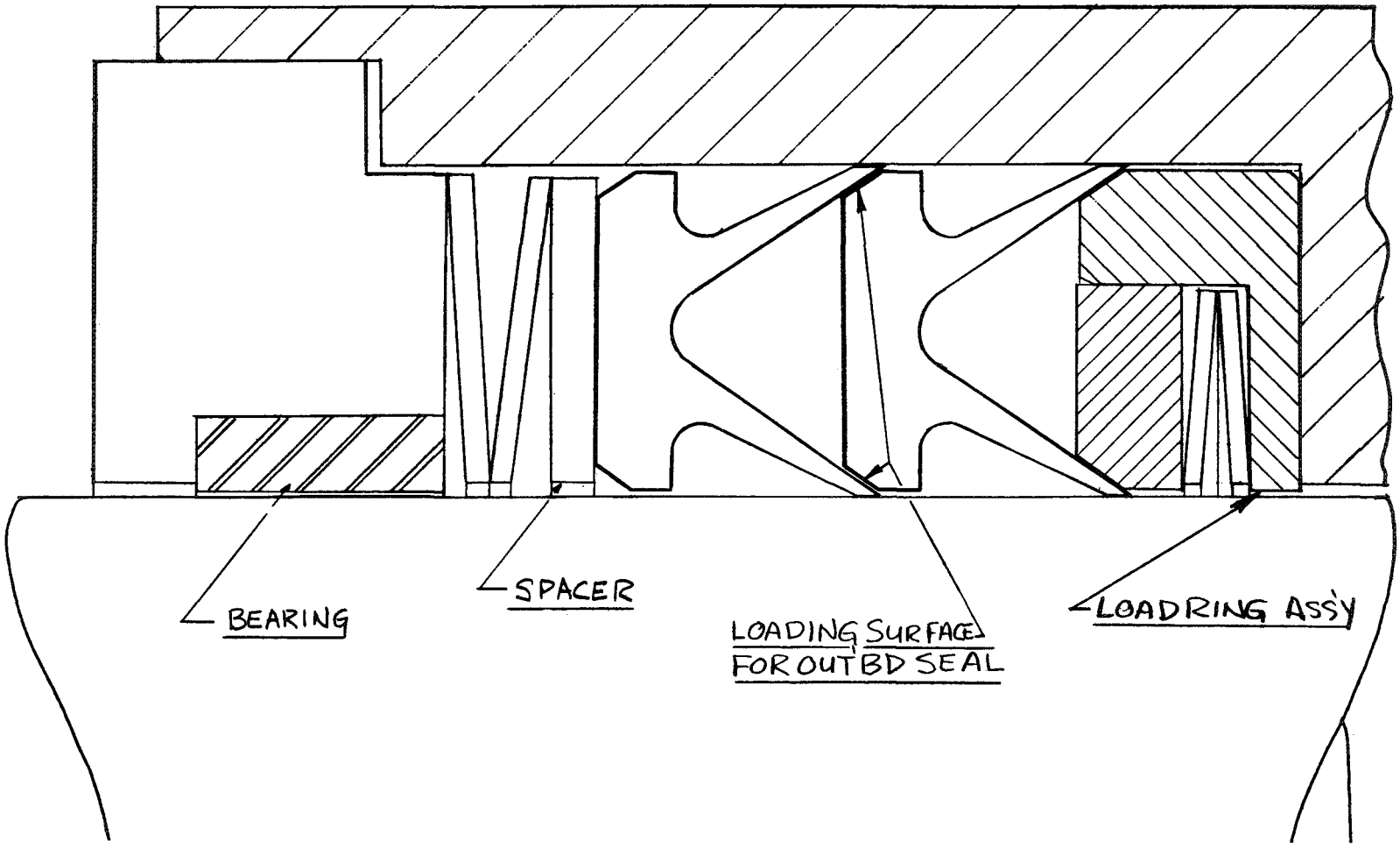

Figure 18. Tapered Leg V-Seal Assembly (Design HB-1)

The "U" shaped seal (Design C-1), shown in Figure 19, is similar in design to the 30° V-seal except that the lower angle (14°) results in longer seal legs, which tends to increase the flexibility of the seal. The seal is designed to provide a deflection of 0.0028 inch (0.0071 cm) with a load of 7 pounds per inch (1226 N/m). This configuration also utilizes the dual arrangement for more efficient seal loading.

Figure 20 depicts a wedge loaded lip seal (Design D), wherein the sealing zone of the lip is confined in a tapered seat by axial forces generated by spring washers. The spring load assures contact between the seal and piston rod. As wear occurs, the springs urge the sealing lip further into the tapered seat to maintain contact with the rod surface. This seal is designed for a maximum wear compensation of 0.015 inch (0.038 cm). However, this was achieved at a fairly high stress level of 4000 psi (2.76×10^7 N/m^2).

Figure 21 depicts a polyimide lip seal (Design E) which is reinforced with a high strength steel (H-11 type) outer lip. The reinforcing lip also acts as a hoop spring to provide the initial seal contact load and also serves as a wear compensating device. The spring is designed to provide a uniform circumferential load of 3 pounds (13.34 N), which is capable of producing a seal deflection of 0.006 inch (0.0152 cm). As shown in Figure 21, the seal is also pressure loaded, which augments the spring load.

Shown in Figure 22 is Design F, which is another modification of the original V-seal design. The "V" is configured to an included angle of approximately 135°. The wide angle results in a uniform seal section and provides a smooth transition from one surface to another to minimize stress concentrations and bending moment.

The conical lip seal (Design G) shown in Figure 23, is designed to utilize the slightly higher tensile properties of the polyimide sheet material. Sealing is accomplished by an initial interference fit over the piston rod. Using the polyimide sheet material, a high enough preload (interference) could be generated to provide seal contact throughout the entire operating temperature range. Testing of a similar design during the previous contract work (ref. 1) produced promising results at low and high pressures.

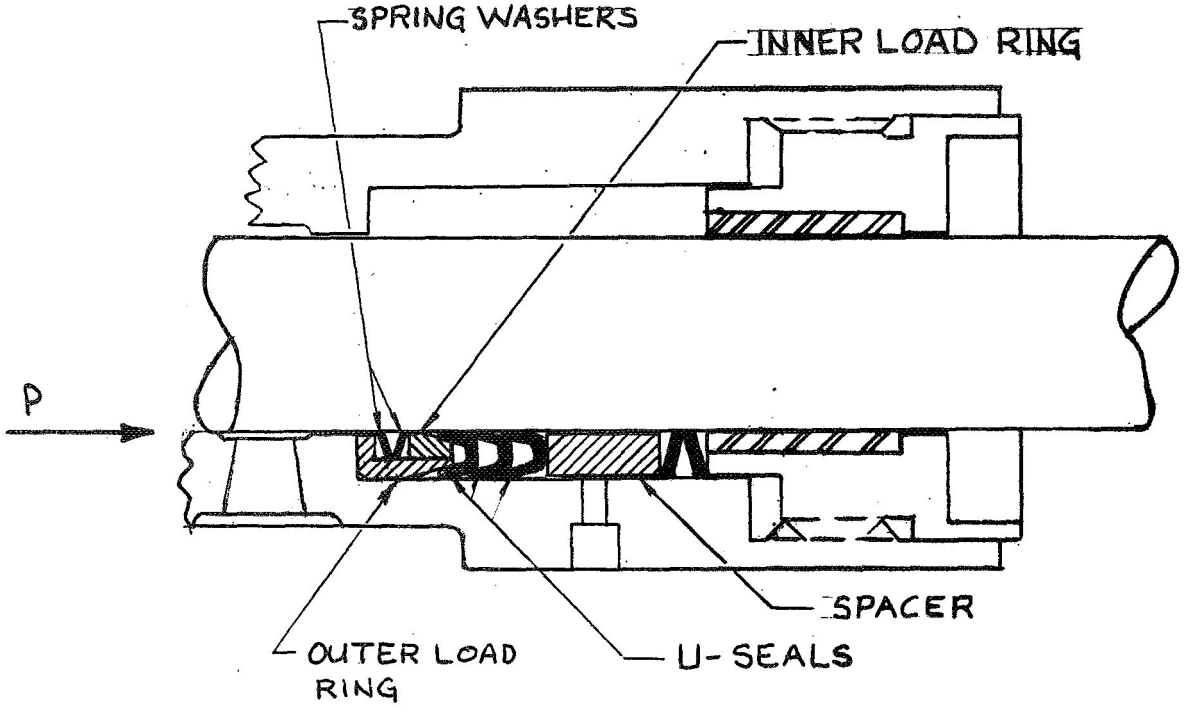

Figure 19. U-Seal with Dual Load Ring
(Design C-1)

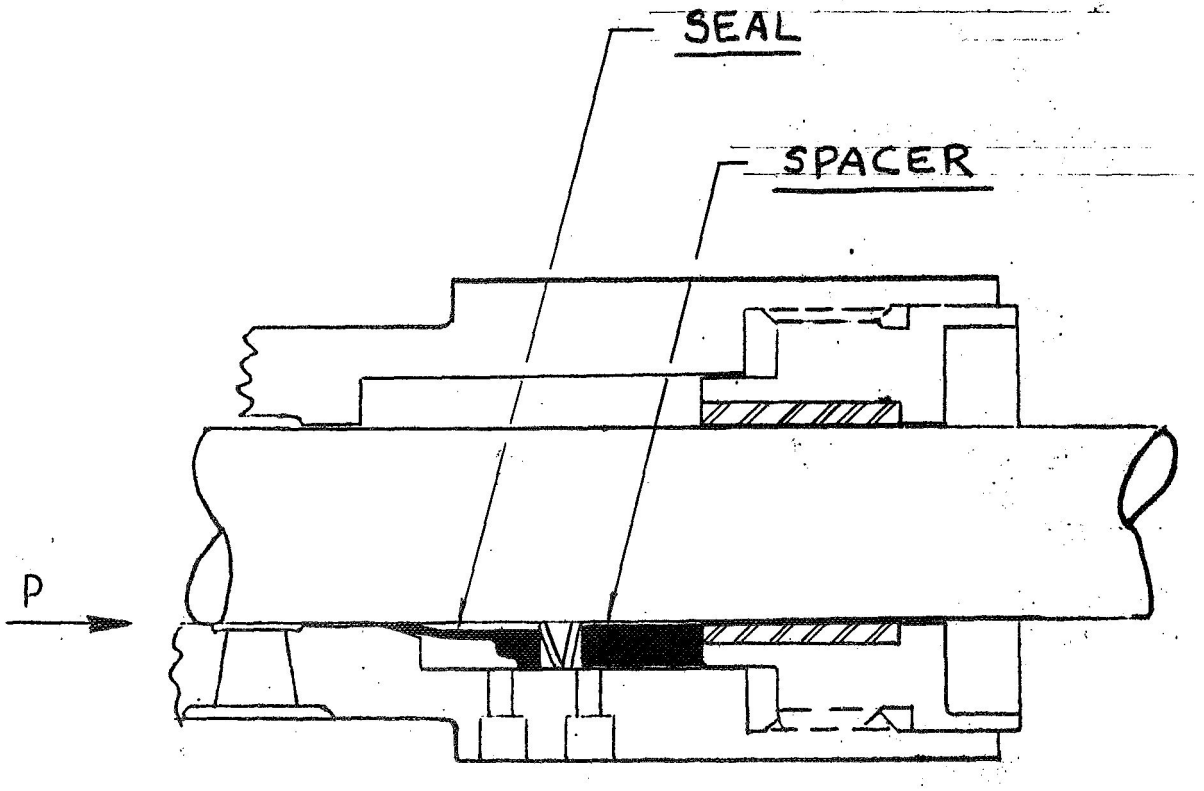

Figure 20. Wedge Loaded Lip Seal
(Design D)

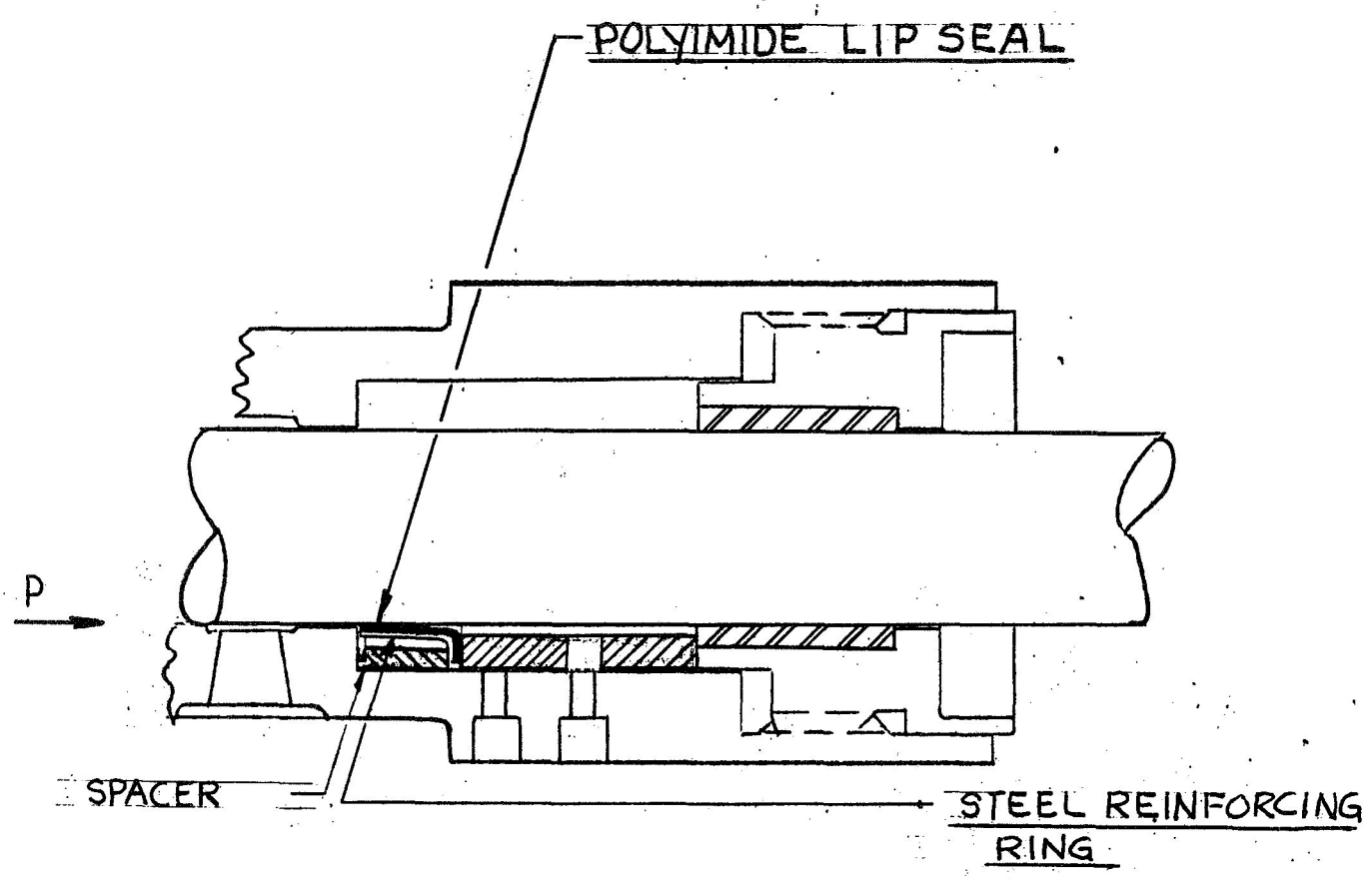

Figure 21. Spring Loaded Lip Seal
(Design E)

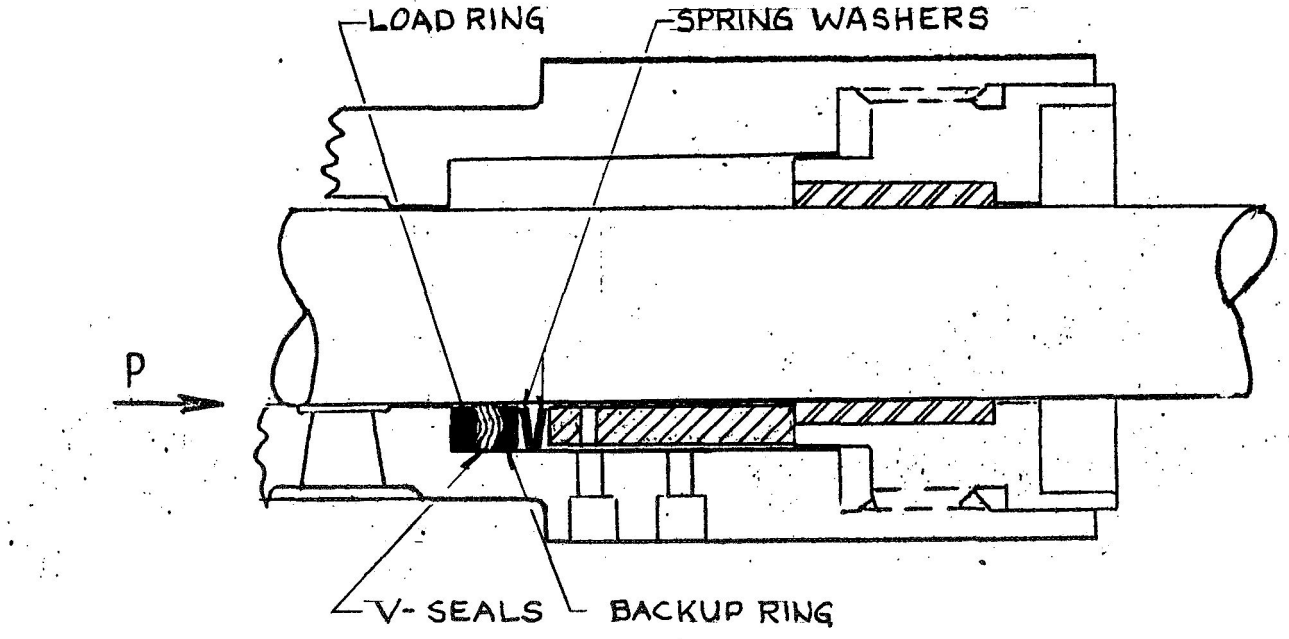

Figure 22. Wide Angle V-Seal
(Design F)

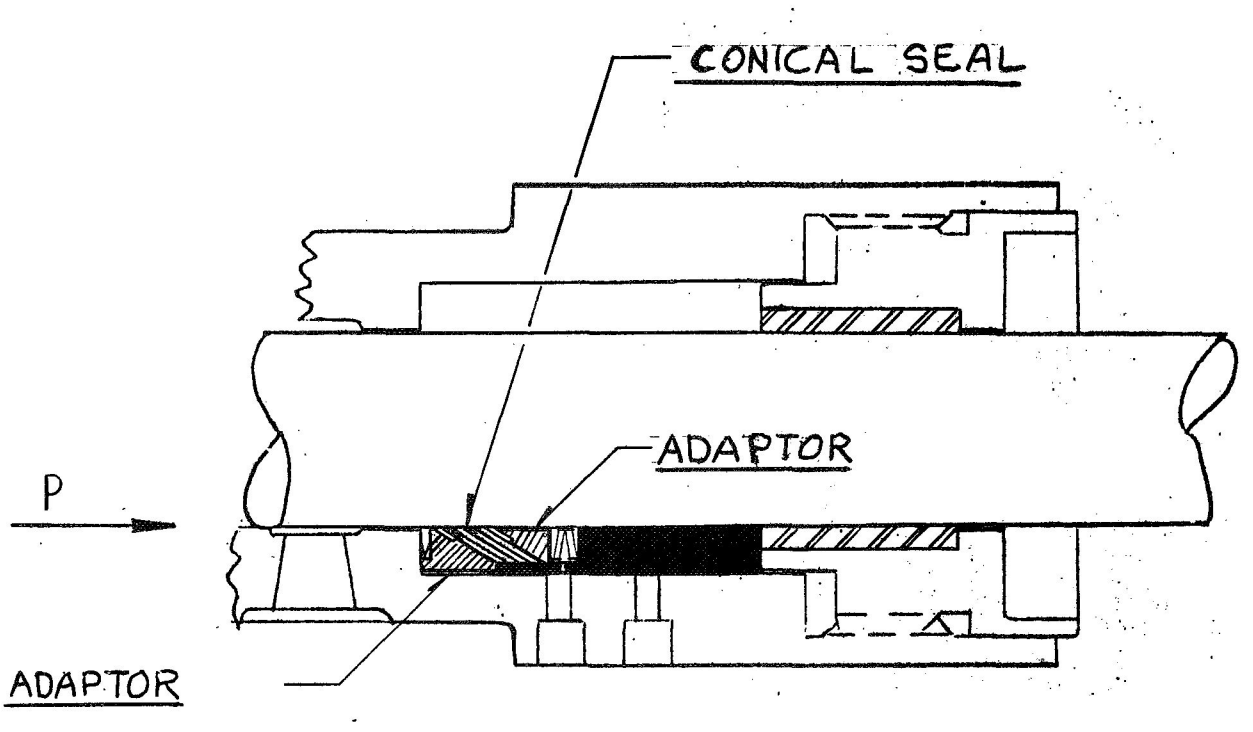

Figure 23. Conical Lip Seal
(Design G)

D. PRELIMINARY EVALUATION OF CANDIDATE SEAL CONFIGURATIONS

1. General

Preliminary tests were conducted on the candidate seals to validate the basic assumptions used in the design of the seals. As the objective of the design phase was to improve the loading characteristics of the seals so that maximum seal deflection could be obtained while subjecting the seal to the lowest stress level possible, seal deflection, leakage, and friction were the criteria used in evaluating the new designs. The original V-seal design was included in the testing to obtain baseline data for evaluating the new designs.

2. Test Procedures and Apparatus

The test apparatus for the load-deflection tests (Figure 24) consist of a seal gland, loading cylinder, direct reading force gage, and a dial indicator for measuring seal deflection. The tests were run with axial seal loads up to 200 pounds (889N), as this was the loading used in the endurance test configuration.

Seal friction, wear compensation, and leakage were determined using the test apparatus shown in Figure 25. This test setup consists of a double-ended cylinder which houses the test seal and piston rod; one end of the cylinder is sealed off with teflon sealing rings to minimize frictional changes due to pressure variations. The piston rod was machined such that the diameter of the rod varied from 0.998 to 0.9885 inch (2.53 to 2.51 cm). The decreasing diameters were made in steps, and were intended to simulate wear and subsequent loss of sealing contact between the shaft and seal. The ability of the seal to respond (deflect) to these changes provided an indication of the seal's capacity to compensate for wear.

The test procedure is as follows. Initially, the seal is positioned over the portion of the rod that has the normal design dimensions, and the applicable seal load is applied. With the test cylinder pressurized to 100 psi (6.9×10^5 N/m^2), the rod is shifted so that the seal is in contact with the

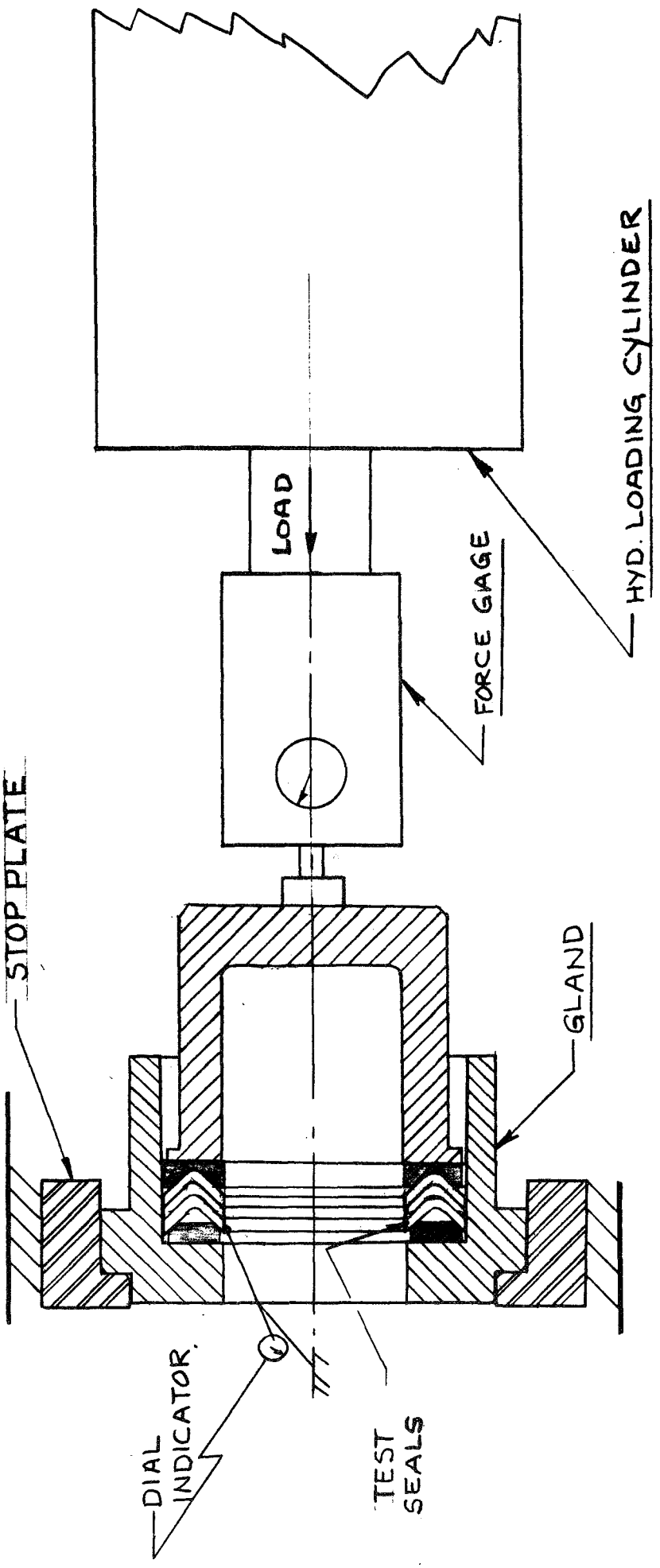

Figure 24. Load-Deflection Test Apparatus

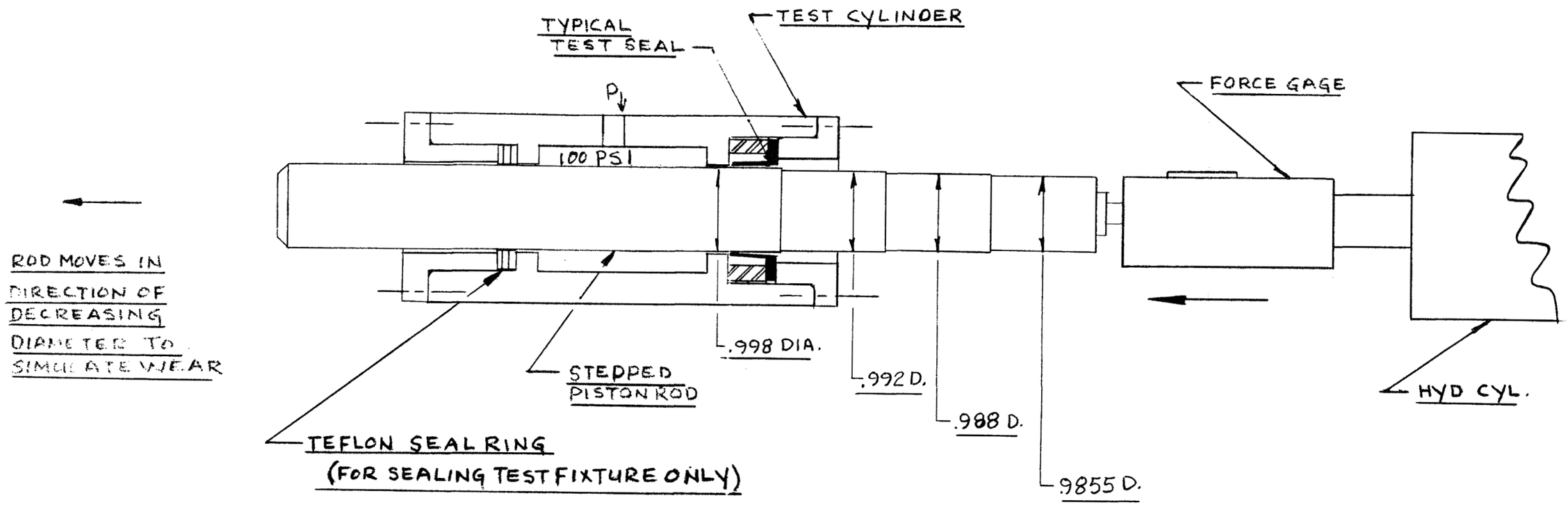

Figure 25. Seal Friction, Wear Compensation, and Leakage Test Apparatus

reduced diameter portion. Both leakage and friction are checked; if no leakage is observed, the rod is shifted so that the seal is in contact with the next smaller diameter. This procedure is continued until leakage occurs. At this point, testing is discontinued and the data evaluated to determine if the point of leakage matches the design deflection of the seal. In most cases, the point of leakage for a specific seal was predictable based on the measured lip deflection of that seal.

3. Load Deflection Tests

The data obtained from the load-deflection tests are shown in Figures 26 through 34 . These data are presented in terms of seal radial deflections versus seal radial load and are compared to the calculated values for each seal. A summary of the theoretical and actual design characteristics of the seals is given in Table 5.

Figure 26 shows the load-deflection values for a single 45° V-seal (Design A) in its original configuration. For comparison, the seal was also evaluated using the modified backup ring and dual load ring. As shown in Figure 26, the load-deflection curve with the original backup and load ring configuration flattened out rapidly, as expected. Some improvements were obtained using the modified backup ring, which provided slightly greater seal deflections. Substantial increases in seal deflections were obtained using the dual load ring and original backup. Further increases in seal deflections were obtained when the modified backup was used inconjunction with the modified load ring. The deflections obtained with this configuration were slightly higher than the calculated deflection curve up to the design point. The test data indicates that adequate seal deflections can be achieved with moderate loading by improving the efficiency of the loading system.

Subsequent load-deflection tests were run with the original 45° V-seal with three seals stacked in series, as this was the actual design arrangement. For comparison purposes, deflection tests using the original one-piece load ring and the modified load ring were made. The data shown in Figures 27 and 28 demonstrate the greater seal deflections obtainable with the modified

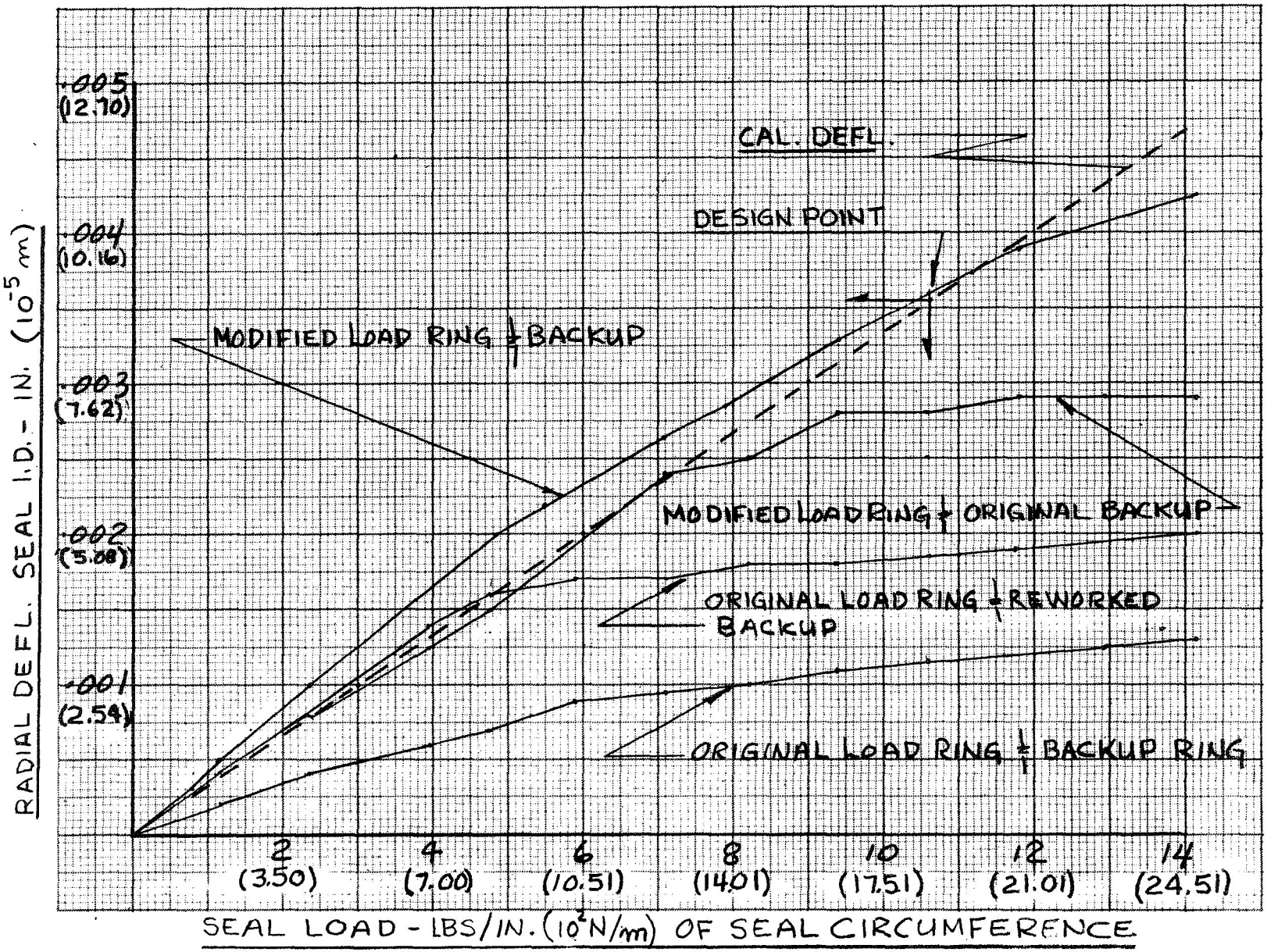

Figure 26. Seal Load vs Seal Deflection - 45° V-Seal (Design A)

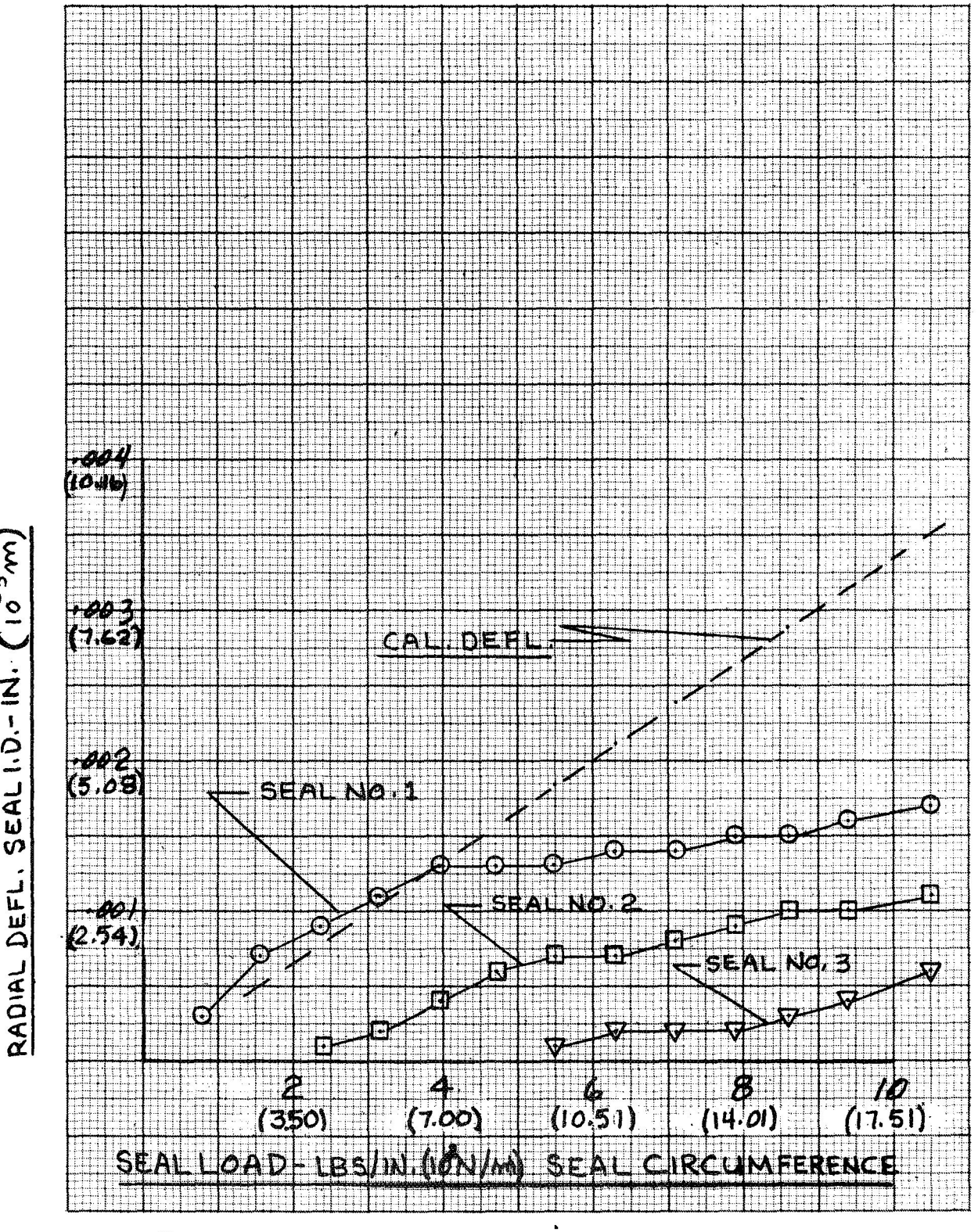

Figure 27. Seal Radial Deflection vs Seal Radial Load - 45° V-Seal (Design A with Original Load Ring and Backup Ring)

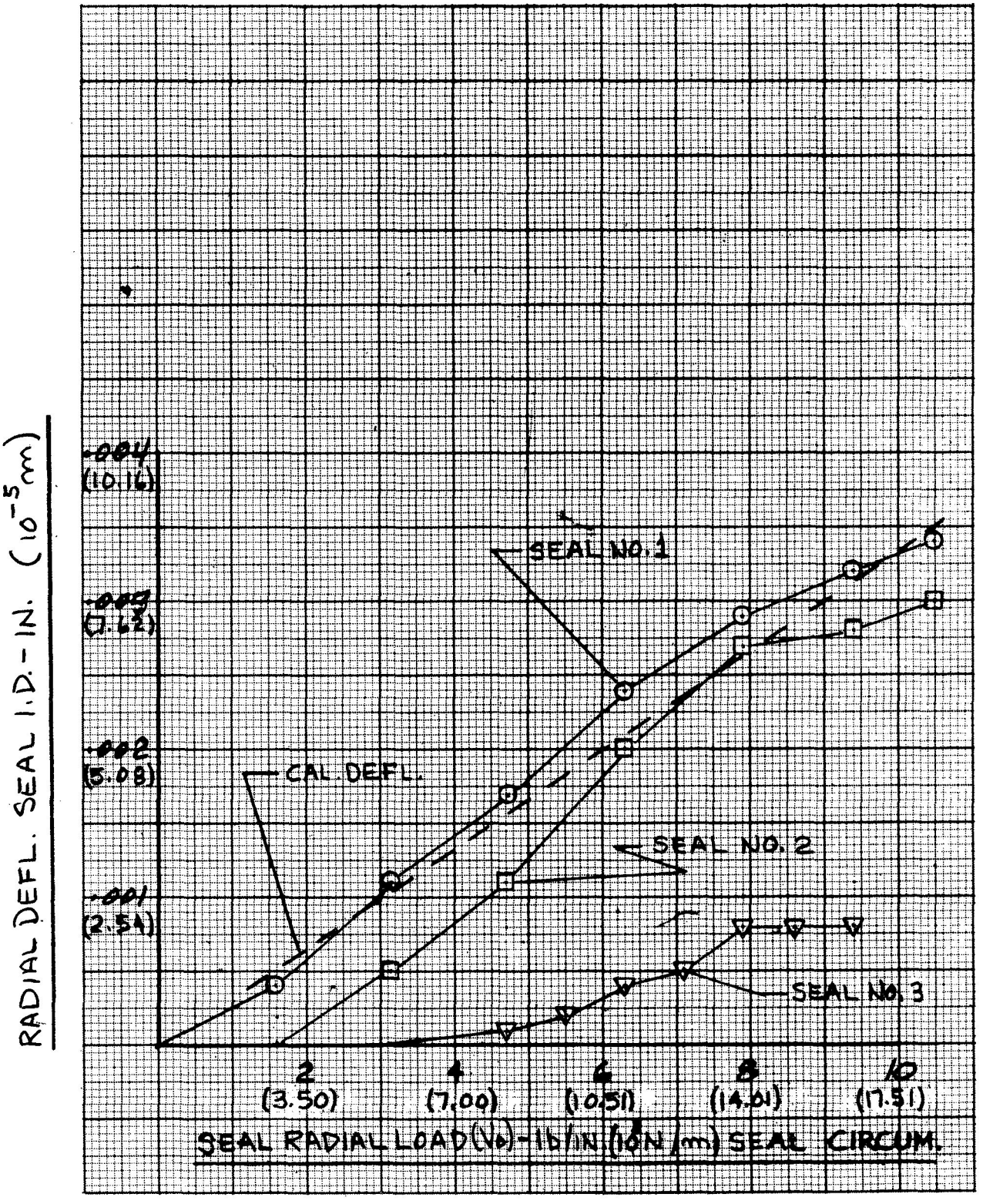

Figure 28. Seal Radial Deflection vs Seal Radial Load - 45° V-Seal (Design A with Dual Load Ring)

load ring. However, deflection of the sealing legs was not uniform for the three seals in the assembly. The greatest amount of deflection was exhibited by the first seal, which was in contact with the load ring. The deflections obtained on the middle seal were slightly less than the values exhibited by the first seal. The third seal, located at the end of the stack, showed very little deflection. This condition is believed to have been caused by friction between the seals. Deflection values obtained on the original seal configuration showed a rapid leveling off despite increasing load, which seemed to indicate a bottoming condition.

Seal deflections obtained with the 30° V-seal (Design B-1), which is one of the improved configurations, showed good correlation with the theoretical deflection values. As shown in Figures 29 and 30, variations in deflections for the I. D. and O. D. of all three seals at any given load condition are small.

For the tapered leg V-seal (Design HB-1) deflection of the I. D. surface and O. D. surfaces of the seal also correlate well with the calculated values. For the I. D. surface (Figure 31), the actual deflections are slightly higher than the calculated values up to the design load of 4. 5 pounds (20. 0N). Deflection of the O. D. surface (Figure 32) was slightly lower than the theoretical value at the design load; however, the actual deflections meet the design requirements.

Load-deflection characteristics of the U-seal (Design C-1) are depicted in Figure 33. The No. 1 seal shows good adherence to the theoretical curve. However, seals No. 2 and 3 exhibited a considerable drop-off from the design curve. This could be attributable to high friction between the seals as the low angle of the legs may have produced a wedging effect between the seals.

Load-deflection values (Figure 34) obtained on the wedge loaded lip seal (Design D) were considerably lower than the calculated values. High friction between the seal lip and metal wedge is believed to have been the cause for the variations.

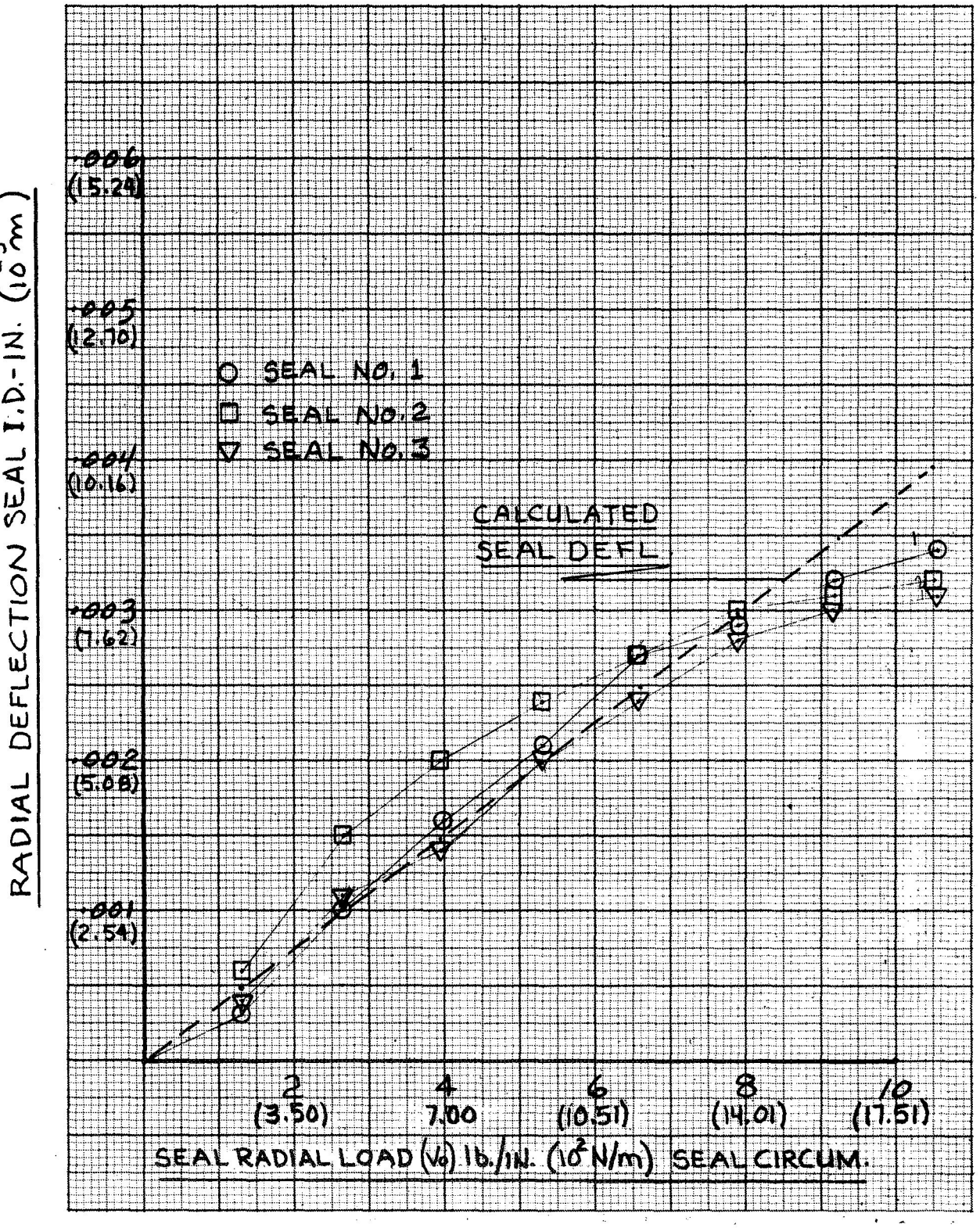

Figure 29. Seal I. D. Radial Deflection vs Radial Load - 30° V-Seal (Design B-1)

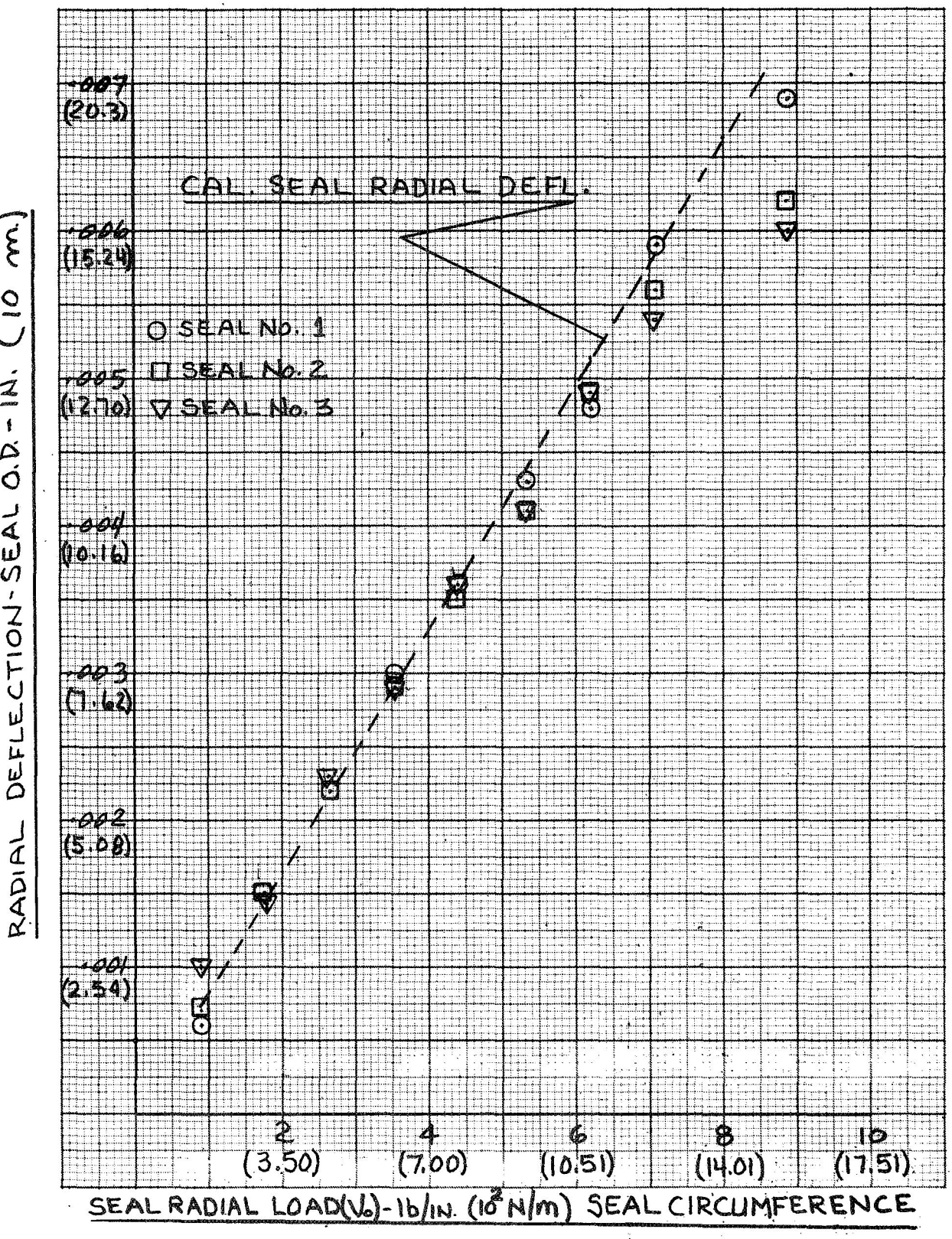

Figure 30. Seal O. D. Radial Deflection vs Seal Radial Load - 30° V-Seal (Design B-1)

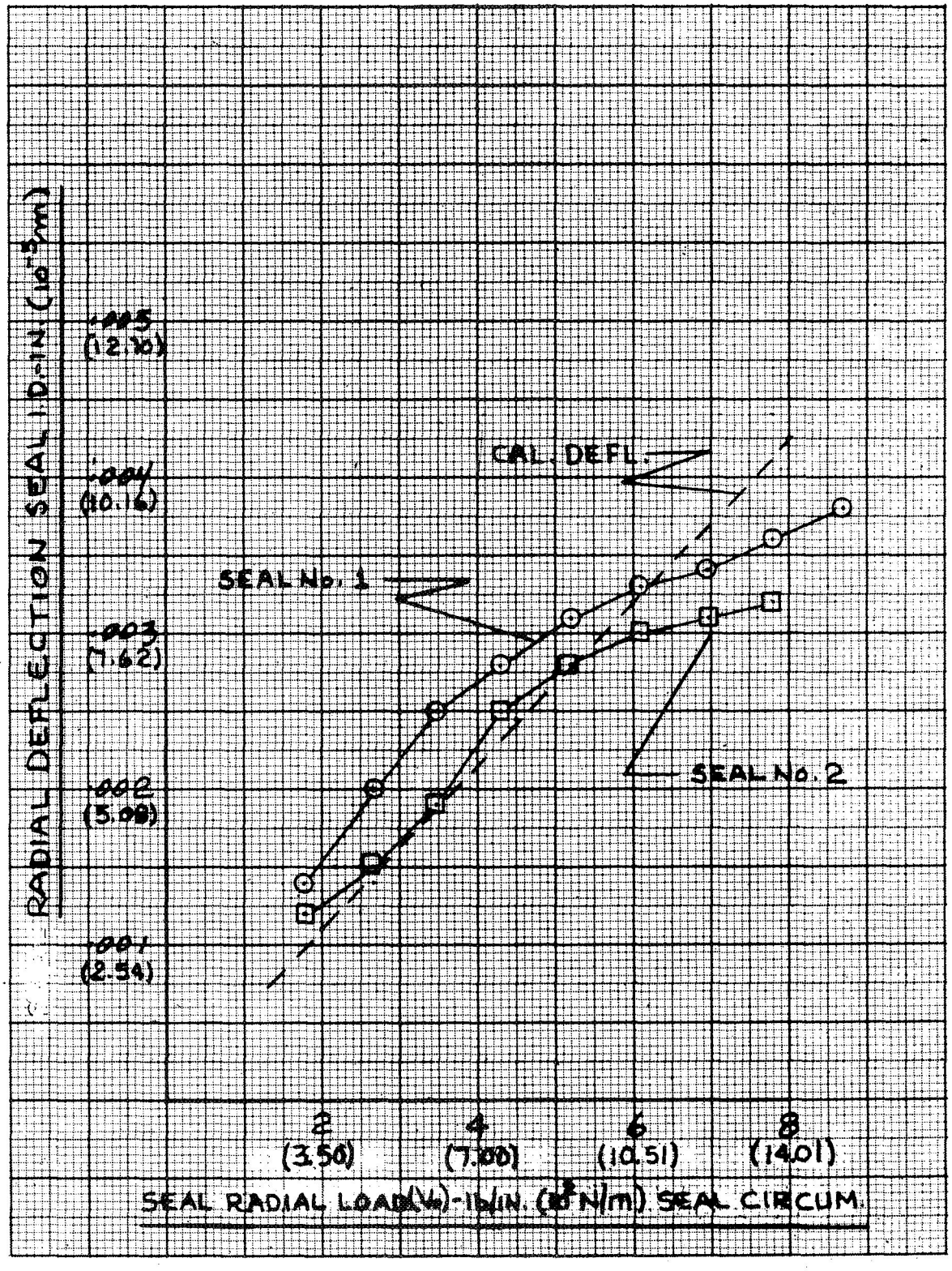

Figure 31. Seal I. D. Radial Deflection vs Seal Radial Load - Tapered Leg V-Seal (Design HB-1)

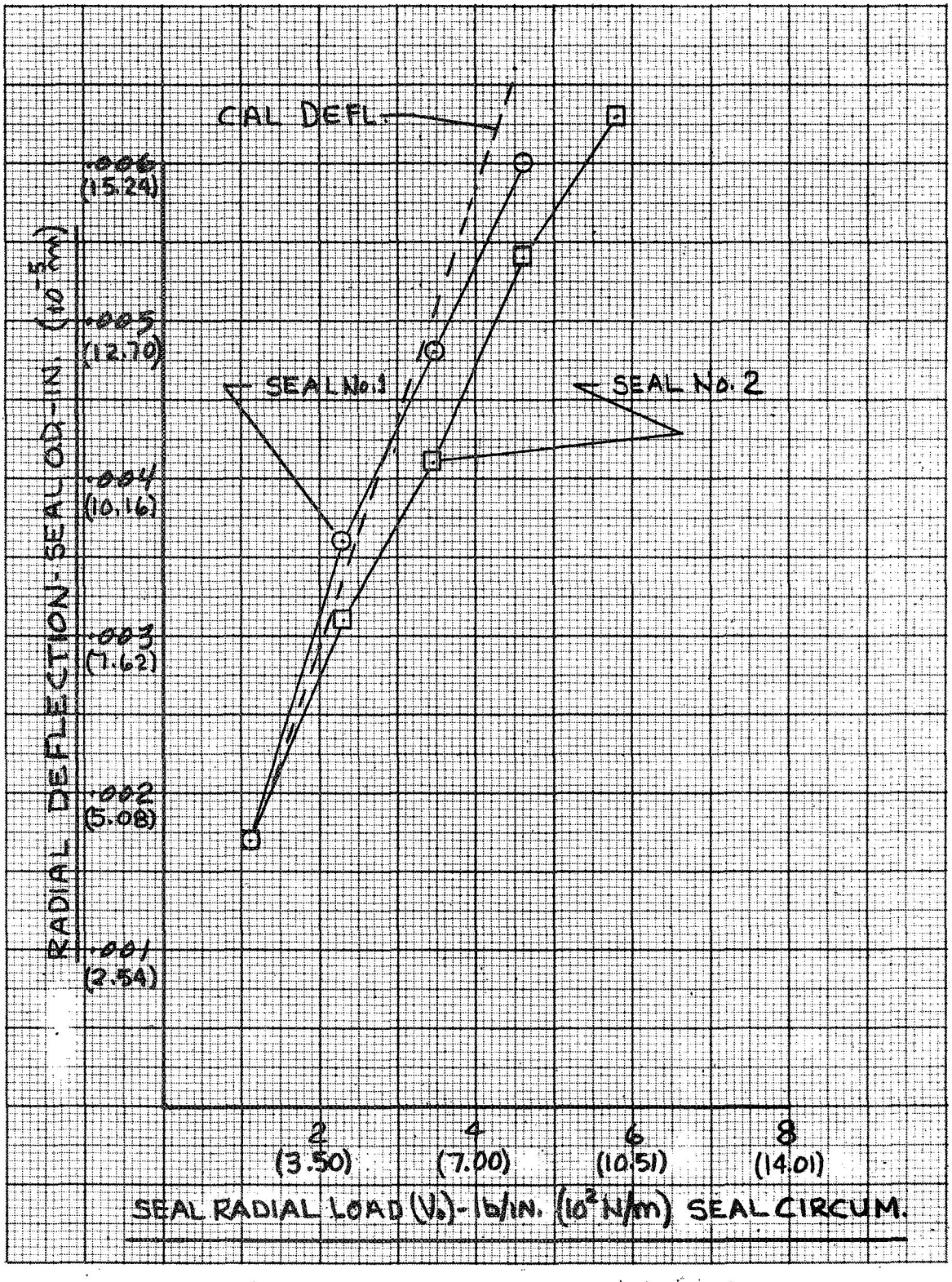

Figure 32. Seal O. D. Radial Deflection vs Seal Radial Load - Tapered Leg V-Seal (Design HB-1)

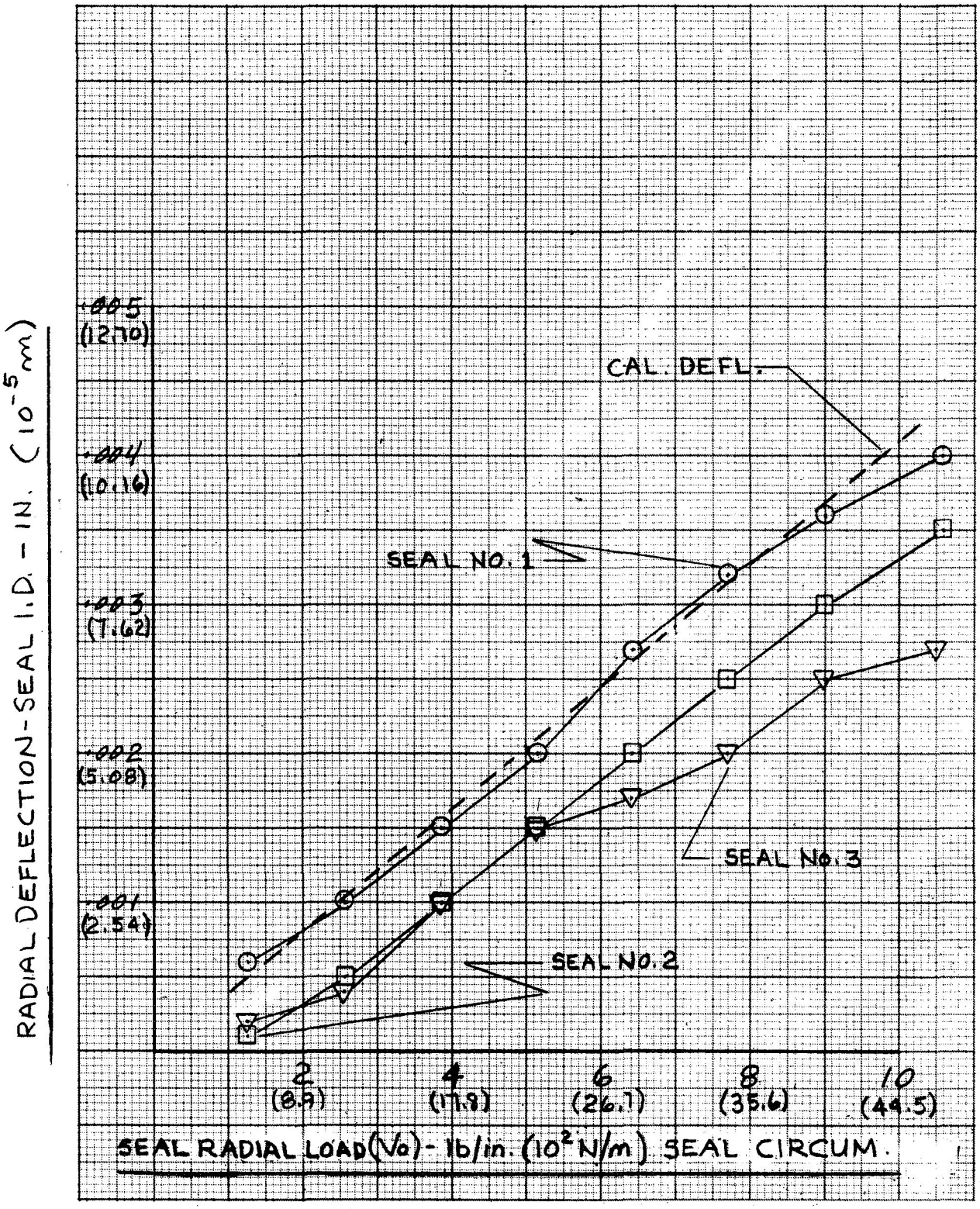

Figure 33. Seal Radial Deflection vs Seal Radial Load - U-Seal (Design C-1)

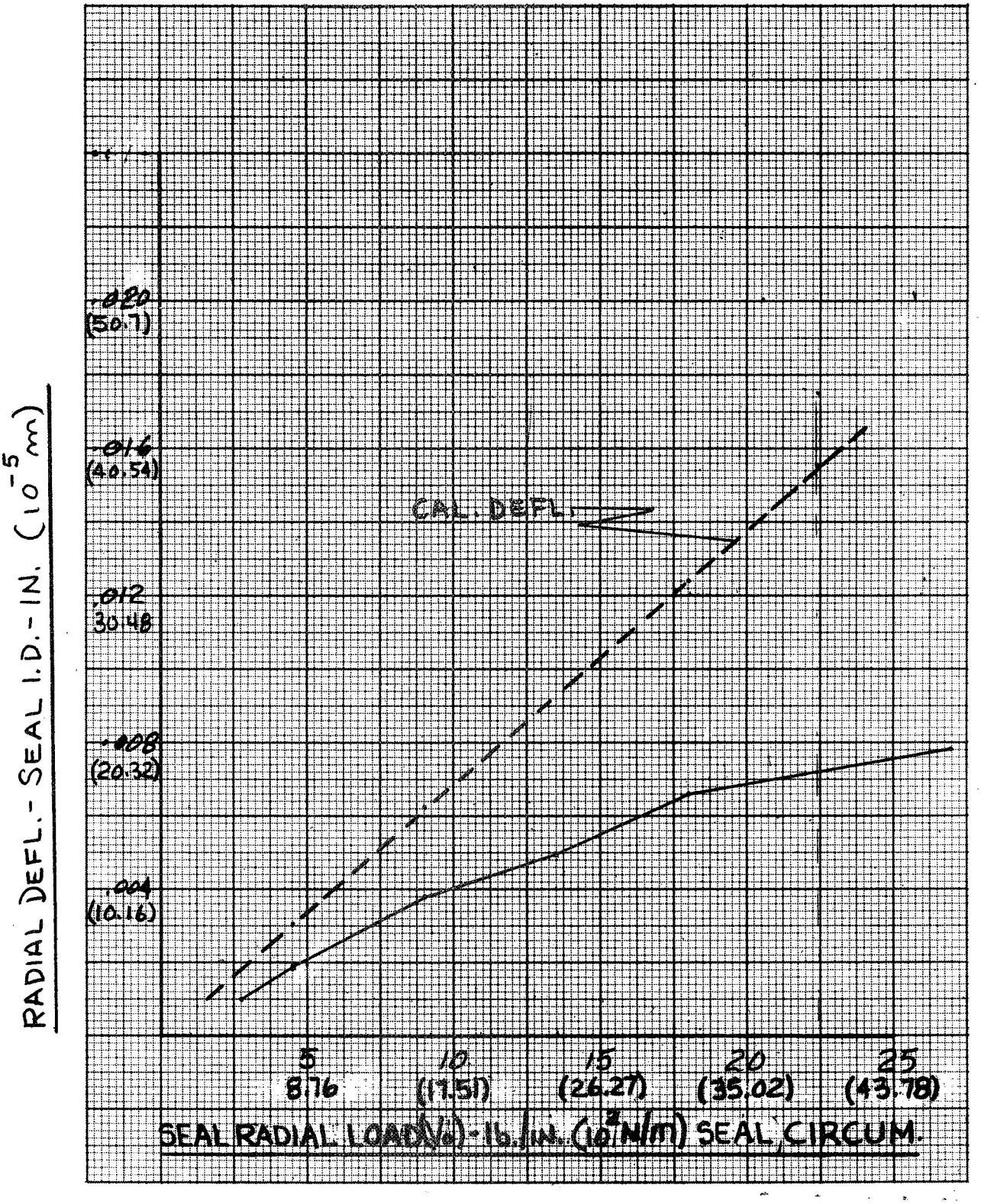

Figure 34. Seal Radial Deflection vs Seal Radial Load - Wedge Seal (Design D)

4. Seal Friction, Wear Compensation, and Leakage Tests

Table 5 shows the correlation between the wear compensating ability of the seal and the measured deflection of the same seal. The original V-seal (45°) design leaked at less than 0.006 inch (0.01524 cm) wear, which was expected, as the average deflection of the seal was 0.002 inch (0.0051 cm). By substituting the modified load ring in place of the standard (one-piece) load ring, the same seal was able to accommodate 0.006 inch (0.01524 cm) wear with no leakage. This compared well with the measured deflection of the seal using the modified load ring, which was approximately 0.005 inch (0.0127 cm). The 30° V-seal with the standard load ring also exhibited leakage at 0.006 inch (0.1524 cm) wear. However, by replacing the standard load ring with the modified load ring configuration, this seal (Design B-1) was able to tolerate wear of 0.006 inch (0.01524 cm) without leaking. The tapered leg V-seal (Design HB-1) was also able to accommodate wear of 0.006 inch (0.01524 cm). Design C-1 (U-seal) also showed good response to wear.

The wedge loaded lip seal (Design D) showed the best wear compensating ability. This configuration was able to maintain a seal at approximately 0.013 inch (0.033 cm) of wear. However, it should be noted that this was accomplished at a much higher loading. The Design E lip seal, which is loaded with a metallic hoop spring, was able to compensate for wear up to 0.006 inch (0.01524 cm). This configuration also exhibited the lowest friction. No leakage was encountered with the wide angle V-seal (Design F) at a simulated wear of 0.013 inch (0.033 cm). The conical lip seal (Design G) also exhibited no leakage when subjected to a simulated wear of 0.013 inch (0.033 cm).

The seal configurations exhibiting the lowest sliding friction values are Designs E, F, HB-1, A-1, and B-1. Seals constructed with low seal angles generally showed higher frictional values.

5. Selection of Candidate Seals

Based on the bench test results and design analyses, the following seals were selected for the high temperature cycling test.

1. V-seal - 30°, with modified load ring (Design B-1).
2. Lip seal No. 2, with slotted hoop spring (Design E).
3. Tapered leg V-seal, modification of 30° V-seal (Design B-1) to include variable thickness seal legs (Design HB-1).

The above designs were selected on the basis of their good balance among the following characteristics: 1) deflection, 2) wear compensating ability, 3) friction, and 4) minimum operating stresses. These configurations were evaluated in conjunction with the original V-seal design (Design A) in the endurance test. Detailed drawings of the test seals are shown in Appendix C.

TABLE 5. SUMMARY OF SEAL FRICTION, WEAR COMPENSATION, AND LEAKAGE *OF CANDIDATE SEAL CONFIGURATIONS*

Seal Configuration		Method of Loading	Diametral Wear Compensation in. (10^{-4}m)	Cal Seal I. D. Radial Defl at Design Load		Actual Seal I. D. Radial Defl at Design Load in. (10^{-4}m)	Sealing Stress psi (10^5N/m^2)	Friction lb (N)
				in. at lb/in.	10^{-4} m at 10^3 N/m			
Design A	45° V-seal (orig design) Std load ring	Belleville springs	Leaked at < 0.006 <(1.52)	0.0036 at 10.6	0.914 at 1.86	0.0012 (0.305)	350 (24.13)	95 (423)
Design A-1	45° V-seal Modified load ring	Belleville springs Dual loading	No leak at 0.006 (1.52)	0.0036 at 10.6	0.914 at 1.86	0.0027 (0.686)	350 (24.13)	90 (400)
Design B	30° V-seal Std load ring	Belleville springs	Leaked at < 0.006 <(1.52)	0.0028 at 7.0	0.711 at 1.23	0.0025 (0.735)	216 (14.89)	110 (488)
Design B-1	30° V-seal Modified load ring	Belleville springs Dual loading	No leak at 0.006 (1.52)	0.0028 at 7.0	0.711 at 1.23	0.0027 (0.686)	216 (14.89)	90 (400)
Design C-1	U-seal (14°) Modified load ring	Belleville springs Dual loading	No leak at 0.006 (1.52)	0.0028 at 7.0	0.711 at 1.23	0.0024 (0.61)	210 (14.48)	160 (712)
Design D	Lip seal No. 1	Wedge loaded	No leak at 0.013 (3.30)	0.015 at 22.4	3.81 at 3.92	0.007 (1.78)	280 (19.31)	130 (578)
Design E	Lip seal No. 2	Hoop spring	No leak at 0.006 (1.52)	0.003 at 3.0	0.76 at 0.525	0.0027 (0.686)	130 (8.96)	29 (129)
Design F	Flat seal Wide angle (133°)	Belleville springs	No leak at 0.013 (3.30)	0.006 at 16	1.52 at 2.80	0.007 (1.78)	265 (18.27)	64 (285)
Design G	Conical seal	Interference fit	No leak at 0.013 (3.30)	0.008 at 15	2.03 at 2.63	0.008 (2.03)	500 (34.48)	120 (534)
Design HB-1	Tapered leg V-seal Modified load ring	Belleville springs Dual loading	No leak at 0.006 (1.52)	0.0025 at 4.5	0.635 at 0.788	0.0027 (0.686)	150 (10.32)	72 (320)

SECTION II
HIGH TEMPERATURE CYCLING TEST

A. GENERAL

Testing of the candidate seals was conducted concurrently in two separate test actuators, using chlorinated phenyl methyl silicone fluid. The actuators were operated continuously at 500°F ± 20°F, (260°C ± 11°C) with shut-down over the weekend. The seals were tested to failure or completion of 20 million short-stroke cycles. The high frequency short-stroke cycling operation was selected based on the judgement that bending fatigue was the principal cause of seal failure during the previous program and the observation that the greatest wear occurred during rapid short stroke operation. Seal failure as defined in Exhibit A of Contract NAS 3-11170 (Appendix A), was that point when fluid leakage exceeded 1 drop per minute (approximately 3 cc/hr). The basic cycling rig used in Contract NAS 3-7264 (Ref. 1) was modified for the testing.

B. TEST RIG

A schematic layout of the high temperature cycling rig is shown in Figure 35. Figure 36 shows the rig as installed in the high temperature oven. The test rig is basically the same as the one used in the work sponsored under NASA contract NAS 3-7264. The rig consists of a hydraulic power supply package, the actuator drive, and the seal test actuators.

The power supply consists of an electric motor-driven variable-delivery pump, which is capable of supplying a flow of 10 gpm at pressures to 4000 psi (2.76×10^7 N/m^2). This hydraulic unit powers the servo controlled actuator which drives the seal test actuators. The stroke length and cycling speed of the driving actuator are controlled by a cam and variable speed electric motor, respectively. The stroke length is regulated by positioning the servo valve drive link on the cam. The drive link also serves as the feedback device to close the servo loop. Pressure taps are installed in the actuator piston chambers to monitor cylinder pressure. By monitoring the pressures in the actuating cylinder, an indication of seal friction can be obtained throughout the testing. As the pressure in the driving actuator is a function of the load being driven, a steady-state pressure value can be established during testing.

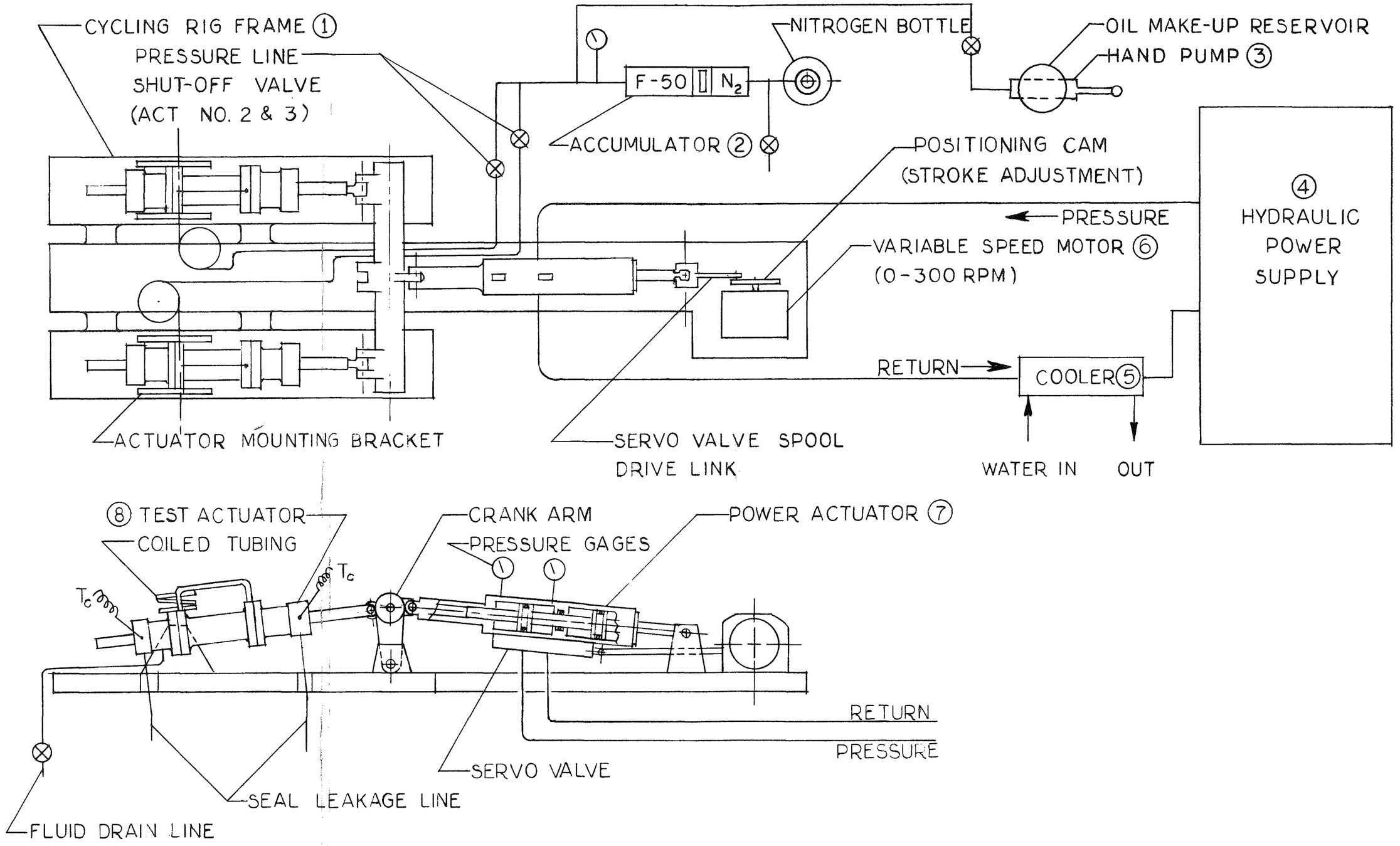

Figure 35. High Temperature Cycling Rig Layout

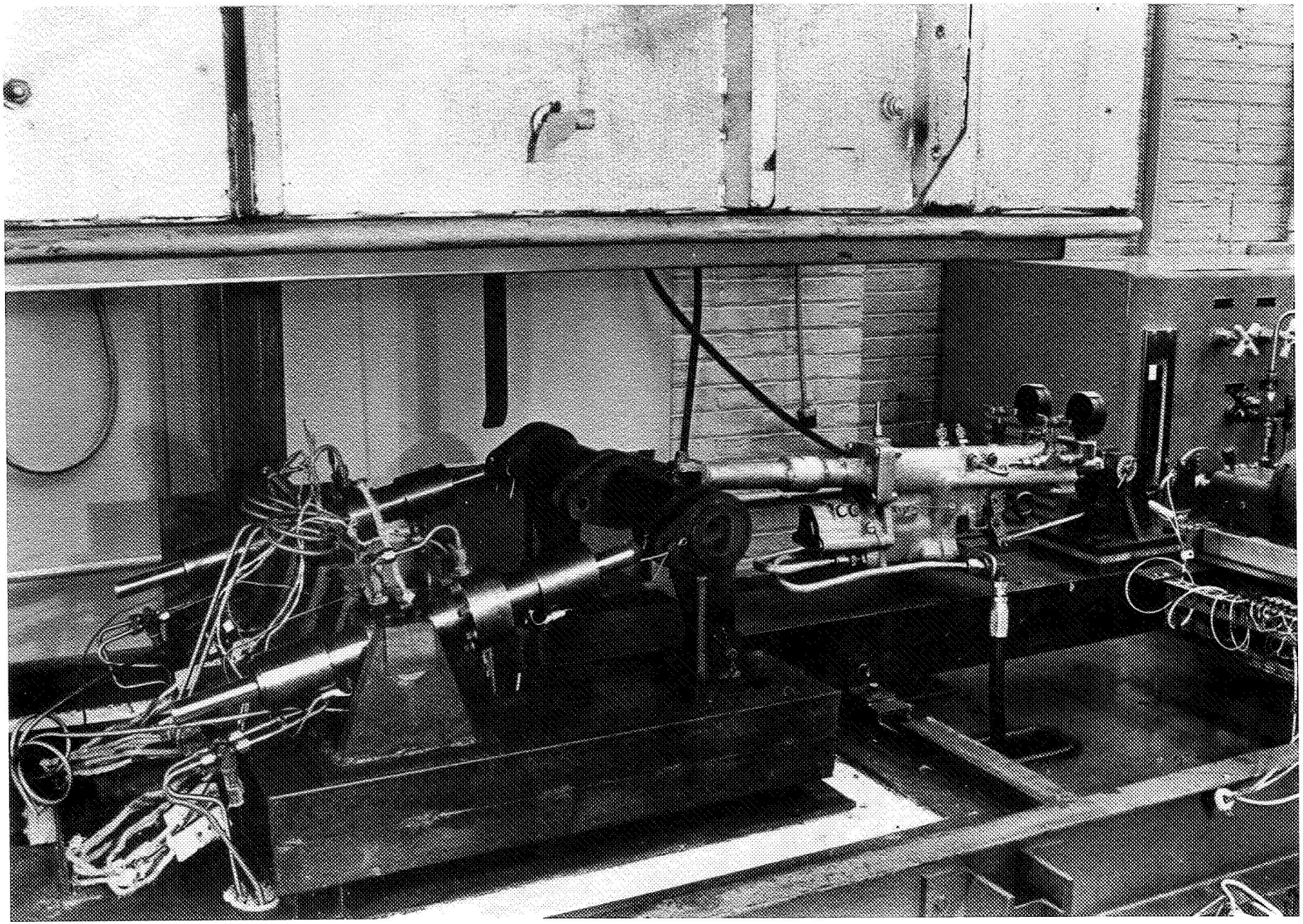

Figure 36. High Temperature Cycling Rig Installation

Thereafter, any increase in seal friction or driving load would result in an increase in pressure over the steady-state value, thus warning the operator of an impending malfunction.

The test actuators are attached to a common crank arm. Each actuator contains two different seal configurations. Pressurized fluid is supplied to the actuators from an accumulator under a nitrogen charge. Pressure lines to the actuators are routed separately; shut-off valves are installed on each line to permit shut-down of the failed actuator. A floating piston is incorporated in the accumulator to provide a barrier between the oil and nitrogen. The accumulator also serves as a fluid make-up system to compensate for leakages.

Filling of the system is accomplished with a hand pump. Leakage drain lines are provided on each end of the actuator to monitor seal leakage. System fluid drain lines are also installed on each actuator to facilitate draining. Thermocouples for monitoring fluid and seal temperatures are also provided.

C. TEST AND INSTRUMENTATION PLAN

The four seal configurations selected for the high temperature cycling test were evaluated in two double-ended actuators. The actuators are designated as actuator No. 2 and actuator No. 3, and were assembled with the following seals.

Actuator No. 2

A - end - 45° V-seal (Design A)
B - end - 30° V-seal (Design B-1)

Actuator No. 3

A - end - Lip seal No. 2 (Design E)
B - end - Tapered leg V-seal (Design HB-1)

Conditions governing the tests were as follows:

1.	Fluid temperature	500 °F ± 20°F (260°C ± 11°C)
2.	Fluid pressure	100-150 psig ($6.9 - 10.4 \times 10^5$ N/m^2)
3.	Seal temperature	500°F (260°C)
4.	Piston rod stroke (total)	0.2-in. ± 0.020-in. (5 mm ± 0.5 mm)

5.	Cycling rate	300 cpm ± 25 cpm
6.	Test duration	20 million cycles
7.	Failure point	Leakage exceeding 1 drop per minute (3 cc/hr)

During the high temperature cycling test, the following data were recorded.

1. Ambient temperature
2. Fluid-in temperature
3. Fluid temperature adjacent to seal
4. Seal temperature (approximate)
5. Fluid pressure
6. Fluid leakage

The locations of the above data pickup points are shown in Figure 37. In addition to these data, the number of thermal cycles, mechanical cycles, and mechanical cycling rates were recorded.

D. TEST RESULTS

1. General

Results of the high temperature cycling test are summarized in Table 6. Of the four seals tested, Design B-1 and Design HB-1, which are improved versions of the original V-seal design, successfully completed the 20-million cycle test. Both seals were subjected to a total of 1172 hours of operation of which 80% of the time was at 500°F (260°C). Leakage accumulated at the end of the test was 27.5 cc and 25.5 cc for Design B-1 and HB-1, respectively. The original V-seal design developed excessive leakage after 11.3 million cycles. Testing of the spring loaded lip seal (Design E) was terminated after 3.3 million cycles when leakage exceeded 1 drop per minute. Details of the performance of the seals during the testing follows:

2. 30° V-Seal (Design B-1)

Initial seal leakage (Figure 38) was noticed after 2.8 million cycles and appeared to have ceased after 4.4 million cycles, at which point a total of 6.5 cc was collected. There was essentially no increase in leakage from that

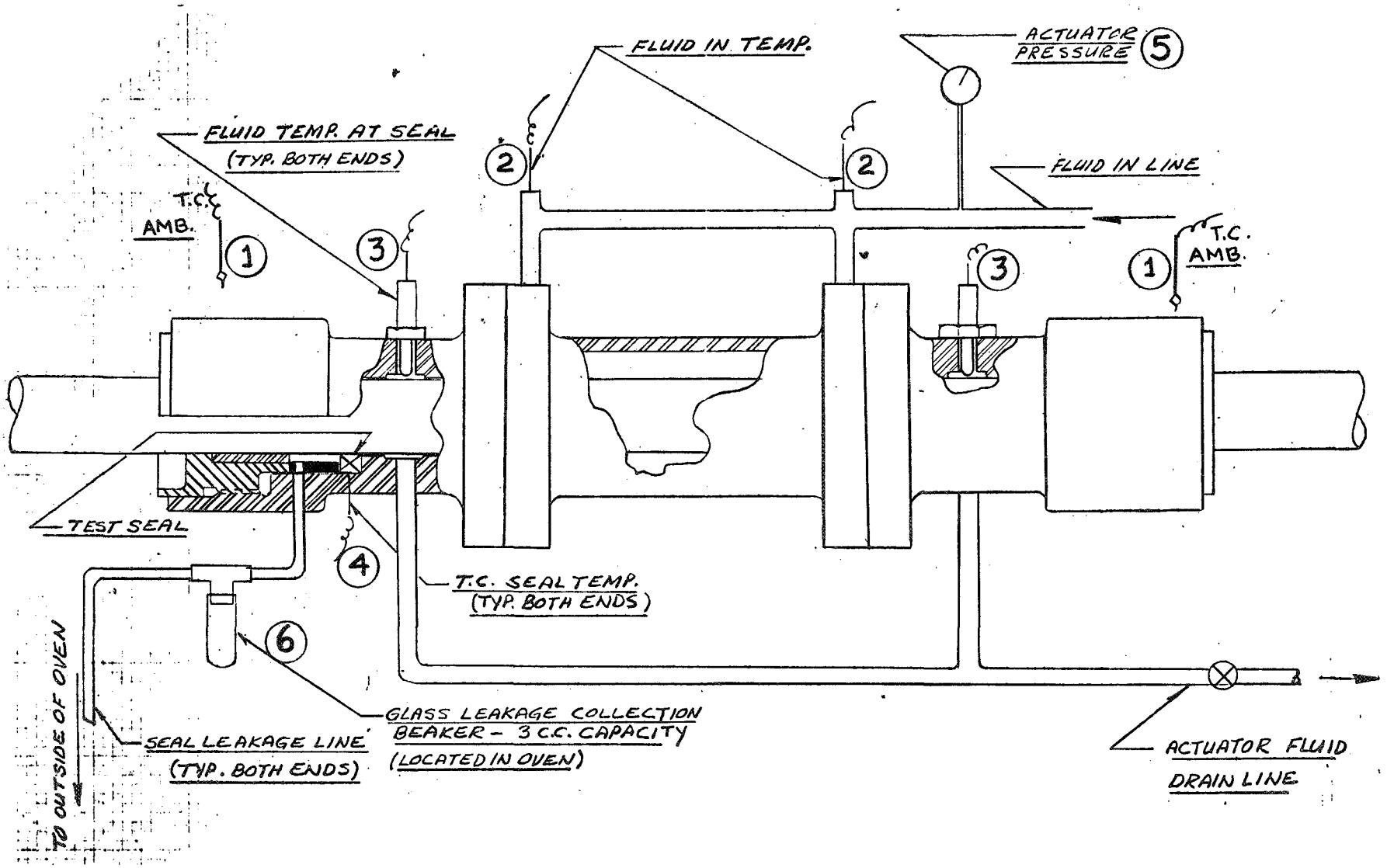

Figure 37. Instrumentation Schematic - Test Actuator

TABLE 6. SUMMARY OF HIGH TEMPERATURE CYCLING TEST

Seal Configuration	Total Test Time (hrs)	Time at 500°F (260°C) (hrs)	Total Cycles	Cycles at 500°F (260°C)	Accumulated Leakage (cc)
Design A, 45° V-Seal	730.5	586	13,248,747*	10,548,000	180 cc/hr, test discontinued
Design B-1, 30° V-Seal	1172	937	21,353,066	17,866,000	27.5
Design E, Spring Loaded Lip Seal	220	178	3,394,000	3,204,000	21 cc/hr, test discontinued
Design HB-1, Tapered Leg V-Seal	1172	937	21,353,066	17,866,000	25.5
Design F, Wide-Angle V-Seal (replaced Design E)	1044	824	18,820,000	15,832,000	103.3
Design F, Wide-Angle** V-Seal (replaced Design A)	534	416	9,788,323	7,488,000	79

* Seal failure occurred at 11.3 million cycles, but seal was kept under test to obtain additional data.

** Test stopped without failure at conclusion of program.

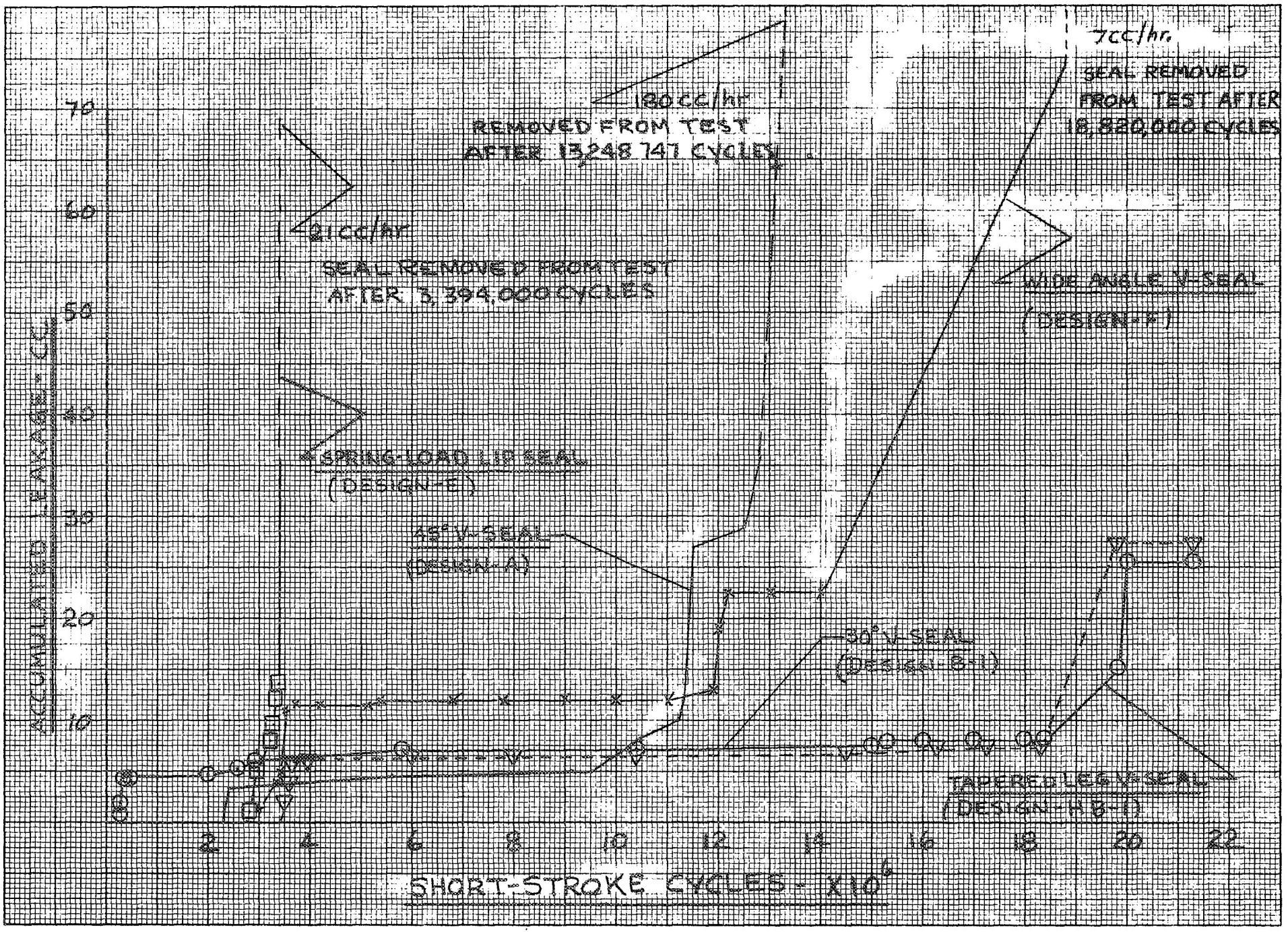

Figure 38. Cumulative Seal Leakage - High Temperature Cycling Test

point on until after 18 million cycles at which time a slight increase in accumulated leakage was noticed. As shown in Figures 39 and 40, the seals were in excellent condition except for a small circumferential crack on the outside surface of the No. 3 (outboard) seal. As this seal was exposed to an air atmosphere, it was suspected that the crack was due to high temperature air aging effects.

A comparison of dimensions recorded before and after testing (Table 7) shows that the O.D. surface of all three seals exhibited shrinkage of 0.002 to 0.004 inch (0.0051-0.0102 cm) from the original dimensions. As the O.D. is a static surface, material wear was not considered in determining the final dimensions. Actual seal wear on the I.D. surface was somewhat difficult to determine because the inside diameter of the seal undergoes shrinkage due to exposure to elevated temperatures. Therefore, if dimensional change is used as a measure of wear, the dimension that the seal assumes after shrinkage must be used as the reference dimension in determining the amount of wear. Using an average of 0.4% shrinkage of the inside diameter from Table 2, seal wear was determined as follows:

$$\text{Seal Wear} = \text{Final Seal Dia} - (\text{Orig Dia} - (0.004 \times \text{Orig Dia}))$$

Based on the above method of wear determination, wear on the three seals ranged from 0.0045 to 0.007 inch (0.011 to 0.018 cm). The higher wear was experienced by the No. 3 outboard seal. This condition could be expected as the outboard seal received less lubrication.

3. Tapered Leg V-seal (Design HB-1)

This seal accumulated a total of 25.5 cc of leakage during the test. Of this total, 4.5 cc was collected during the initial 400,000 cycles of operation. As shown in Figure 38, the tapered leg V-seal was the only seal that exhibited slight leakage during initial cycling. This may be attributable to the fact that the seal utilizes a very light (4.5 pound/inch) (788N/m) sealing load as compared to the other seals. Consequently, the seal required a longer break-in period to establish full contact with the rod. A gradual decrease in the rate of leakage accumulation after the break-in period, was evidenced (Figure 38) and seems to support the foregoing

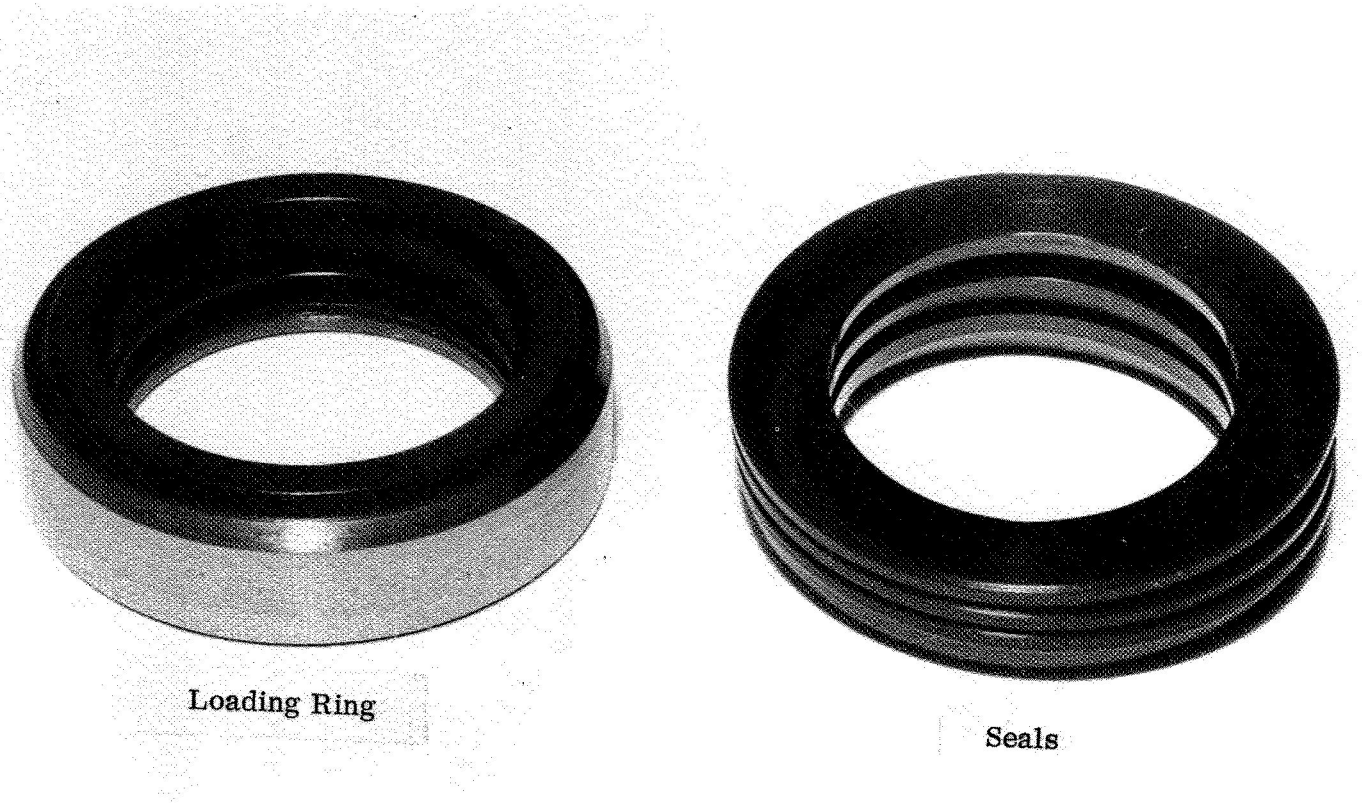

Figure 39. 30° V-Seal (Design B-1) and Loading Ring after 21,353,066 Cycles

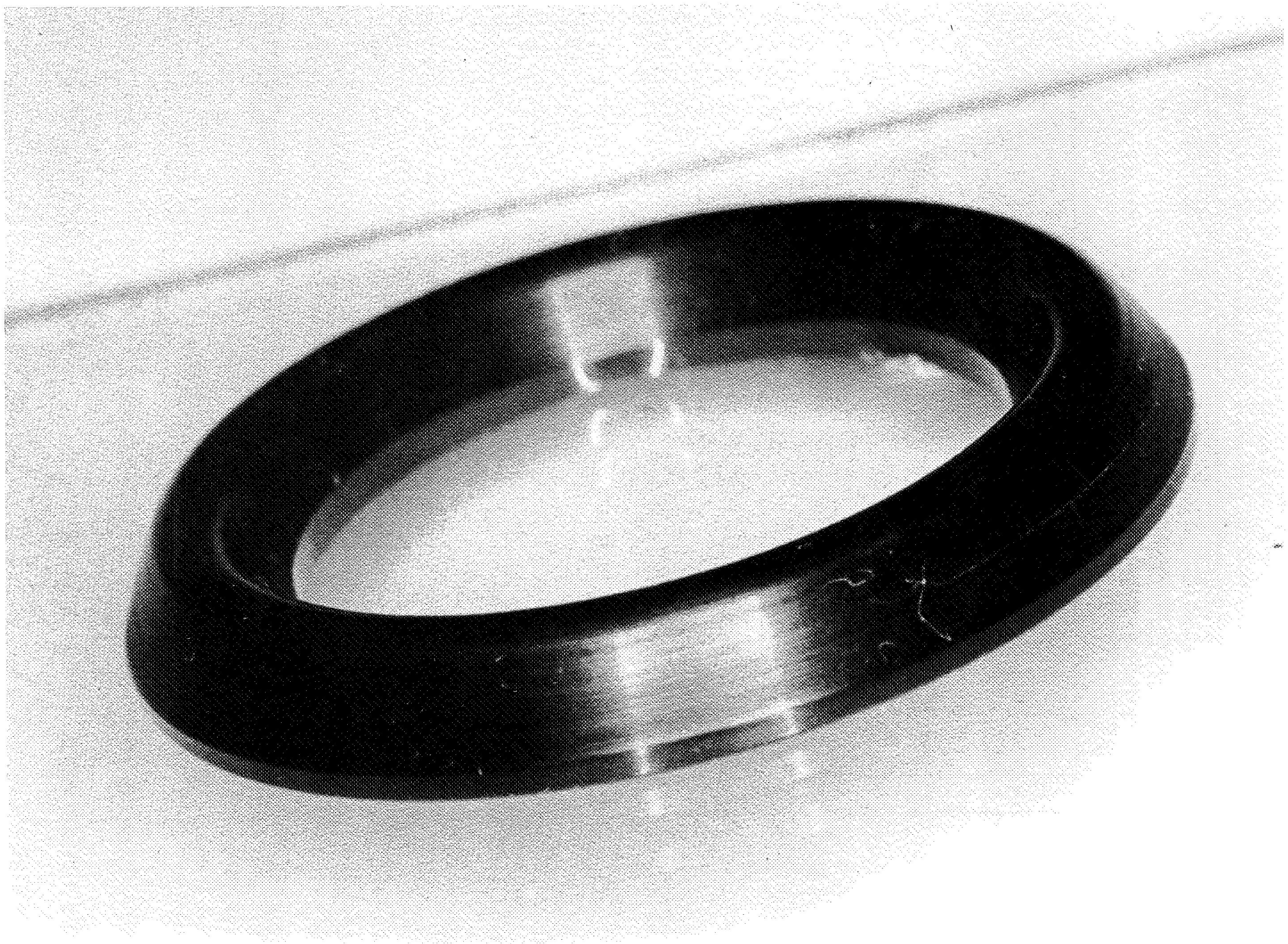

Figure 40. 30° V-Seal (Design B-1) Outboard Element after 21,353,066 Cycles

TABLE 7. COMPARISON OF SEAL DIMENSIONS - BEFORE AND AFTER TESTING

Seal Configuration	I.D. Dimensions								O.D. Dimensions				
	Before Test (in.)	(cm)	I.D. W/Shrink. (in.)	(cm)	After Test (in.)	(cm)	Wear (in.)	(cm)	Before Test (in.)	(cm.)	After Test (in.)	(cm)	% Chge
Design A (45° V-Seal)													
Seal No. 1	0.995	2.527	0.991	2.517	1.001	2.542	0.010	0.0254	1.504	3.820	1.494	3.796	0.67
Seal No. 2	0.996	2.529	0.991	2.517	1.005	2.553	0.014	0.0355	1.503	3.817	1.494	3.796	0.6
Seal No. 3	0.996	2.529	0.991	2.517	1.004	2.550	0.013	0.033	1.504	3.820	1.495	3.797	0.6
Design B-1 (30° V-Seal)													
Seal No. 1	0.999	2.537	0.995	2.527	1.000	2.540	0.005	0.0127	1.497	3.802	1.495	3.797	0.13
Seal No. 2	0.999	2.537	0.995	2.527	0.9995	2.528	0.0045	0.0114	1.497	3.802	1.494	3.796	0.2
Seal No. 3	1.000	2.540	0.996	2.529	1.003	2.548	0.007	0.0178	1.497	3.802	1.493	3.792	0.27
Design HB-1 (Tapered V-Seal)													
Seal No. 1	0.999	2.537	0.995	2.527	0.999	2.537	0.004	0.0101	1.497	3.802	1.492	3.789	0.33
Seal No. 2	0.999	2.537	0.995	2.527	1.003	2.548	0.008	0.020	1.498	3.805	1.493	3.792	0.33
Design E Spring loaded lip seal	0.994	2.524	-	-	0.995	2.527	0.001	0.00254	1.040	2.640	1.035	2.627	0.48
Design F (Wide-Angle V-Seal)													
Seal No. 1	0.999	2.537	0.995	2.527	1.003	2.548	0.008	0.020	1.498	3.805	1.495	3.797	0.2
Seal No. 2	0.999	2.537	0.995	2.527	1.000	2.540	0.005	0.0127	1.498	3.805	1.495	3.797	0.2
Seal No. 3	0.999	2.537	0.995	2.527	0.999	2.537	0.004	0.0101	1.498	3.805	1.493	3.792	0.33

assumption. Following the break-in period, leakage was practically zero up to the 18 million cycle mark before a slight increase in accumulated leakage was noted.

The condition of the seals (Figure 41) was good, and there was no evidence of cracking. Wear at the sealing surface, as indicated in Table 7, was approximately 0.004 and 0.008 inch (0.010 and 0.020 cm) respectively, on the No. 1 seal and No. 2 seal. The O.D. surfaces of both seals exhibited shrinkage of approximately 0.005 inch (0.0127 cm) from the original dimensions.

4. 45° V-Seal, Original Design (Design A)

The 45° V-seal, which was the control specimen, developed excessive leakage (180 cc/hr) after approximately 11.3 million cycles. As indicated in Figure 38, the rise in leakage started at about the 9 million cycle mark and increased rapidly. The leakage usually occurred during the cool-down portion of the thermal cycle and reached its highest rate at approximately 300-320°F (149-160°C). From this point, the leakage decreased as the temperature was further reduced. This pattern indicated that leakage may have been caused by a combination of seal shrinkage and differential thermal contraction between the seal cavity and seal O.D., resulting in loss of contact between the two members. In pursuing this line of reasoning, cycling of the failed seal was continued beyond the failure point to obtain additional leakage data. The seal was finally removed from the test rig after completing a total of 13.2 million cycles.

Based on the data obtained during this latter portion of the test, a graphical presentation relating leakage, temperature, and differential contraction between the seal O.D. and the seal cavity is shown in Figure 42. The leakage data was obtained after approximately 11.3 and 12.8 million cycles of operation. As shown in this figure, leakage during the cooling period was highest at approximately the temperature at which the seal O.D. started to contract away from the seal cavity. Since the loading device was limited in its capability to deflect the O.D. of the seal to compensate for this condition, leakage occurred.

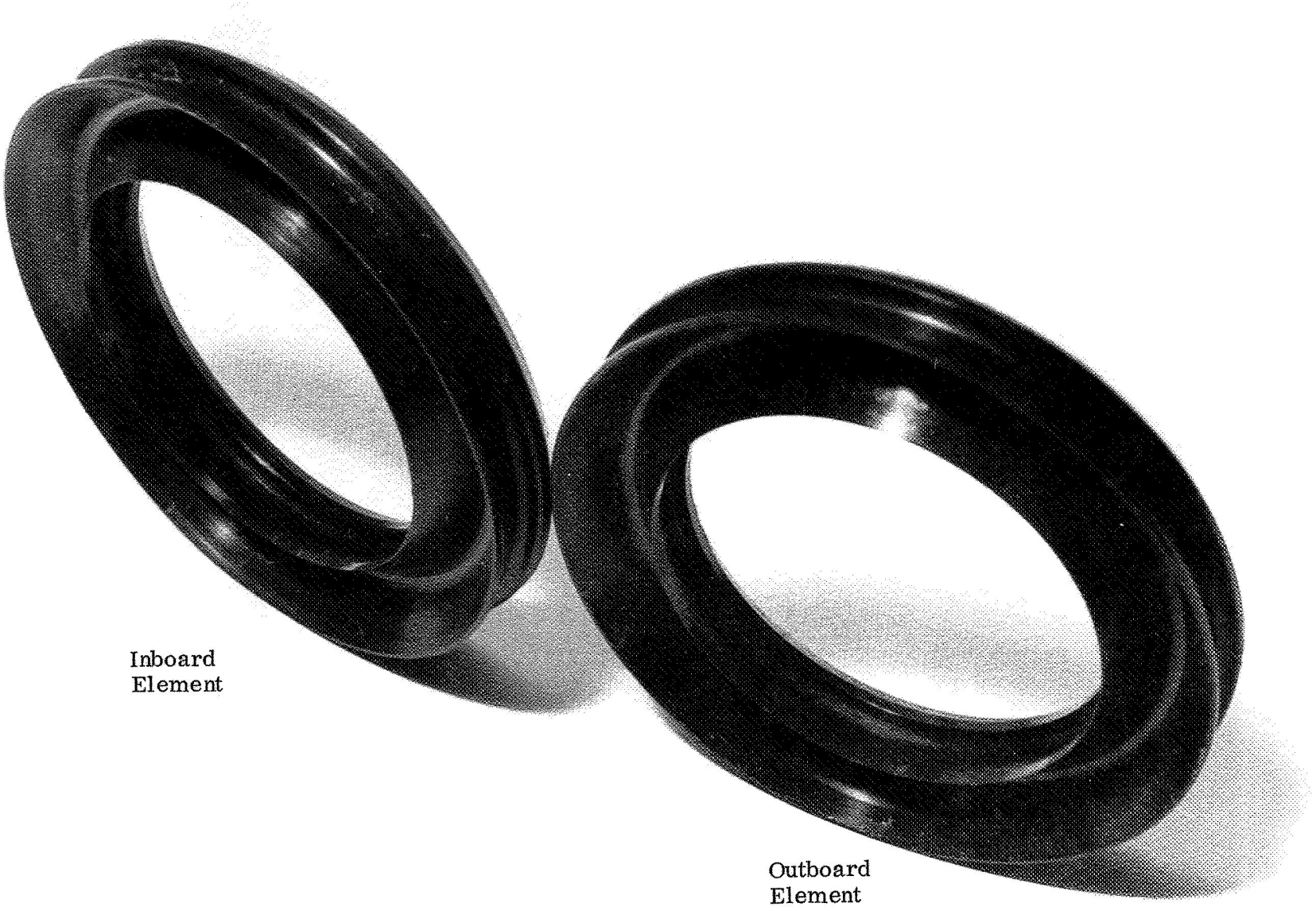

Figure 41. Tapered Leg V-Seal (Design HB-1) after 21,353,066 Cycles

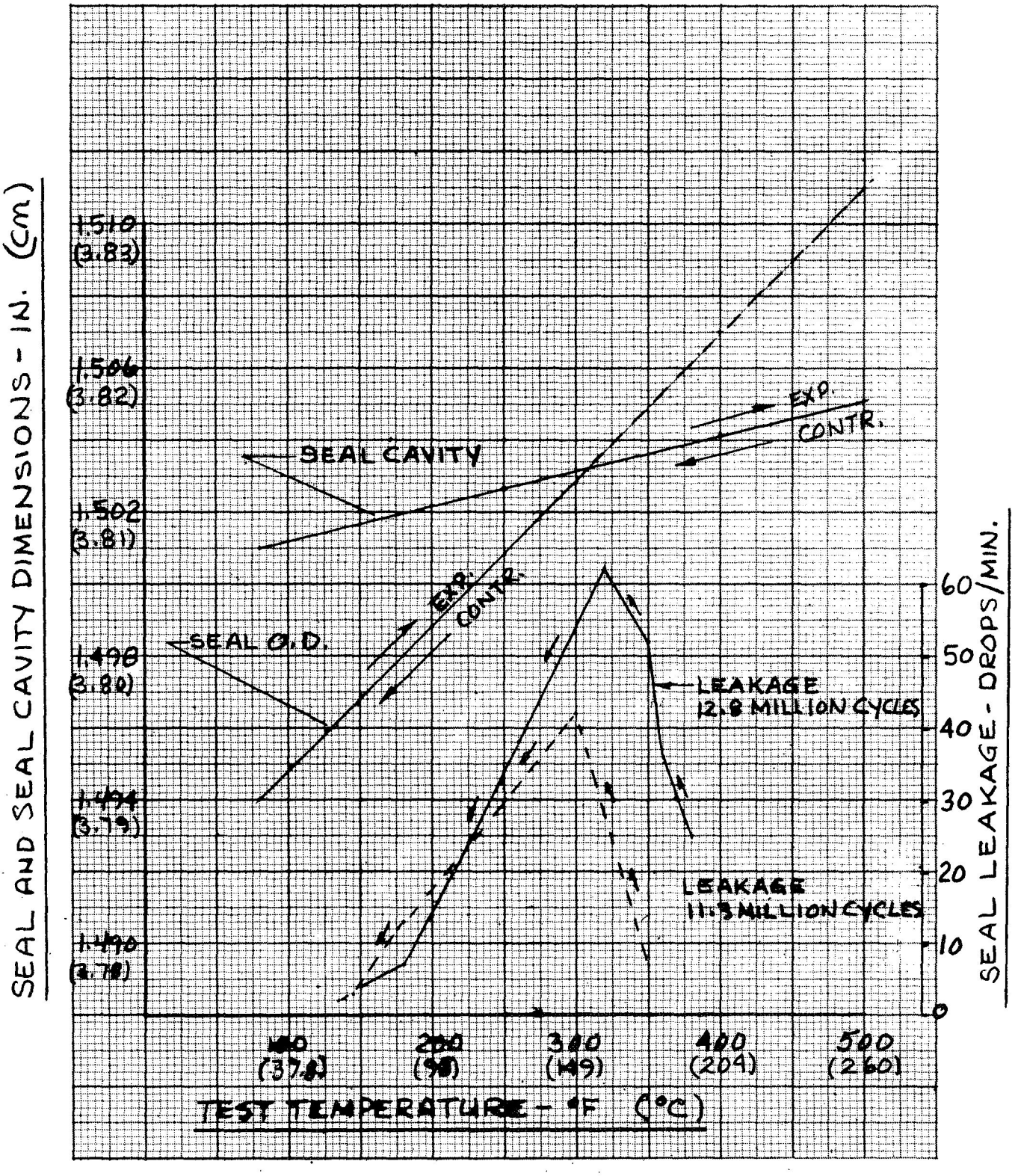

Figure 42. 45° V-Seal (Design A) Leakage during Cooling

Examination of the failed seals revealed incipient cracks (see Figures 43 and 44) near the inside radius of the seals. Erosion of material (Figure 43) from the dynamic sealing portion of the seal nearest to the load ring was also noticed. Both of the foregoing conditions were exhibited by the 45° V-seals in prior testing (Reference 1), wherein failures occurred at a comparable number of cycles and in a similar manner. Excessive seal loading is believed to have caused both conditions.

Of the seals tested, this configuration exhibited the greatest amount of wear (0.010 to 0.014-in.) (0.0254 to 0.0355 cm) at the dynamic surface. The higher seal loading employed by this design is believe to be the main contributing factor to the higher wear. Shrinkage of the O.D. surfaces was considerably higher than that experienced by the other "V" type seals tested. However, this may be partially due to the fact that the 45° V-seal was designed with a 0.004-inch (0.010 cm) interference fit at the O.D. surface on assembly. The interference fit produces additional stresses on the material which are additive to the thermal stresses and stresses resulting from the seal load.

5. Spring Loaded Lip Seal (Design E)

Essentially zero leakage was exhibited by this seal during approximately 2.75 million cycles of operation. Leakage developed at this point (Figure 38) and increased rapidly during the final 0.65 million cycles of operation. It is believed that the leakage experienced during the test occurred between the sealing lip and the slotted spring. Although a tight fit existed between the seal and the spring during initial assembly, a clearance developed due to the shrinkage of the polyimide after several thermal cycles and provided a leakage path for the fluid. Visual inspection of the seal confirmed the existence of this condition. Figure 45 shows the wear spots on the inside surface of the sealing lip. As this surface does not normally contact the rod surface, the wear marks could only occur due to fluid under pressure seeping between the small clearance between the sealing lip and metal spring, causing the seal to collapse against the piston rod. This leakage eventually worked its way back to the flange portion of the seal and leaked to atmosphere. As shown in Table 7, wear at the sealing surface was approximately 0.001 inch (0.00254 cm).

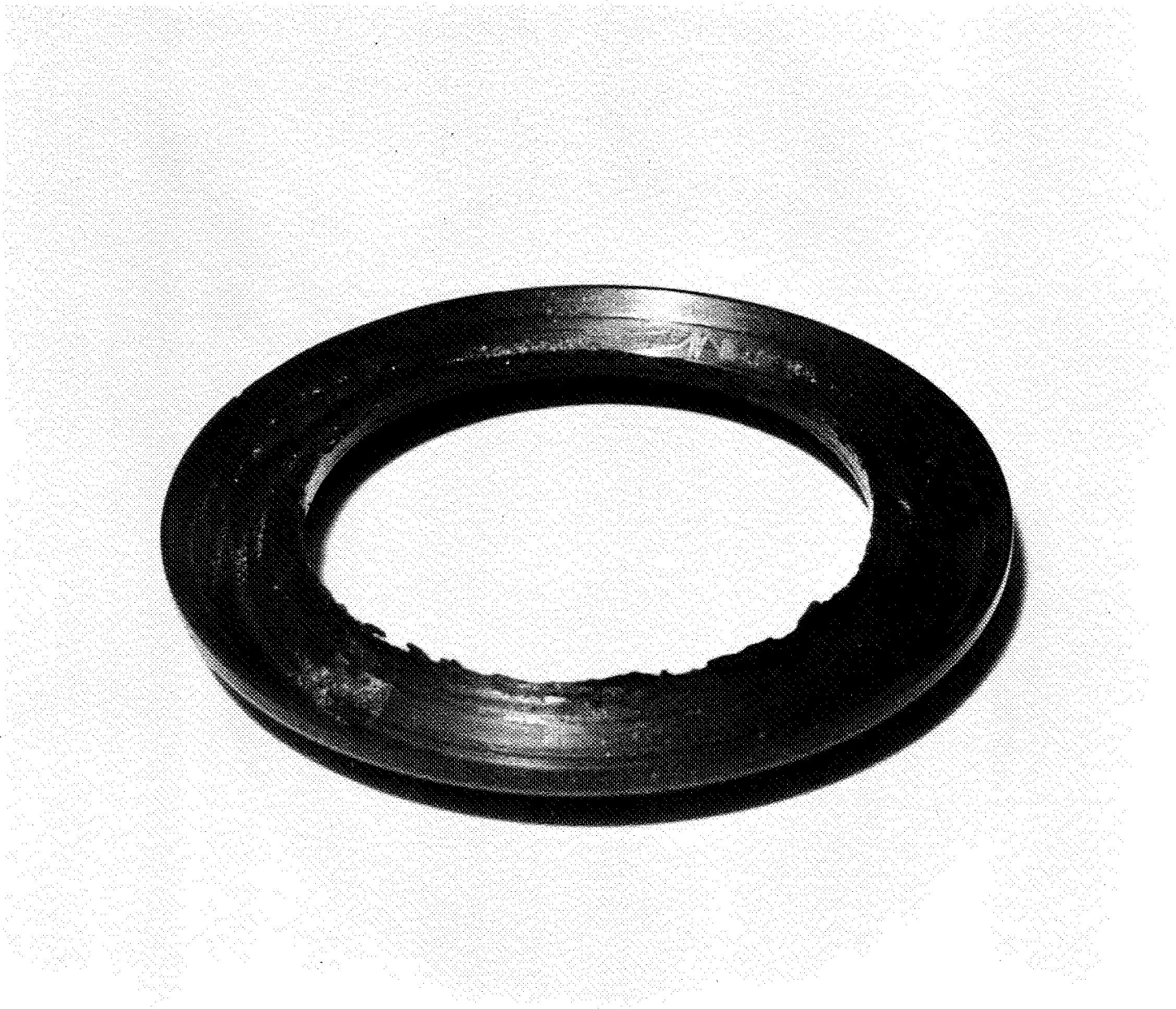

Figure 43. 45° V-Seal (Design A) Inboard Element after 13,248,747 Cycles

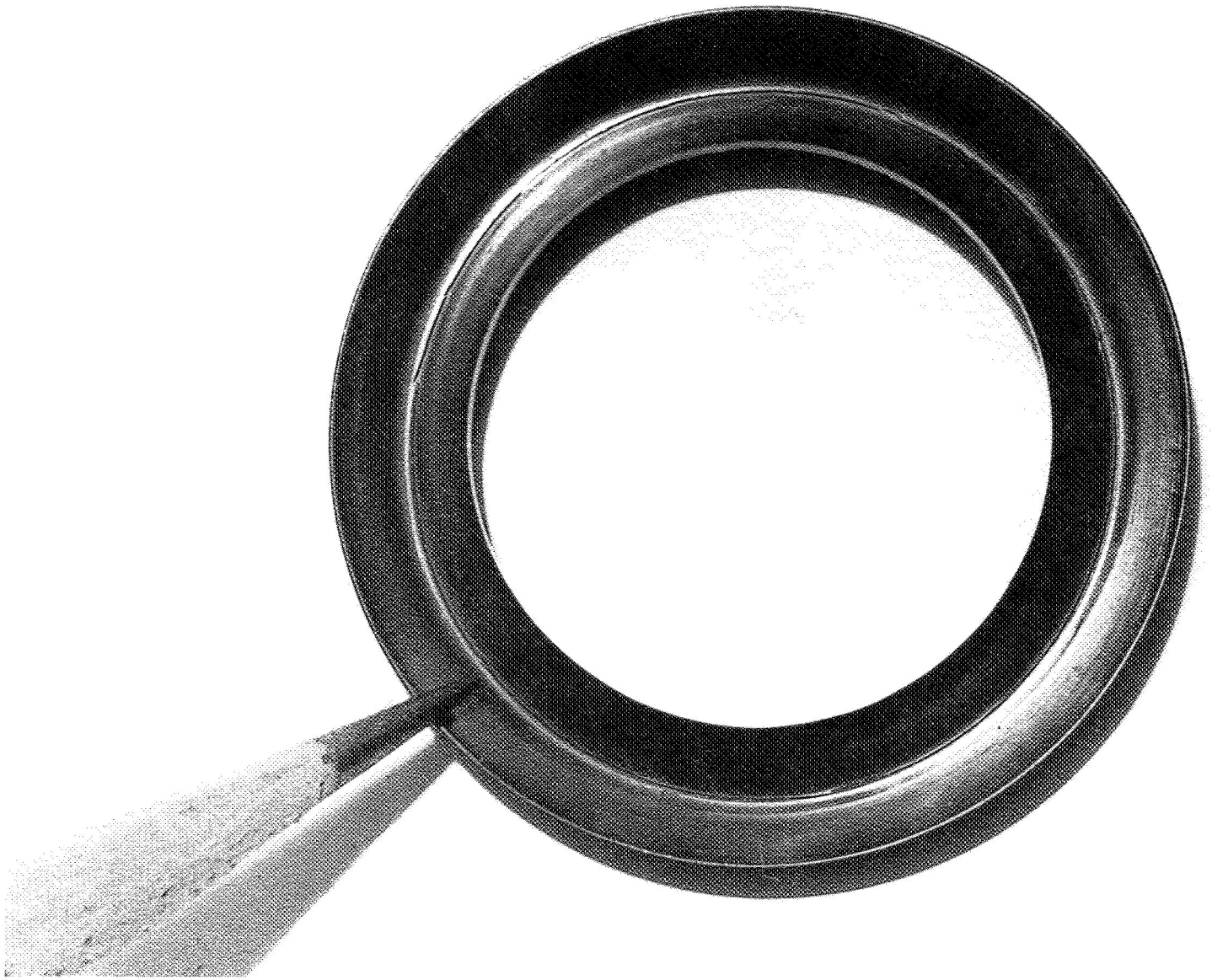

Figure 44. 45° V-Seal (Design A) Outboard Element after 13,248,747 Cycles

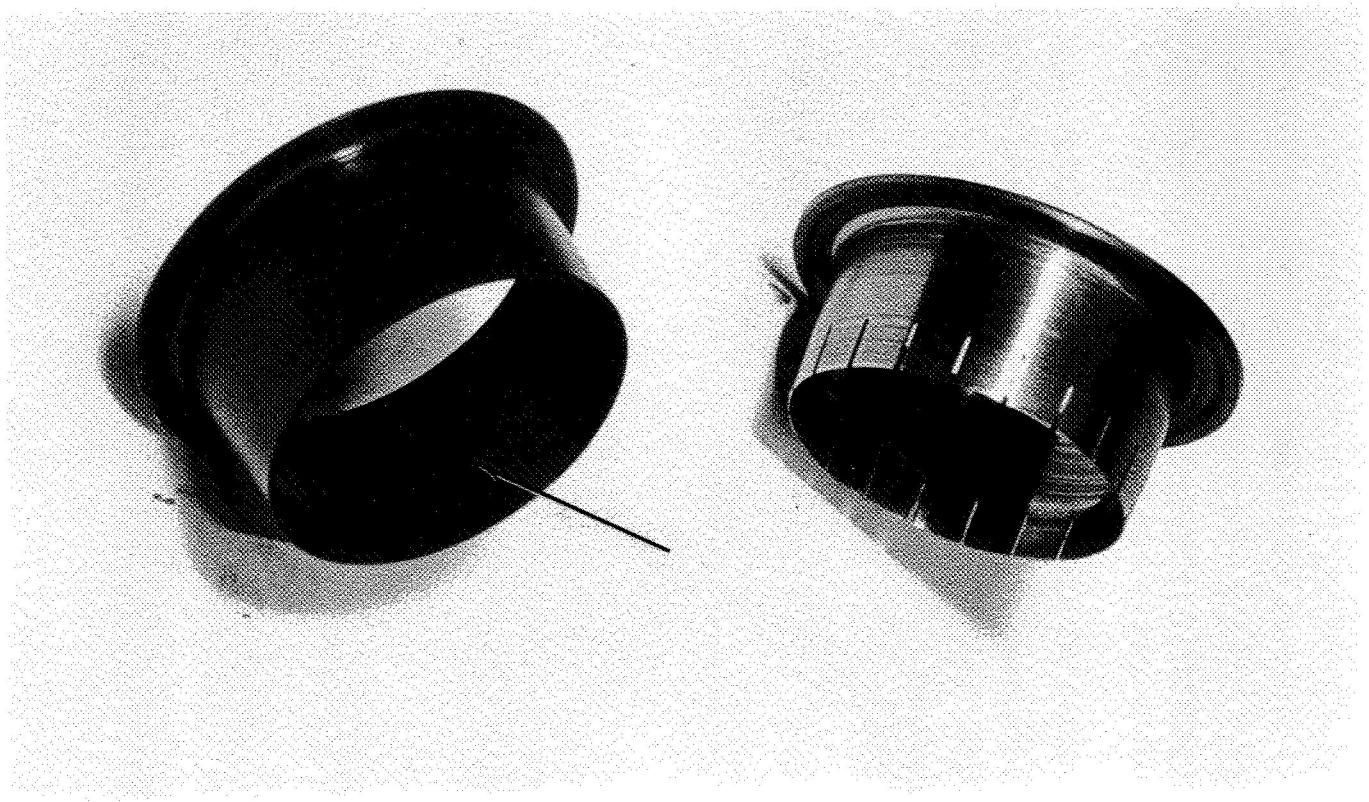

Figure 45. Spring Loaded Lip Seal (Design E) after 3,394,000 Cycles

6. Wide-Angle V-Seal (Design F)

This seal, which replaced the spring-loaded lip seal (Design E) in the test, successfully completed 18.8 million cycles before excessive leakage developed (Figure 38). Total accumulated leakage during the test was 103.3 cc. Inspection of the seal (Figure 46) revealed circumferential cracks on all three elements. Erosion and cracks were noted on the sealing surface of the extreme outboard element (Figure 47). The greatest amount of wear (0.008 inch) (0.020 cm) was experienced by the seal that was in contact with the load ring.

A second set of wide-angle V-seals was tested for approximately 9.8 million cycles. This set of seals was used as a replacement for the 45° V-seal, which failed earlier. Testing of this seal was discontinued when the normal test program was completed.

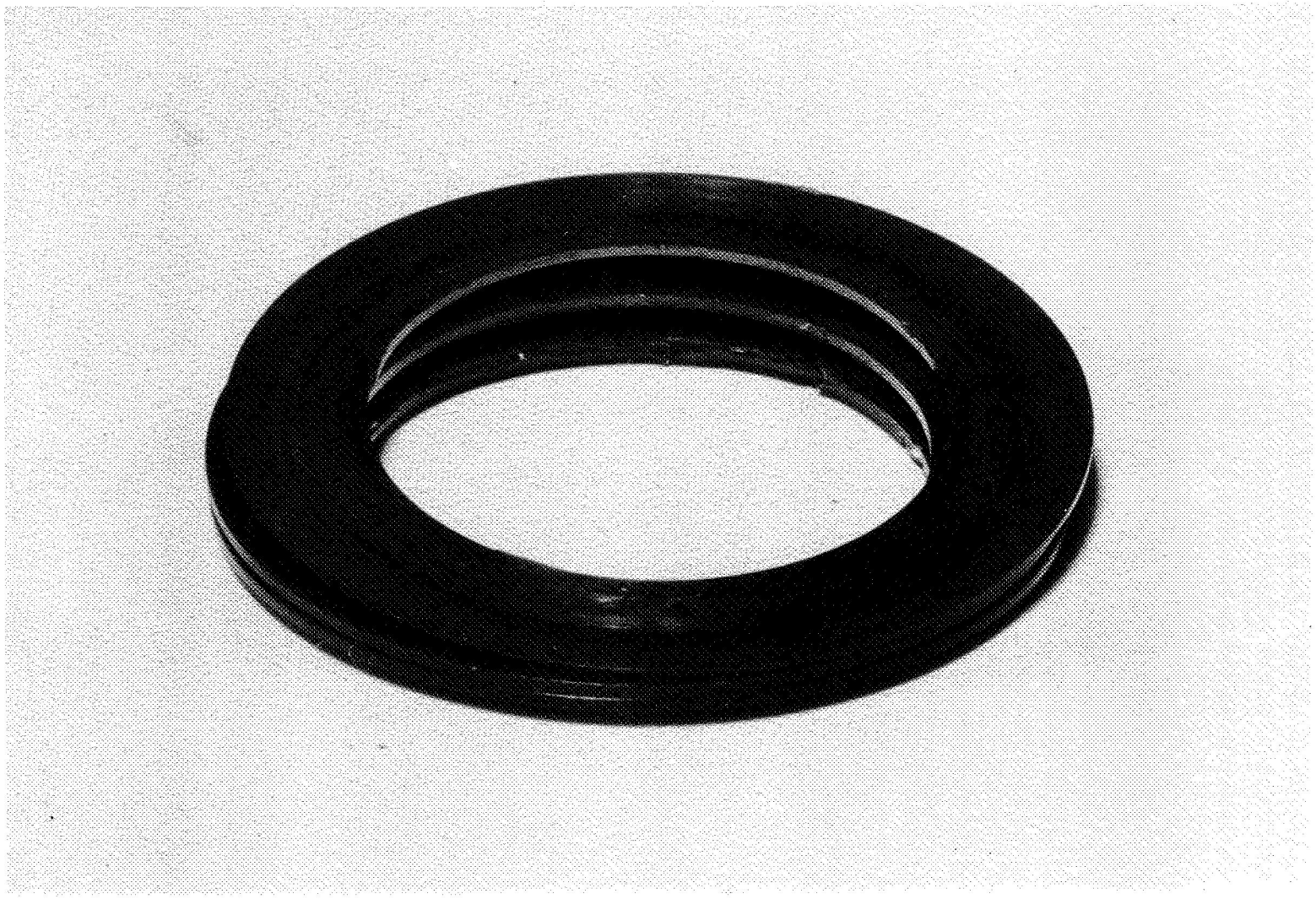

Figure 46. Wide-Angle V-Seal (Design F) after 18,820,000 Cycles

Figure 47. Wide-Angle V-Seal (Design F) Outboard Element after 18,820,000 Cycles

SECTION III
CONCLUSIONS

The major tasks of this program were accomplished as planned. Based on the results obtained, substantial progress has been made toward the development of polyimide rod seals for high temperature hydraulic actuator applications. Conclusions that can be drawn from this work are summarized below:

1. The capability of polyimide rod seals to meet the specified goal of 20 million cycles at temperatures to 500°F (260°C) with a leakage rate of less than one drop per minute, was successfully demonstrated by Designs B-1 (30° V-seal) and HB-1 (tapered leg V-seal).

2. For Design B-1 (30° V-seal), improved flexibility was obtained with the use of longer seal legs. Asymmetrical loading provided by a dual load path loading device resulted in a more uniform and controllable seal load.

3. The use of a linearly tapered seal section in Design HB-1 provided a minimum stress seal design. This approach reduced the tendency for the polyimide to crack by minimizing the bending stresses at the critical notch sensitive area of the seal.

4. The primary causes of failure of the 45° V-seal were excessive seal loading and uneven distribution of the load, which resulted in circumferential cracking at stress concentrations exceeding the strength of the polyimide. Failure occurred in a similar manner, and after a similar number of stress cycles, to earlier tests conducted under a different type of operational cycle (simulated flight cycle).

5. Although the spring-loaded lip seal (Design E) exhibited a short operating life, the concept shows considerable potential because of its simple design and low operating friction.

6. In the design of polyimide seals, careful consideration should be given to the thermal properties of the material. Thermal stresses due to differential expansion and contraction at the sealing surfaces represent a major portion of the overall seal stresses and must be taken into consideration in the seal design. Shrinkage of the polyimide due to thermal aging appears to be an inherent characteristic of the material. Consequently, proper seal loadings to provide the necessary deflections to compensate for this condition should be incorporated in the seal design.

APPENDIX A

NAS3-11170

EXHIBIT "A"

I Scope of Work

The work to be performed shall consist of investigations to extend the performance of polyimide rod seals for use with hydraulic fluids in advanced aircraft, including (1) futher development of the polyimide V-seal evolved under Contract NAS3-7264, (2) develop other seal designs which most effectively use the mechanical properties of the polyimide material, and (3) conduct high temperature cycling tests on the most promising seal configurations to determine their operating endurance limits.

II Statement of Work

The Contractor shall furnish the necessary personnel, facilities, services and materials and otherwise do all things necessary for, or incident to, the work described below:

TASK I - SEAL DESIGN DEVELOPMENT

A. V-Seal Analyses and Redesign

1. The V-seal evaluated in Contract NAS3-7264 shall be redesigned based on a thorough analysis of its configuration, physical properties, and known performance and failure modes. The following general procedure shall be used for this analysis:

a) All relevant dimensional data of the specimens tested in Contract NAS3-7264 shall be reviewed.

b) Large-scale (10x normal) layouts shall be made of the specimen seal installations. These layouts shall be representative of conditions before and after testing and also of conditions at both room and elevated temperature to account for thermal expansion. This shall permit study of the relationship of the cavity and rod to the posture of the seal elements, load ring, and backup ring under various conditions.

c) Free body diagrams shall be prepared from the layouts with probable deflection modes indicated.

d) Stress analyses shall be performed in an effort to match established theory to the manner and time of the failures. Known physical properties of the material and estimates of kinematic conditions during operation shall be utilized in the analyses.

e) Concurrent with the above, the dimensional stability of the material shall be evaluated. V-seal specimens shall be subjected to thermal cycling and high-temperature soaking under confined and unconfined conditions.

EXHIBIT "A"

2. A design study shall be conducted using the results from this analytical study and other applicable information to improve the V-seal design concept. Some techniques that shall be considered include:

   a) Use of longer V-sections through reducing the included angle to lower the stress level while obtaining the required deflections.

   b) Use of a constant-stress geometry to minimize stress concentration (more gradual transitions from one section to another).

   c) Reinforcing the V-section with a higher modulus material (metallic) to prevent overstressing of the sealing elements.

   d) Use of improved loading devices to provide better load distribution; i.e., asymmetrical as opposed to symmetrical loading, and use of flexible material (e.g., Rulon) as interleaf between V-seals for more uniform axial load transmission.

3. The Contractor shall evaluate fabrication and molding techniques to determine the most suitable method for producing unfilled polyimide seals. The feasibility of using rolled polyimide sheet material for seal fabrication shall be considered. The V-seal design shall utilize any improved fabrication methods.

4. V-seals shall be fabricated to the new design and bench tested to ascertain the benefits of the improvements. These tests shall determine friction, leakage, seal deflection, and compensation of wear under simulated wear conditions.

B. Other Seal Designs

In addition to the V-seal, four other concepts shall be evolved that offer the potential of utilizing the mechanical properties of the polyimide to best advantage. Simple stress analysis shall be conducted to aid in design selection. The most promising seal designs shall be fabricated, and design parameters such as friction, loading, leakage, and wear compensation shall be determined through bench testing.

TASK II - SEAL FABRICATION AND TEST RIG LAYOUT

Based on the results of the seal design and testing in Task I, four (4) sets each of the most promising seal configuration shall be fabricated. In addition, a layout drawing of the test rig with accompanying parts list shall be prepared. The parts list shall indicate the items furnished at no cost by the Contractor as well as those items furnished by NASA.

EXHIBIT "A"

TASK III - HIGH TEMPERATURE CYCLING TESTS

A. Seal Evaluation

1. The Contractor shall select with the approval of the NASA Project Manager, the three most promising one-inch seal configurations developed in Task I and the V-seal design developed under Contract NAS3-7264 for testing as described below.

2. The seals shall be tested in the double ended test actuators used under Contract NAS3-7264 or equivalent. Each actuator shall be used to test two different seal designs concurrently, and two actuators shall be tested in the same rig used under Contract NAS3-7264 with four seal designs being tested concurrently.

3. The Contractor shall conduct high frequency short stroke cycling tests on the four selected seal designs. The selected test sequence is based on bending fatigue as the likely cause of prior failure and the observation the primary wear problems developed in the short stroke cycle operation. The tests shall be conducted at a fluid temperature of 500°F, ± 20°F and fluid pressure of 100 to 150 psig. (The seal temperature shall be no less than the fluid temperature.) The cycling rate shall be 300 cpm ± 25 cpm. Piston rod total stroke length shall be maintained at .020 inch (± .020.) The test fluid shall be chlorinated phenyl methyl silicone supplied by the Contractor unless otherwise directed by the NASA Project Manager. The test shall be run to failure or completion of 20 million short-stroke cycles. Seal failure shall be defined as leakage in excess of one drop per minute (approximately 3 cc per hour). Prior to conducting the test, the Contractor shall submit a test plan and instrumentation plan for the NASA Project Manager approval.

B. Data Requirements

The minimum data recorded during tests of the seals shall be as follows:

1. Oil temperature
2. Oil leakage
3. Number of cycles and rate
4. Oil pressure

C. Calibration and Additional Data Requirements

1. Apparatus and instruments used shall be calibrated prior to the start and at scheduled intervals during the program.

2. An equipment log shall be maintained for each apparatus and instrument. Dated entries shall be made for all calibrated results, all uses of the equipment, all inspection data, and all maintenance operations on the equipment.

3. Technical record logs shall be established by the Contractor and dated entries made to provide a means for documenting the history of each seal throughout its testing cycle. The logs shall contain all information needed to reach a decision as to whether the seals developed meet the specified requirements.

4. The above logs shall be fully maintained and be available for review by the NASA Project Manager.

5. All data recorded under this contract shall be made available to the NASA Project Manager upon request.

D. Additional Reporting Requirements

As an additional requirement, the Final Report shall include in an appendix all pertinent analysis performed during the program and a set of detailed drawings of the test seals.

APPENDIX B
SEAL ANALYSES

A. GENERAL

Design analyses of the spring-loaded lip seal (Design E) and the wide angle V-seal (Design F) are presented in the following sections. The analyses provided the basis for the design of the two seal configurations. In determining the load-deflection characteristics of these seals, appropriate formulas from R. J. Roark's "Formulas for Stress and Strain" were applied. For the design of the hoop spring used in seal Design E, reference was made to the work by A. M. Wahl - Mechanical Springs, second edition (Reference 4).

B. SPRING-LOADED LIP SEAL

This configuration, Figure 21, consists of a polyimide sealing lip and slotted metal hoop spring. The latter provides the necessary closing force on the seal lip to effect a seal against the piston rod. The spring also acts as a wear compensating device.

The method of analysis was similar to that used in the V-seal studies (see Section I). The principle factor governing the design of the seal was the differential thermal expansion between the polyimide seal and the piston rod at 500°F (260°C). Therefore, the seal loading had to be of sufficient magnitude to restrain the seal from expanding so that intimate contact between the seal and piston rod could be maintained at the 500°F (260°C) operating condition.

The differential expansion ($\Delta\ell$) between the seal and piston rod at 500°F (260°C), was determined in the following manner:

$\Delta\ell$ = seal expansion-rod expansion at 500°F (260°C).

Using coefficients of expansion of

27.5×10^{-6} in./in./°F for the polyimide and

5.6×10^{-6} in./in./°F for the 440C piston rod;

$\Delta\ell = 27.5 \times 10^{-6}$ in./in./°F x 430°F x 1 in. - 5.6×10^{-6} in./in./°F x 430 x 1 in.

$\Delta\ell$ = 0.0094 in. (0.024 cm)

Therefore in the design of the seal, an external load capable of deflecting the seal by 0.0094 in. (0.024 cm) diametrally must be incorporated to overcome the effects of thermal expansion.

Values of seal load, seal cross-sectional thickness, and operating stresses were determined by applying classical formulas for stress analysis of thin walled cylinders. From R. J. Roark's "Formulas for Stress and Strain" (Reference 2), the following equations were derived.

For radial deflection (R.D.),

$$R.D. = \frac{-V_o}{2D\lambda^3} \tag{B-1}$$

where: $D = \frac{Et^3}{12(1-\nu^2)}$; and

$$\lambda = \sqrt[4]{\frac{3(1-\nu^2)}{R_2^2 t^2}} = \frac{[3(1-\nu^2)]^{1/4}}{\sqrt{Rt}}$$

Substituting for D and λ, Equation (B-1) becomes

$$R.D. = \frac{-V_o}{\frac{2Et^3}{12(1-\nu^2)} \quad \frac{3^{3/4}(1-\nu^2)^{3/4}}{R^{3/2} t^{3/2}}} = -\frac{6V_o R^{3/2}(1-\nu)^{1/4}}{3^{3/4} Et^{3/2}} \tag{B-2}$$

Hoop stress (δ_2) due to seal loading is determined from

$$\delta_2 = -\frac{2V_o}{t} \lambda R \text{ (at end)} \tag{B-3}$$

substituting for λ Equation (B-3) becomes:

$$\delta_2 = -\frac{2(3)^{1/4} V_o (1-\nu^2)^{1/4} \sqrt{R}}{t^{3/2}} \text{ (at end)} \tag{B-4}$$

The hoop bending stress (δ_2') is obtained from:

$$\delta_2' = +\nu\delta_1' \tag{B-5}$$

Where (δ_1') the meridional bending stress is:

$$\delta_1' = \frac{1.932\,V_o}{\lambda t^2} \tag{B-6}$$

Substituting for λ, Equation (B-6) becomes

$$\delta_1' = \frac{1.932\,V_o}{\frac{t^2\,3^{1/4}\,(1-\nu)^{1/4}}{\sqrt{R}\,\sqrt{t}}} = \frac{1.932\,V_o\sqrt{R}}{(3^{1/4})\,t^{3/2}\,(1-\nu)^{1/4}} \tag{B-7}$$

Hoop stress due to fluid pressure

$$\delta_2 = \frac{PR}{t}$$

Given the following conditions, Equation (B-2) was rearranged to solve for the seal load (V_o).

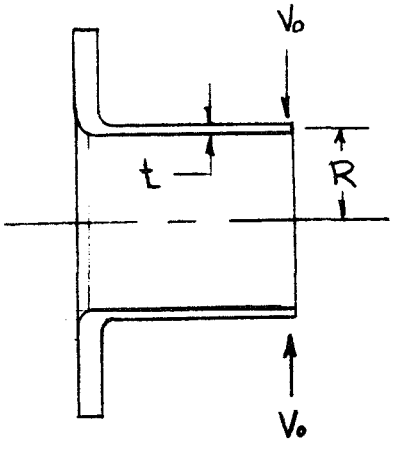

POLYIMIDE SEALING LIP

Modulus of Elasticity of polyimide	(E)	-	250,000 psi at 500°F
Poisson's ratio	(ν)	-	.45
Seal radius	(R)	-	.5 in.
Seal thickness	(t)	-	.018 - .020 in.
Tensile yield strength	F_{TY}	-	6000 psi at 500°F
Seal radial deflection	(R.D.)	-	0.0047 in. at 500°F

$$R.D. = - \frac{6 V_o (.5)^{3/2} (.946)}{2.28 (250 \times 10^3) t^{3/2}} \quad \text{(B-2)}$$

$$R.D. = .00339 \times 10^{-3} \left(\frac{V_o}{t^{3/2}}\right)$$

$$V_o = \frac{.0047 \times .0042}{.00339 \times 10^{-3}}$$

V_o = 3 pounds per inch (525 N/m) of seal circumference

The hoop stress resulting from the seal load (V_o) was determined from Equation (B-4).

$$\delta_2 = - 2(1.316)\ 3\ (.946) \frac{\sqrt{.5}}{t^{3/2}} \quad \text{(B-4)}$$

δ_2 = 2180 psi (1.5×10^7 N/m^2)

From Equation (B-7), the bending stress resulting from the seal load was:

$$\delta_1' = \frac{1.932\ V_o \sqrt{R}}{(3^{1/4})\ t^{3/2} (1-\nu)^{1/4}} \quad \text{(B-7)}$$

$$\delta_1' = 1.1 \left(\frac{V_o}{t^{3/2}}\right)$$

$$\delta_1' = 1.1 \times \frac{3}{.00242}$$

δ_1' = 1365 psi (9.41×10^6 N/m^2)

The above values obtained for loop stress and bending stress are well within the strength envelope of the polyimide. The seal cross-sectional thickness (t) of .018-.020 inch (0.046-0.051 cm) was selected in order to obtain the most flexible seal possible.

The slotted hoop spring depicted below was configured to provide a series of spring taps, which produced a uniform load of 3 pounds (525 N/m). The tabs were designed based on a simple cantilever spring of constant width loaded at the free end.

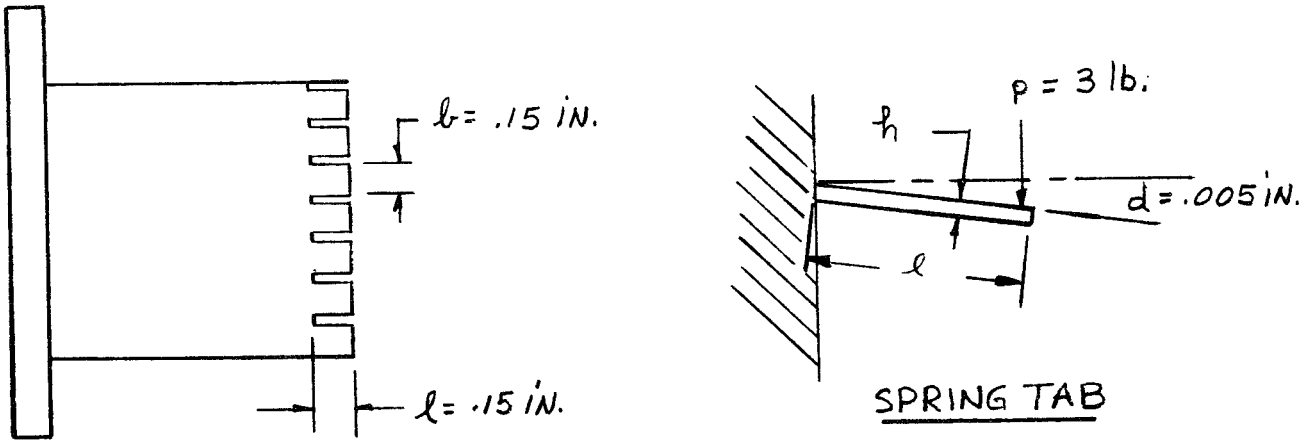

Figure 48. Hoopspring

In the above case the well known cantilever formula for deflection (Reference 4) is

$$d = \frac{p\ell^3}{3EI} \qquad \text{(B-8)}$$

where ℓ = length of spring

E = modulus of elasticity

$I = \frac{bh^3}{12}$ = moment of inertia, where b = width, h = thickness

An H-11 type (Vascojet 1000) steel, heat treated to provide a tensile yield strength of approximately 180,000 psi at 600°F, was selected as the spring material. Using the data shown in Figure 48, the thickness (h) of the spring was determined from Equation (B-8).

$$d = \frac{p\ell^3}{3E} \quad \frac{bh^3}{12} \qquad \text{(B-8)}$$

Rearranging and solving for h, Equation (B-8) becomes:

$$h = \sqrt[3]{\frac{12\, p\ell^3}{3Ebd}}$$

$$h = \sqrt[3]{\frac{4 \times 3 \times (.15)^3}{29 \times 10^6 \times (.15) \times (.005)}}$$

h = .0123 inch (0.031 cm)

The nominal bending stress at the built-in end of the spring is

$$\delta = \frac{6p\ell}{bh^2} \qquad \text{(B-9)}$$

$$\delta = \frac{6(3)(.15)}{.15\,x(.0123)^2}$$

$$\delta = 120{,}000 \text{ psi } (8.27 \times 10^8 \text{ N/m}^2)$$

C. WIDE ANGLE V-SEAL (DESIGN F)

This seal configuration, shown in Figure 49, consists of three sealing elements, a backup ring, and loading ring. The wide angle (133°) construction provides a gradual transistion from one surface to another to minimize stress concentration. Loading of the inner and outer sealing surfaces is accomplished by two spring washers, which are capable of producing an axial force of approximately 100 pounds (445N).

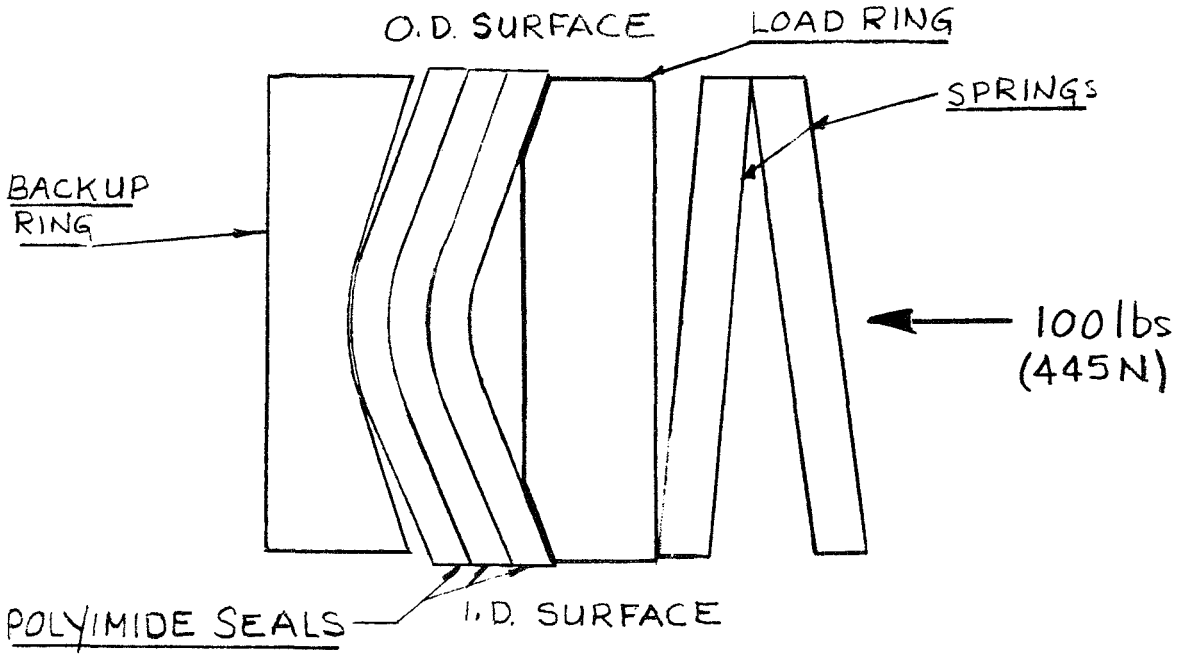

Figure 49. Wide Angle V-Seal

Analysis of the stress and deflection characteristics of this seal was based on techniques used in the stress analysis of flat plates (Reference 4). As shown below the seal was evaluated as a circular plate with a concentric circular hole.

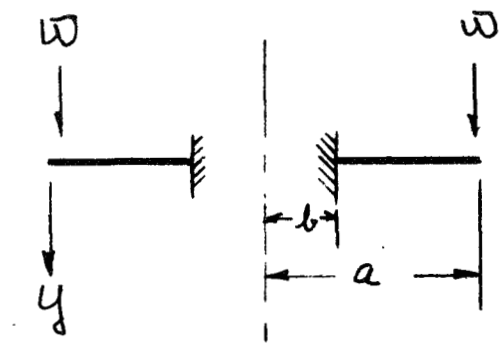

CONDITION-A

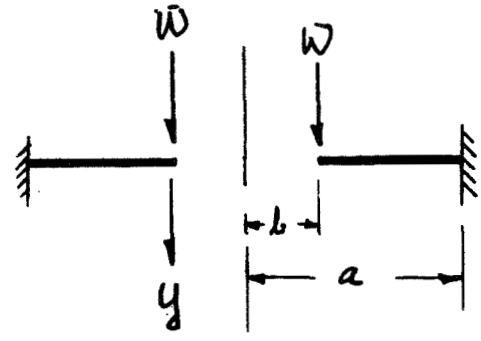

CONDITION-B

O.D. DEFLECTION

I.D. DEFLECTION

For condition "A" deflection of the O.D. surface, the inner edge is assumed fixed and a uniform load acting along the outer edge. In this case the maximum radial stress occurs at the inner surface. From Reference 4, the stress and deflections were determined as follows:

$$\text{Max. } \delta_r \text{ (at inner edge)} = \frac{3\bar{w}}{2\pi t^2}\left[\frac{2a^2(m+1)\log a/b + a^3(m-1) - b^2(m-1)}{a^2(m+1) + b^2(m-1)}\right] \qquad \text{(B-10)}$$

$$\text{Max. y (at outer edge)} = -\frac{3\bar{w}(m^2-1)}{4m^2\pi Et^3}\left[\frac{a^4(3m+1) - b^4(m-1) - 2a^2b^2(m+1) - 8ma^2b^2\log a/b - 4a^2b^2(m+1)(\log a/b)^2}{a^2(m+1) + b^2(m-1)}\right] \qquad \text{(B-11)}$$

Notations:

δ_r = radial stress - psi

y = vertical deflection - in.

$\bar{w}$ = applied load = $\frac{50}{2\pi \times .75 \times 3}$ = 3.5 pounds/inch

$m = \frac{1}{\nu} = \frac{1}{.45} = 2.22$

$(m+1) = (2.22 + 1) = 3.22$, $(m - 1) = 1.22$

a = 0.75 in., b = 0.625 in., t = 0.02 in., E = 250,000 psi at 500°F

$\frac{a}{b} = \frac{.75}{.625} = 1.20$; $\log \frac{a}{b} = .079$; $a^2 = .562$; $b^2 = .39$

$$\text{Max. } \delta_r = \frac{3(3.5)}{2\pi \times .02^2}\left[\frac{2 \times .562 \times 3.22 \times .079 + .562 \times 1.22 - .39 \times 1.22}{.562 \times 3.22 + .39 \times 1.22}\right] \quad \text{(B-10)}$$

$$= 4200 \times .218$$

$$\delta_r = 915 \text{ psi } (6.31 \times 10^6 \text{ N/m}^2)$$

$$\text{Max. } y = -\frac{3(3.5)(3.9)}{4(4.9)\pi\, 250{,}000 \times .000008}\left[\frac{2.425 - .1864 - 1.416 - .309 - .0177}{1.812 + .477}\right] \quad \text{(B-11)}$$

Max. $y = -.334 \times .217$

Max. $y = -.0725$ in. (0.184 cm).

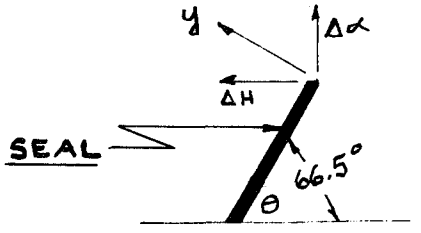

Deflection for O.D. is $\Delta\alpha = y \cos\theta = .0725 \times .3987 = .028$ in. (0.071 cm).

For condition B

$$\text{Max. } \delta_r \text{ (at outer edge)} = \frac{3\bar{w}}{2\pi t^2}\left[1 - \frac{2mb^2 - 2b^2(m+1)\log a/b}{a^2(m-1)+b^2(m+1)}\right] \quad \text{(B-12)}$$

Max. y (at inner edge) =

$$-\frac{3\bar{w}(m^2-1)}{4\pi m^2 E t^3}\left\{a^2 - b^2 + \frac{2mb^2(a^2-b^2) - 8ma^2 \log a/b + 4a^2b^2(m+1)(\log a/b)^2}{a^2(m-1) + b^2(m+1)}\right\} \quad \text{(B-13)}$$

Notations:

$m = 2.22,\ a = 0.625,\ b = 0.498,\ t = .02$

$E = 250,000$ psi at 500°F

$\bar{w} = \dfrac{50}{2\pi \times .498 \times 3} = 5.33$ pounds/inch

$a^2 = 0.390,\ b^2 = 0.248,\ \dfrac{a}{b} = 1.255,\ \log \dfrac{a}{b} = .0986$

$$\text{Max. } \delta_r = \frac{3 \times 5.33}{2 \times \pi \times .0004}\left[1 - \frac{2 \times 2.22 \times .248 - 2 \times .248 \times 3.22 \times .098}{.3906 \times 1.22 + .248 \times 3.22}\right] \qquad \text{(B-12)}$$

$$\text{Max. } \delta_r = \frac{15.99}{.00251}\left[1 - \frac{1.102 - .157}{.477 + .799}\right]$$

$$\text{Max. } \delta_r = 6370 \times .257$$

$$\text{Max. } \delta_r = 1640 \text{ psi } (1.13 \times 10^7 \text{ N/m}^2)$$

$$\text{Max. } y = -\frac{3(5.33) \times 3.9}{4 \times \pi \times 4.9 \times 2} \times \left\{ .142 + \frac{.157 - .169 + .012}{.447 + .799} \right\} \qquad \text{(B-13)}$$

$$= - .518 \times .142$$

$$\text{Max. } y = - .0735 \text{ inch}$$

Deflection for I.D. is $\Delta\alpha = y \cos \theta = .0735 \times .398 = .029$ inch (0.074 cm)

APPENDIX C

DRAWINGS

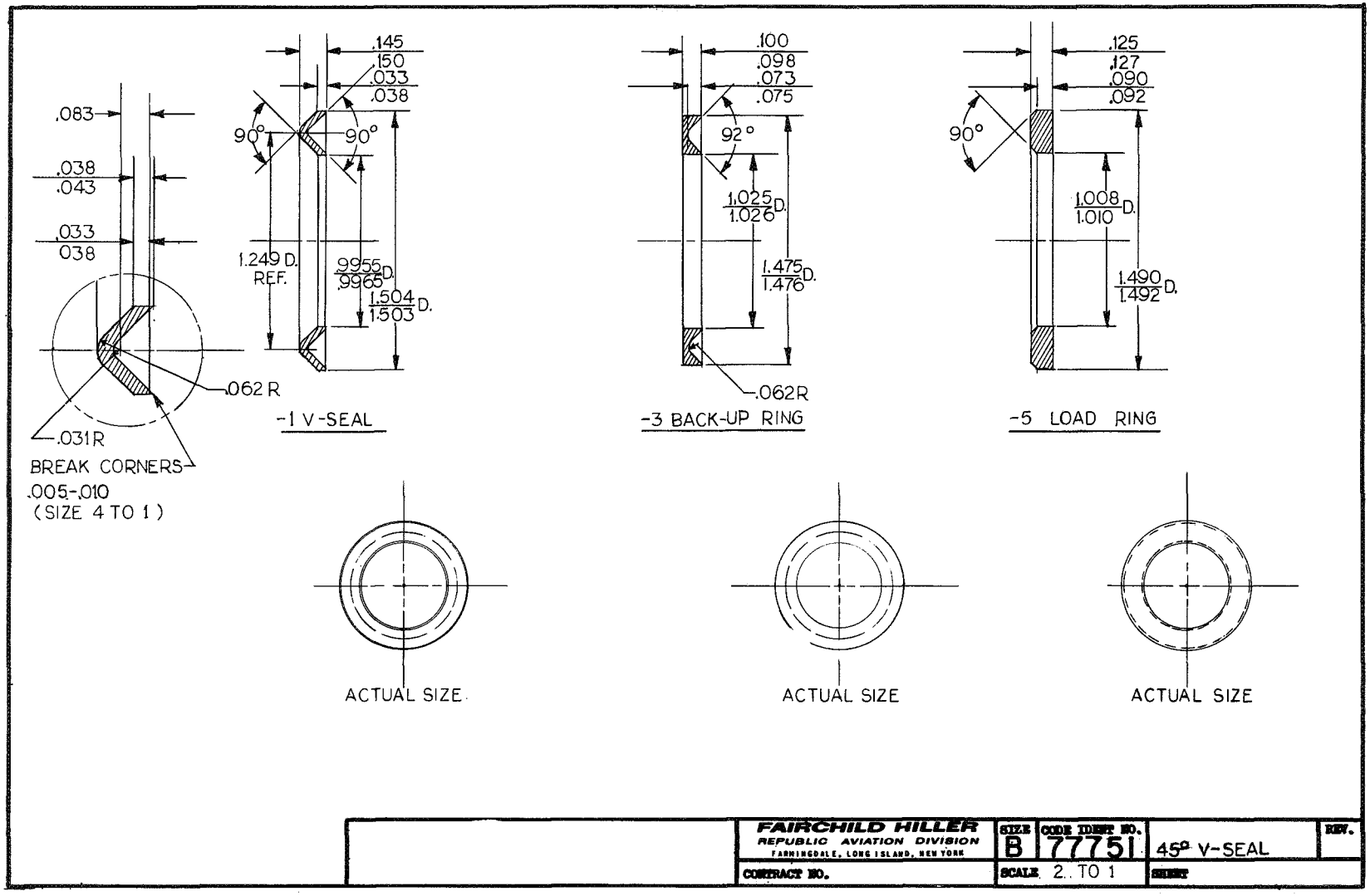
.083
.038
.043
.033
038
.062 R
.031R
BREAK CORNERS
.005-.010
(SIZE 4 TO 1)
.145
.150
.033
.038
90°
90°
1.249 D.
REF.
.9955
.9965 D.
1.504
1.503 D.
-1 V-SEAL
.100
.098
.073
.075
92°
1.025
1.026 D.
1.475
1.476 D.
.062R
-3 BACK-UP RING
.125
.127
.090
.092
90°
1.008
1.010 D.
1.490
1.492 D.
-5 LOAD RING
ACTUAL SIZE
ACTUAL SIZE
ACTUAL SIZE
FAIRCHILD HILLER
REPUBLIC AVIATION DIVISION
FARMINGDALE, LONG ISLAND, NEW YORK
SIZE B
CODE IDENT NO. 77751
45° V-SEAL
REV.
CONTRACT NO.
SCALE 2 TO 1
SHEET

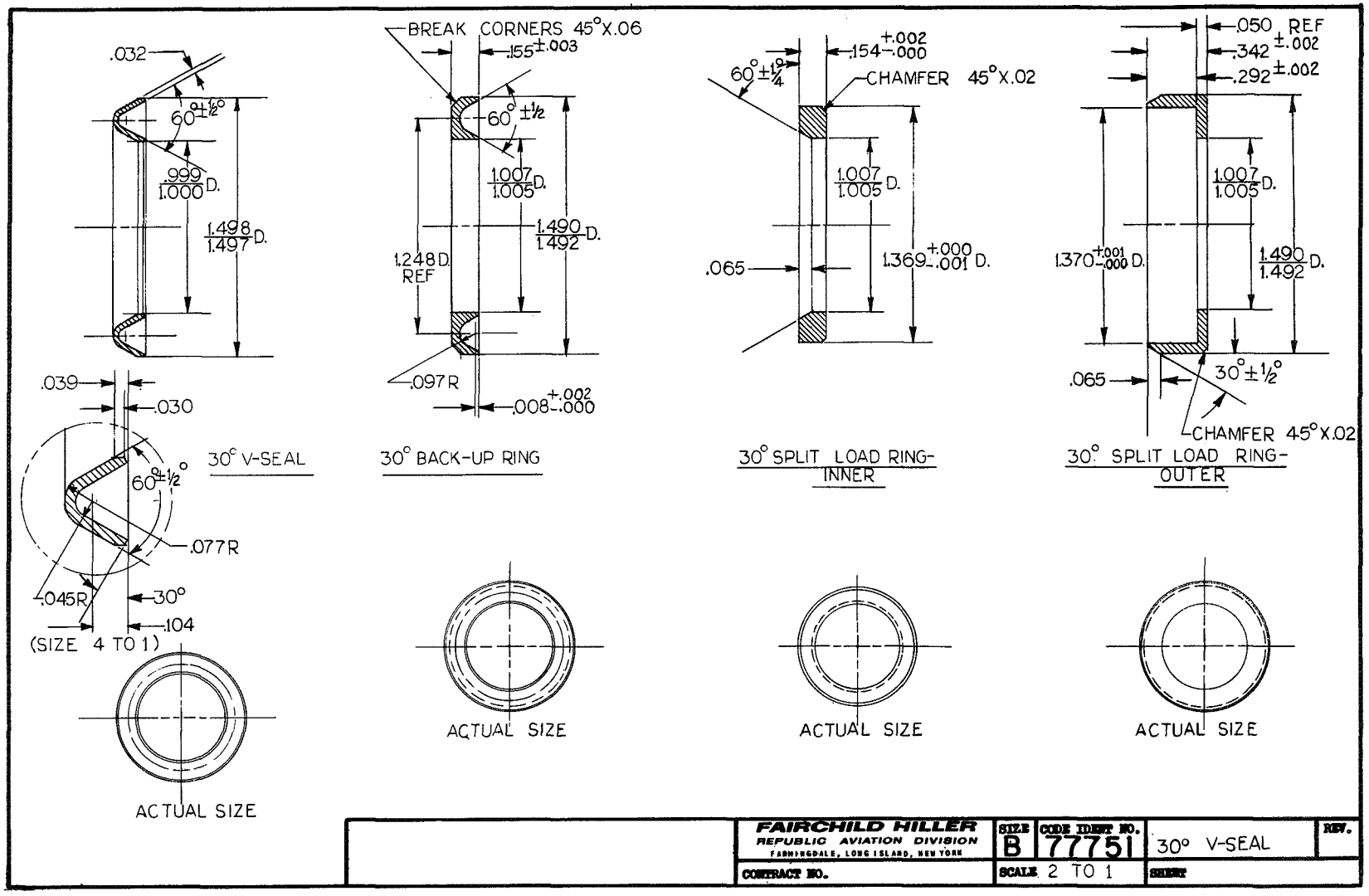
.032
60° ±½°
.999/1.000 D.
1.498/1.497 D.
.039
.030
60° ±½°
.077R
.045R
30°
.104
(SIZE 4 TO 1)
30° V-SEAL
ACTUAL SIZE
BREAK CORNERS 45° X.06
.155 ±.003
60° ±½
1.007/1.005 D.
1.490/1.492 D.
1.248 D. REF
.097R
.008 +.002 -.000
30° BACK-UP RING
ACTUAL SIZE
60° ±¼°
.154 +.002 -.000
CHAMFER 45° X.02
1.007/1.005 D.
.065
1.369 +.000 -.001 D.
30° SPLIT LOAD RING-INNER
ACTUAL SIZE
.050 REF
.342 ±.002
.292 ±.002
1.007/1.005 D.
1.370 +.001 -.000 D.
1.490/1.492 D.
.065
30° ±½°
CHAMFER 45° X.02
30° SPLIT LOAD RING-OUTER
ACTUAL SIZE
FAIRCHILD HILLER
REPUBLIC AVIATION DIVISION
FARMINGDALE, LONG ISLAND, NEW YORK
SIZE B
CODE IDENT NO. 77751
30° V-SEAL
REV.
CONTRACT NO.
SCALE 2 TO 1
SHEET

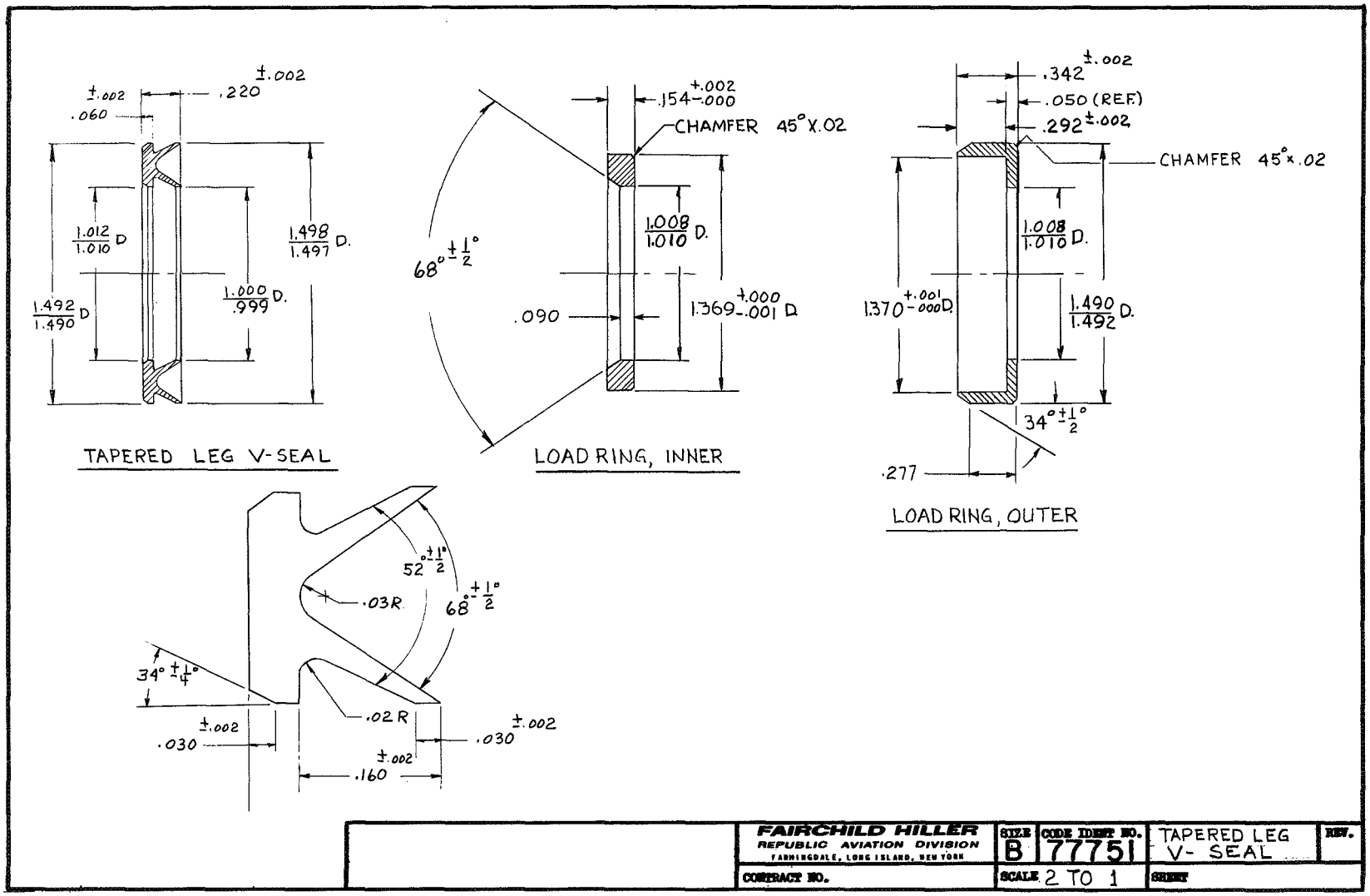
±.002
.060
±.002
.220
1.012/1.010 D
1.498/1.497 D.
1.492/1.490 D
1.000/.999 D.
TAPERED LEG V-SEAL
+.002
.154 -.000
CHAMFER 45° X.02
68° ± 1/2°
1.008/1.010 D.
.090
1.369 +.000 -.001 D
LOAD RING, INNER
±.002
.342
.050 (REF.)
.292 ±.002
CHAMFER 45° x .02
1.008/1.010 D.
1.370 +.001 -.000 D.
1.490/1.492 D.
34° ± 1/2°
.277
LOAD RING, OUTER
52° ± 1/2°
.03R
68° ± 1/2°
34° ± 1/4°
±.002
.030
.02 R
±.002
.030
±.002
.160
FAIRCHILD HILLER
REPUBLIC AVIATION DIVISION
FARMINGDALE, LONG ISLAND, NEW YORK
SIZE B
CODE IDENT NO. 77751
TAPERED LEG V- SEAL
REV.
CONTRACT NO.
SCALE 2 TO 1
SHEET

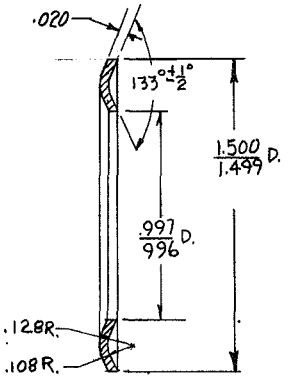

-1 V-SEAL

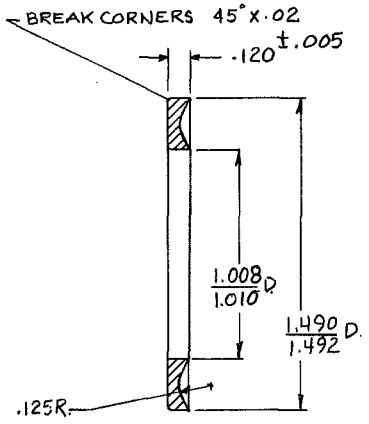

-3 BACK UP RING

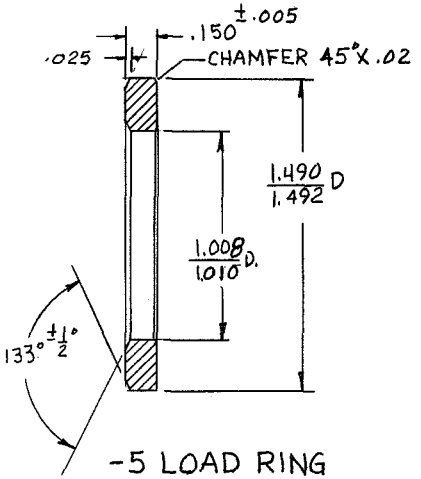

-5 LOAD RING

	FAIRCHILD HILLER REPUBLIC AVIATION DIVISION FARMINGDALE, LONG ISLAND, NEW YORK	SIZE B	CODE IDENT NO. 77751	WIDE ANGLE V-SEAL
	CONTRACT NO.	SCALE 2 TO 1	SHEET	REV.

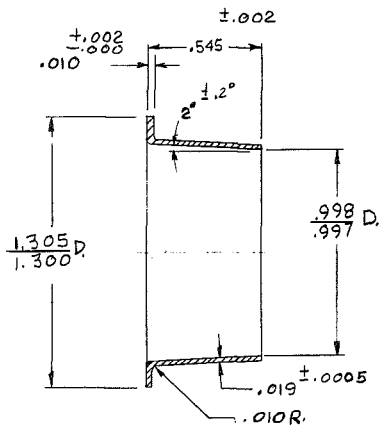

POLYIMIDE LIP SEAL

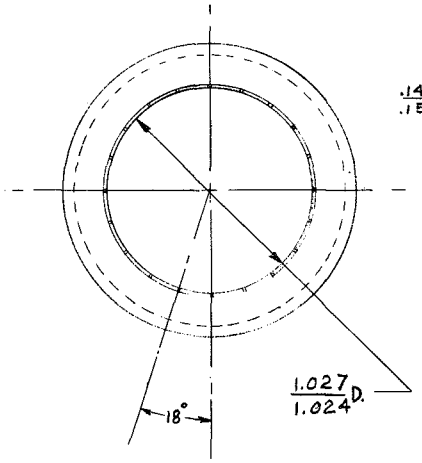

20 SLOTS - EVENLY SPACED
18° APART

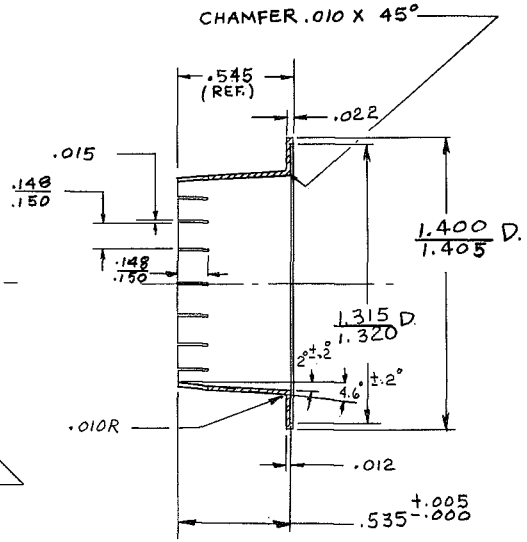

HOOP SPRING

NOTE:
HEAT TREAT SPRING AS FOLLOWS:
(1) PREHEAT AT 1500°F, (2) HOLD AT 1850°F. FOR 20 TO 30 MINS. IN NEUTRAL ATMOSPHERE AND COOL TO RM. TEMP., RATE OF COOLING FR 1850°F TO 1200°F IN 60 SEC. (3) TEMPER (NEUTRAL ATMOS) IMMEDIATELY UPON REACHING RM. TEMP. FOR 3 HRS. AT 1050°F, AIR COOL AND RETEMPER FOR ADDITIONAL 3 HRS. AT 1050°F AND AIR COOL. (BRIGHT SURFACE REQD) TEST BUTTON HARDNESS TO BE Rc 48-52.

FAIRCHILD HILLER REPUBLIC AVIATION DIVISION FARMINGDALE, LONG ISLAND, NEW YORK	SIZE B	CODE IDENT NO. 77751	SPRING-LOADED LIP SEAL	REV.
CONTRACT NO.	SCALE 2 TO 1		SHEET	

REFERENCES

1. Lee, J., "High Temperature Hydraulic System Actuator Seals For Use in Advanced Supersonic Aircraft," NASA CR-72354, 1967.

2. Roark, R. J., "Formulas for Stress and Strain," Third Edition, 1954.

3. "Vespel Precision Parts from du Pont Polyimide Resins," Commercial Brochure, E. I. du Pont de Nemours & Co. (Inc.), 1967.

4. Wahl, A. M., "Mechanical Springs," Second Edition, 1963.

FINAL REPORT, CR 72563, DISTRIBUTION LIST FOR
CONTRACT NAS3-11170

	Addressee	Number of Copies
1.	NASA-Lewis Research Center Aeronautics Procurement Section 21000 Brookpark Road Cleveland, Ohio 44135 Attention: Leonard W. Schopen, MS 77-3	1
2.	NASA-Lewis Research Center Technical Utilization Office 21000 Brookpark Road Cleveland, Ohio 44135 Attention: P. E. Foster, MS 3-19	1
3.	NASA-Lewis Research Center Fluid System Components Division 21000 Brookpark Road Cleveland, Ohio 44135	
	Attention: A. Ginsburg, MS 5-3	1
	E. E. Bisson, MS 5-3	1
	C. H. Voit, MS 5-3	1
	R. L. Johnson, MS 23-2	2
	W. R. Loomis, MS 23-2	3
	M. A. Swikert, MS 23-2	1
	D. P. Townsend, MS 6-1	2
	H. E. Sliney, MS 23-2	1
	W. F. Hady, MS 23-2	1
4.	FAA Headquarters 800 Independence Avenue, SW Washington, D. C. 20553	
	Attention: General J. C. Maxwell	1
	F. B. Howard	1
5.	NASA Headquarters 600 Independence Avenue, SW Washington, D. C. 20546	
	Attention: N. F. Rekos (RAP)	1
	A. J. Evans (RAD)	1
	J. Maltz (RRM)	1
6.	NASA-Langley Research Center Langley Station Hampton, Virginia 23365	
	Attention: Mark R. Nochols	1

	Addressee	Number of Copies
7.	Air Force Aero Propulsion Laboratory Wright-Patterson AFB, Ohio 45433 Attention: APEL, J. L. Morris	1
8.	NASA-Lewis Research Center Air-Breathing Engines Division 21000 Brookpark Road Cleveland, Ohio 44135 Attention: J. H. Childs, MS 60-4	1
9.	Air Force Materials Laboratory Wright-Patterson AFB, Ohio 45433 Attention: MANL, R. Adamczak MANL, R. L. Benzing MANE, R. E. Headrick MANL, H. Schwenker MAAM, R. D. Hughes MAAE, P. House	1 1 1 1 1 1
10.	Air Force Systems Engineering Group Wright-Patterson AFB, Ohio 45433 Attention: SEJDF, S. Prete	1
11.	United Aircraft Corporation Pratt & Whitney Aircraft Division East Hartford, Connecticut Attention: R. P. Shevchenko P. Brown	1 1
12.	General Electric Company Gas Turbine Division Evendale, Ohio 45215 Attention: B. Venable J. A. Fallon J-56 C. S. Boardman J-155	1 1 1
13.	NASA-Lewis Research Center 21000 Brookpark Road Cleveland, Ohio 44135 Attention: Library, MS 60-3 Fred Macks, MS 3-15	2 1
14.	NASA-Lewis Research Center 21000 Brookpark Road Cleveland, Ohio 44135 Attention: Reports Control Office, MS 5-5	1

	Addressee	Number of Copies
15.	NASA-Scientific & Technical Information Facility P. O. Box 33 College Park, Maryland 20740 Attention: NASA Representative	6
16.	Department of the Army U. S. Army Aviation Material Labs. Fort Eustis, Virginia 23604 Attention: J. W. White Propulsion Division	1

Avco Corporation
379 West 1st Street
Dayton, Ohio 45402
Attention: R. J. McBride (1)

Crane Packing Company
6400 W. Oakton Street
Morton Grove, Illinois
Attention: Harry Tankus (1)

Moog Servocontrols Inc.
Proner Airport
East Aurora, New York (1)

Mechanical Technology Inc.
Latham, New York
Attention: M. B. Peterson (1)

SKF Industries, Inc.
Engineering & Research Center
King of Prussia, Penn. 19406
Attention: W. B. Tuffin (1)

Westinghouse Electric Corp.
Research Laboratories
Beulah Road, Churchill Borough
Pittsburgh, Pennsylvania 15235
Attention: Dave Boes

The Bendix Corporation
Aerospace Division
South Bend, Indiana
Attention: Librarian (1)

B. F. Goodrich Company
Aerospace & Defense Products Division
Troy, Ohio
Attention: L. S. Bialkowski (1)

U. S. Army Ordnance
Rock Island Arsenal Laboratory
Rock Island, Illinois 61201
Attention: R. LeMar (1)

NASA-Manned Spacecraft Center
Houston, Texas 77058
Attention: R. Bricker, ES5 (1)

Chevron Chemical Company
Oronite Division
200 Bush Street
San Francisco, California 94120
Attention: T. S. McClure (1)

Kendall Refining Company
Main Office
Bradford, Pennsylvania
Attention: L. D. Dromgold (1)

Monsanto Research Corporation
1515 Nicholas Road
Dayton, Ohio 45407
Attention: Charles J. Eby (1)

Sundstrand Aviation - Rockford
2421 Eleventh Street
Rockford, Illinois 61101
Attention: L. A. Sibert, 763M (1)

Hydroacoustics Laboratory
General Dynamics Electronics
1400 North Goodman Street
P. O. Box 226
Rochester, New York 14601
Attention: Griffith May (1)

E. I. DuPont deNemours & Company
Plastic Department
Wilmington, Delaware 19898
Attention: David Hamlin (1)
N. W. Todd (1)

Boeing Company
J. J. Werts Developmental Projects
Airplane Department
Box 707
Renton, Washington 98055
Attention: M. L. Holmdahl (1)

Pennsylvania State University
Department of Chemical Engineering
University Park, Pennsylvania 19406
Attention: Dr. E. E. Klaus (1)

Southwest Research Institute
8500 Culebra Road
San Antonio, Texas 78205
Attention: P. M. Ku (1)

General Motors Corporation
Allison Division
Plant No. 8
Indianapolis, Indiana
Attention: E. M. Deckman (1)

Fairchild Controls Corporation
225 Park Avenue
Hicksville, Long Island, New York
Attention: B. J. Hawkins (1)

New York Airbrake Company
Watertown Division
Stratopower Section
Starbuck Avenue
Watertown, New York (1)

Aerojet-General Corporation
20545 Center Ridge Road
Cleveland, Ohio 44116
Attention: W. L. Snapp (1)

Dow Chemical Company
Abbott Road Buildings
Midland, Michigan
Attention: Dr. R. Gunderson (1)

Esso Research & Engineering Co.
P. O. Box 8
Linden, New Jersey 07036
Attention: Mr. Jim Moise (1)

U. S. Naval Research Laboratory
Washington, D. C.
Attention: Dr. William Zisman (1)

U. S. Naval Air Material Center
Aeronautical Engine Laboratory
Philadelphia, Pennsylvania
Attention: A. L. Lockwood (1)

Department of the Navy
Bureau of Ships
Washington 25, D. C.
Attention: Hary King, Code 634A (1)

Chicago Rawhide Mfg. Co.
1311 Elston Avenue
Chicago 22, Illinois
Attention: R. Blair

Koppers Company, Inc.
Metal Products Division
Piston Ring & Seal Department
7709 Scott Street
Baltimore, Maryland 21203
Attention: T. C. Kuchler (1)

Borg-Warner Corporation
Weston Hydraulics Limited
Van Nuys, California
Attention: K. H. Knox (1)

Pressure Technology Corp. of America
453 Amboy Avenue
Woodbridge, New Jersey
Attention: A. Bobrowsky (1)

Parker Aircraft Company
5827 West Century Blvd.
Los Angeles 9, California
Attention: K. L. Thompson (1)

Stein Seal Company
20th and Indiana Avenue
Philadelphia, Pennsylvania 19132
Attention: Dr. Stein (1)

Sealol Company
100 Post Road
Providence, Rhode Island (1)

Huyck Metals Company
P. O. Box 30
45 Woodmont Road
Milford, Connecticut
Attention: J. I. Fisher (1)

General Electric Company
Silicone Products Department
Waterford, New York 12188
Attention: J. C. Frewin (1)

McDonnell Douglas Aircraft Co., Inc.
Missile & Space Systems Division
3000 Ocean Park Blvd.
Santa Monica, California
Attention: R. McCord (1)

American Brake Shoe Company
Abex-Aerospace Division
3151 W. Fifth Street
Oxnard, California 93032
Attention: J. A. Mileti (1)

Sperry Rand Corporation
Vickers Incorporated Division
Research & Development Dept.
Troy, Michigan 48084
Attention: Dr. W. W. Chao (1)

Midwest Research Institute
425 Volker Blvd.
Kansas City, Missouri 64110
Attention: Vern Hopkins (1)

Franklin Institute Laboratories
Benjamin Franklin Parkway at
20th Street
Philadelphia 3, Pennsylvania
Attention: E. Thelen (1)

Borg-Warner Corporation
Pesco Products Division
24700 N. Miles Road
Beford, Ohio 44014
Attention: C. M. Hughes (1)

North American Aviation, Inc.
Los Angeles Division
International Airport
Los Angeles 45, California
Attention: D. L. Posner (1)

Curtiss-Wright Corporation
Wright Aeronautical Division
333 West 1st Street
Dayton 2, Ohio
Attention: F. F. Koogler (1)

Monsanto Company
Organic Chemical Division
800 North Lindbergh Blvd.
St. Louis, Missouri 63166
Attention: Dr. R. Hatton (1)
Dr. W. R. Richard (1)

Monsanto Research Corporation
Boston Laboratories
Everett 49, Massachusetts
Attention: Dr. J. O. Smith (1)

Olin Mathieson Chemical Corp.
Organics Division
275 Winchester Avenue
New Haven 4, Connecticut
Attention: Dr. C. W. McMullen (1)

General Dynamics Corporation
Forth Worth, Texas
Attention: L. H. Moffatt (1)

Dow Corning Company
Midland, Michigan
Attention: H. Schieffer

Battelle Memorial Institute
505 King Avenue
Columbus 1, Ohio
Attention: C. M. Allen (1)

I. I. T. Research Foundation
10 West 35th Street
Chicago, Illinois 60616
Attention: Dr. Strohmeier (1)

Clevite Corporation
Aerospace Research
540 East 105th Street
Cleveland, Ohio 44108
Attention: G. F. Davies (1)

E. I. duPont deNemous & Co.
Organic Chemicals Depart.
1007 Market Street
Wilmington, Delaware 19898
Attention: N. D. Lawson (1)

Mobil Oil Company
Research Department
Paulsboro Lab.
Paulsboro, New Jersey 08066
Attention: Dr. E. Oberright (1)

Koontz-Wagner Electric Co., Inc.
343 Lincolnway West
South Bend, Indiana 46601
Attention: J. S. Tjaden

Lockheed Aircraft Corporation
Lockheed Missile & Space Co.
Material Science Lab.
3251 Hanover Street
Palo Alto, California
Attention: Francis J. Clauss (1)

Grumman Aircraft Engineering Corp.
Bethpage, New York 11714
Attention: William Mayhew (1)
F. Wakefield (1)
M. Tarase (1)

Hughes Aircraft Company
International Airport Station
P. O. Box 98515
Los Angeles 9, California (1)

W. S. Shamban & Company
11543 W. Olympic Blvd.
West Los Angeles, California 90064
Attention: Sherman Gauley (1)